Computational studies on adsorption behavior of hydrogen- and oxygen-related species on diamond (111) surfaces

Samar Moustafa Abd-elnaeem

January, 2014

Dissertation

Computational studies on adsorption behavior of hydrogen- and oxygen-related species on diamond (111) surfaces

Graduate School of Natural Science & Technology
Kanazawa University

Major Subject:
Electrical Engineering and Computer Science

Course:
Electronic Science

School registration No. (1123112101)

Name: Samar Moustafa Abd-elnaeem

Chief advisor: Prof. Takao Inokuma

ACKNOWLEDGEMENTS

*First of all, all praises and thanks to **ALLAH,** ALMIGHTY, for His blessing in completing this thesis, and indeed, throughout my life. He gives me the strength, and always protects, helps and guides me.*

*I would like to express my deep gratitude and appreciations to my supervisor **Prof. Takao Inokuma** for the continuous support of my M.sc and Ph.D study and research, for his patience, his efforts and time. I appreciate his fruitful discussion, valuable comments and helpful guidance throughout this work .*

*I would like also to express my sincere gratitude to **Associate Professor. Norio Tokuda** for his valuable discussions during this research.*

I would like to thank all members in the "Thin Film laboratory" and all stuff of Kanazawa University for the assistance they provided during my staying and studying in Kanazawa.

Also, my sincere thanks are due to all staff members of physics department, faculty of science, Assuit University, Egypt, for their encouragement.

*This research would not have been possible without the financial support from the Ministry of Education, Culture, Sports, Science and Technology in Japan (**MEXT**).*

*Finally I am indebted to my family, especially my beloved parents, **Prof. Moustafa** and **Mrs. Zeinab**, my husband and best friend, **Hesham**, my two princesses, **Yomna** and **Haya**, my brothers and sisters and all of my friends for supporting and helping me get through the stressful and difficult times. Without their continuous love, prayers and encouragement, I would not have finished this thesis.*

CONTENTS

Abstract

ABSTRACT

Diamond is an allotrope of carbon that has become one of the most important materials in industry. Because of its many outstanding physical and chemical properties, such as high thermal conductivity, extreme hardness, high transparency for ultraviolet-infrared (UV-IR) radiation, chemical inertness, and low friction coefficient, it has been a very useful material for various technological applications. Nowadays, the chemical vapor deposition (CVD) is the main method to grow diamond film. In the epitaxitial growth of diamond, three low-index faces, (111), (110) and (100), are the main orientations. Among the three orientations, (111) surface is of particular interest because the formation of atomically flat surfaces has been realized by utilizing a lateral growth mode on the (111) face.

Adsorption of foreign atoms on diamond surface can significantly modify its physical and chemical properties. These adsorbates play an important role in thin-film growth by affecting, for instance, adatom adsorption, nucleation and migration on surfaces The most common species that terminate diamond surfaces are hydrogen- (H) and oxygen-related species (e.g., O and OH groups). It has been shown that hydrogenated diamond surfaces can preserve its unique p-type surface conductivity and exhibit significant negative electron affinity. On the other hand, oxygenated surfaces show no surface conductivity and shift the electron affinity from negative to positive. These effects of hydrogen and oxygen to modify the surface properties of diamond are very attractive for use in electronic applications such as Schottky diodes, field effect transistors and pH sensors. Also, adsorbed oxygen atoms on diamond surfaces have also been known to make them hydrophilic while hydrogenated surfaces are hydrophobic.

Also, the investigation of hydrogen and oxygen coexistence on the diamond surfaces could also be important. Previous studies have established that the diamond surface terminated with OH exhibits a negative electron affinity, which makes the material potentially useful in a number of applications, such as photocathodes and cold cathode emitters.

The interaction of hydrogen, oxygen and Hydroxyl group on diamond surfaces becomes an important issue for both diamond technology and surface science study.

However, their behaviors on diamond surfaces seem not to be understood enough. In this study, the potential energies for neutral H, O atoms and OH group on a flat and stepped (a surface with monoatomic step) diamond (111)-(1×1) surface are investigated by a molecular orbital method based on the density functional theory (DFT) in order to clarify the static aspects for the interaction between those adatom and the surface.

Two-dimensional profiles of the potential energy for hydrogen, oxygen atoms and hydroxyl group are presented. The behaviors of surface diffusion and the influence of atomic steps are discussed. The oxygen adatom is found to have much lower energy barrier for migration. On the basis of the variations of potential energy, surface diffusion coefficients of adatoms are calculated. The potential energy for the O adatom is much lowered near the step edge. It is suggested that the oxygen atoms adsorbed on diamond (111) surface favor to be trapped near an atomic step after migration. Also, relaxation of the stepped surfaces with H adatom, O adatom, OH group as well as bare surface was studied. It was found that the carbon atoms at the step edge, which are bonded to H adatom or OH group, reconstructed to lower the surface energy and forms a downward slope in the $11\bar{2}$ direction.

CHAPTER 1

CHAPTER 1

Introduction

1.1. Diamond - the 21st century material?

The present trend in semiconductor technology is directed toward the development of devices capable of operating at higher and higher frequencies. In semiconductor devices this calls for smaller sizes, higher current densities and, hence, higher power dissipation capability. As a result of these conditions, it is becoming necessary for the devices to withstand unusually high operating temperatures. Since Germanium and silicon are presently approaching the limits of their capabilities, they cannot be relied upon for future improvements.

Diamond is a promising semiconductor material with unique physical and chemical properties. Table 1.1 summarizes many of the basic properties of most common used semiconductor materials including diamond. Diamond has the largest electronic energy gap among the elemental semiconductors, and one of the largest known energy gaps of all semiconductors. It has high diffusion energies for impurities and defects, and stable surfaces. The combination of light atomic mass and strong chemical bonding results in diamond having relatively high vibrational frequencies compared with other semiconductors. Related to this, at room temperature and above, the ability of diamond to conduct heat from an active area is unusually high. These properties should allow diamond to be used increasingly in a range of applications, from surface-mediated processes to high-power devices [1]. Developments of the use of diamond require knowledge of a very wide range of properties. Some have been known for many years, such as the thermal expansion of diamond, which is required to make a heterogeneous structure of diamond and another material. Other properties have only been mapped out recently. For example, to obtain complete control of the lattice we need to know the effects not only of impurities but also of the disorder from the isotope content of the lattice. In

yet other areas, exploiting high speed (terahertz) or small dimensions (nanometre), there is still much to learn.

	Ge	Si	GaAs	(6H-) SiC	GaN	**Diamond**
Band gap E_g (eV)	0.66	1.12	1.43	3.03	3.45	**5.5**
Dielectric constant ε_r	16.0	11.9	13.1	9.7	8.9	**5.7**
Breakdown voltage ($\times 10^5$ V/cm)	2.0	3.0	3.5	24	20	**100**
Electron mobility μ_n ($cm^2/V\,s$)	3900	1500	8500	400	1250	**4500**
Hole mobility μ_p ($cm^2/V\,s$)	1900	450	400	100	30	**3800**
Saturation electron drift velocity V_{sat} ($\times 10^7$ cm/s)	1	1	2	2	2.5	**2.7**
Thermal conductivity (W/cm K)	0.6	1.5	0.55	5	1.3	**22**
Melting point ($^\circ$C)	937	1414	1240	2100	2500	**3550**
Young's modulus E (GPa)	103	130	85.9	380	150	**1143**

Table 1.1. Basic properties of most common used semiconductor materials including diamond [2].

1.1.1. Historical review

Diamond is an allotrope of carbon that has been known as gemstone for several thousand years and was recognized by various cultures for its religious or industrial uses [3]. For most of that time it was only valued for its appearance and for its mechanical properties. The word "diamond" has its origin in the ancient Greek "adámas/αδάμας" meaning unbreakable. Besides the property of being the hardest known natural material diamond is mainly appreciated as a gemstone because of its optical properties: the high refractive index and large color a unique brilliance. With the rapid increase in the control of its synthesis, new possibilities have arisen to exploit its electrical and optical properties.

The formation of diamond by artificial means has been an on-going effort for much of the last 150 years. Many of the early attempts at diamond growth did not and still do not fall within the confines of scientific dogma with regard to high-pressure and temperature diamond synthesis; however, some of those early efforts are remarkably similar to those used today to make diamond at low pressures. Empirical observation had shown that natural diamond found in its native kimberlite was probably made deep in the earth and the carbon that diamond was made from was under a very high temperature and a large pressure at the time of formation. It was believed that diamonds could be made synthetically if the very high pressures deep in the earth could be replicated at a high temperature in the laboratory. P. W. Bridgeman worked for many years on the production of high pressures in the laboratory as well as on the high-pressure graphite-to-diamond transformation and could be considered the spiritual father of high-pressure and temperature synthesis of diamond.

Ever since the discovery that diamond was pure carbon in 1797 many attempts were made to convert inexpensive graphite into gemstones. In 1950s, both Allmänna Svenska Elektriska Aktiebolaget (ASEA) in Sweden and General Electric in the United States could produce diamond artificially via the high-pressure–high-temperature press method (HPHT) by developing a technique to raise the pressure in the reaction chamber to more than 8 GPa and the temperature to above 2000°C in order to reproduce the conditions under which natural diamond forms inside the Earth. (Without the use of suitable catalysts the conditions would have to be even more extreme.)

Diamond films were first grown by chemical vapor deposition CVD (low-pressure diamond synthesis) in the mid-1950s by two groups concurrently, Boris Derjaguin and Dimitri V. Fedoseev at Institute of Physical Chemistry of The Academy of Science of the U.S.S.R in Moscow, and William G. Eversole and coworkers of Union Carbide. Both groups used a two-step process of deposition and then etching the graphite. The Japanese have also been working in the area of carbon film deposition, diamond-like carbon, and diamond since the 1960s. They found that an abundance of hydrogen appeared to etch the graphite and allow diamond growth. The Japanese were also the first to explore diamond film deposition with microwave

plasmas, radio frequency plasmas, combustion torches, and hot filaments. In 1980s many more scientists became involved in diamond film growth research primarily in the Soviet Union, Japan, and U.S [4].

Research areas in diamond film growth include mechanistic studies, nucleation studies, morphology studies, diamond-like films, coating applications, device applications heat sink applications, and surface science studies.

1.1.2. Common allotropes of carbon

Carbon is the lightest Group IV element in the periodic table having six electrons in ground-state configuration of $1s^2\ 2s^2\ 2p^2$, with two core electrons and four valence electrons split equally between *s* and *p* orbitals.. Unlike most elements, carbon has several material forms which are known as polymorphs (or allotropes). They are composed entirely of carbon but have different physical structures and, uniquely to carbon, have different names: graphite, diamond, amorphous carbon, graphene, fullerene (e.g. buckyballs, nanotubes, nanowires), lonsdaleite (hexagonal crystal lattice), and others [5].

The properties of the various carbon allotropes can vary widely. For instance, diamond is by far the hardest-known material, while graphite can be one of the softest. Diamond is transparent to the visible spectrum, while graphite is opaque; diamond is an electrical insulator while graphite is a conductor, and the fullerenes are different from either one. Yet these materials are made of the same carbon atoms; the disparity is the result of different arrangements of their atomic structure.

Pure carbon naturally forms two different crystalline materials: diamond, in which all bonds between carbon atoms are the same, and graphite, with two different types of bonds between the atoms. Because diamond is the higher energy form of the two, its natural occurrence is rare compared with that of graphite. In contrast, the lowest energy form of related elements such as silicon (Si) and germanium (Ge) has the same crystal structure as diamond, but no naturally occurring form like graphite [6].

Graphite is the most common form of pure carbon on Earth and in contrast to diamond, each carbon shares one electron with two of its neighbors, and two electrons with the third neighbor. The atoms all bond in planes (two-dimensional hexagonal lattice) which are stacked on top of each other resulting in quite weak forces between different planes. Graphite is therefore a rather soft material and varies also considerably in other physical properties from diamond (Figure 1.1 (a)).

In the case of diamond, *s*- and *p*-states hybridise and form the extremely strong tetrahedral sp^3-bonds. Together with the special three-dimensional arrangement of the atoms in the lattice, the so-called diamond structure, they make diamond so exceptionally hard and also lead to other amazing intrinsic properties such as a high refractive index, extremely high thermal conductivity, and a high melting point (Figure 1.1 (b)).

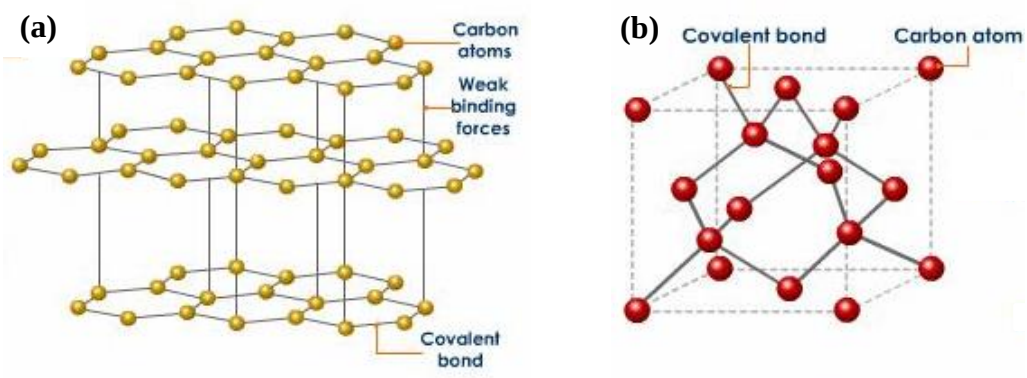

Figure 1.1. Diamond and graphite are two allotropes of carbon: pure forms of the same element that differ in structure **(a)** graphite structure CVD, and **(b)** diamond structure.

A material suitable for an electronic device must not conduct electrical current in its pure state at room temperature. However, it should be possible to tune its conductivity in a controllable manner by introducing trace amounts of impurity atoms (dopants). Such materials are termed "semiconductors." Graphitic carbon conducts electricity at room temperature. In contrast, diamond is a semiconductor with physical properties (such as maximum electric field, saturation velocity, thermal conductivity and band-gap) that make it the ideal material for electronic devices [7,8].

1.1.3. Natural diamond

Diamond can form naturally at depths greater than 150 km in the upper mantle of the Earth [9]. Under conditions of extreme pressure and temperature it is the most stable form of carbon. Over a period of millions of years carbonaceous deposits slowly crystallise into single crystal diamond gemstones. Together with magma the crystals are then brought up to the Earth's crust by kimberlite or lamproite volcanic eruptions. Since this transfer happens within just a few hours the conversion to graphite does not occur and it is possible to mine diamond in the volcanic pipes which contain material that was transported toward the surface by volcanic action, but was not ejected before the volcanic activity ceased. Natural diamond generally contains a significant degree of impurities such as nitrogen or boron.

Natural diamonds have too many defects and impurities for use as semiconductors, regardless of the cost associated with their rarity. Only manufactured semiconductor materials are of the appropriate quality for electronics. Crystalline Si wafers used for electronics have impurity and crystalline defect densities that are lower than the atomic density by a factor of 10^{-11} to 10^{-12}. Electronic-grade Si is the purest bulk material known.

1.1.4. Synthetic diamond

The development of the synthetic processes is a result of the extensive research during the 1940's. Diamond synthesis can be achieved through several routes. The two main methods are high-pressure high-temperature synthesis (HPHT) and chemical vapor deposition (CVD).

HPHT diamond

The first artificial synthesis of diamond was reported in 1955 [10,11] by the *High Pressure High Temperature* (HPHT) method in which the synthesis of diamond essentially duplicates the natural process by converting graphite into diamond under conditions at which diamond is the thermodynamically favored phase. It was achieved by subjecting graphite to high pressure (above 10 GPa) and

high temperature (above 2000° C) in the presence of a transition-metal catalyst. Those metals acted as a solvent-catalyst, which both dissolved carbon and accelerated its conversion into diamond, as shown schematically in Figure 1.2.

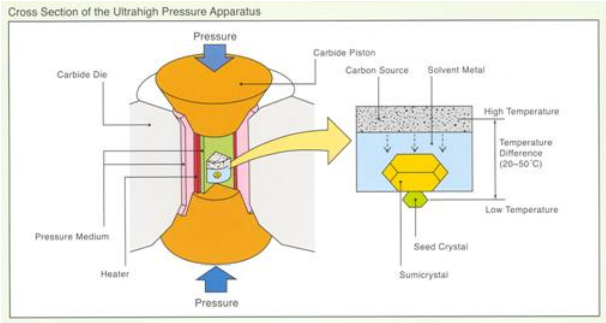

Figure 1.2. Schematic setup of a "Belt" apparatus for the production of HPHT diamonds.

The HPHT disadvantage is that the maximum obtainable crystal size is limited to few millimeters and the diamond crystals contain always impurities from the growth environment. This type of diamond is too expensive and the small area and the nitrogen impurities become it no important for electronic applications. Diamond produced from this method is used as grit in mechanical applications such as polishing, cutting, drilling, thermal management, etc. These applications exploit the extremely high hardness and chemical inertness of diamond. Research in the HPHT synthesis of diamond is still underway in an effort to lower production costs and produce even larger crystals. The difficulties in the direct conversion of graphite to diamond have triggered the development of alternative processes to lower the temperature and pressure.

CVD diamond

Chemical vapor deposition (CVD) offers a process for producing high–crystalline quality diamond under tightly controlled conditions, and was first applied in the 1980s [12,13]. This method involves a gas-phase chemical reaction occurring above a solid surface causing deposition onto that surface. Working at low pressure and high temperature, where carbon is in a metastable regime both diamond and graphite may be produced. Growth conditions can be carefully tuned to reduce graphite formation and favor diamond growth.

A large variety of carbon-containing gas species have been employed to synthesize diamond by CVD. These include methane, aliphatic and aromatic hydrocarbons, alcohols, ketones, amines, ethers and carbon monoxide with methane being the most frequently used reagent. In addition to these carbon carriers, the gas phase usually must contain powerful both non-diamond carbon etchants and surface site preparation species such as hydrogen, oxygen or fluorine atoms.

It has been observed that a necessary condition for diamond growth to occur is the presence of a gas-phase non-equilibrium in the region adjacent to the deposition substrate. The gas-phase non-equilibrium is generated through gas-phase activation achieved typically using one of the three basic methods (Figure 1.3):

. external heating as in hot-filament CVD ;

. plasma activation as in plasma assisted CVD ;

. a combination of thermal and chemical activation as in flame CVD .

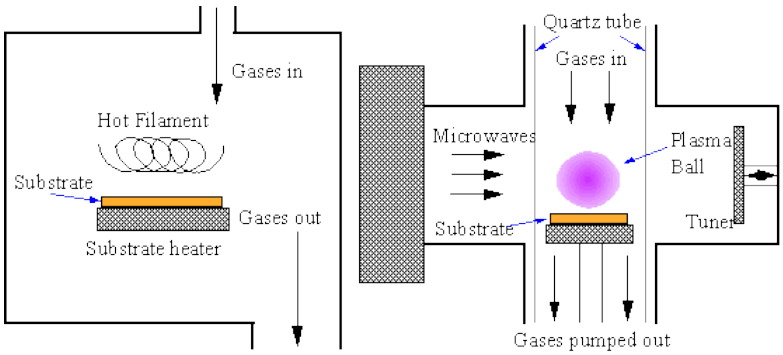

Figure 1.3. Schematic setup of a system of **(a)** Hot filament CVD, and **(b)** Microwave plasma CVD diamond.

While each method differs in detail, they all share features in common. For example, growth of diamond normally requires the substrate to be maintained at a temperature in the range 1000 - 1400 K, and the precursor gas be diluted in an excess of hydrogen. Carbon containing gas and molecular hydrogen are dissociated by the activation energy, forming carbon radicals and atomic hydrogen, which drift toward the substrate by a gradient in temperature and concentration (Figure 1.4). The diamond growth is based on the gas phase chemical reactions which happening

on the substrate surface involving carbon atoms deposited either in the form of diamond and graphite. Diamond growth takes place due to the different reaction rate between hydrogen-graphite and hydrogen-diamond; in optimized conditions atomic hydrogen removes graphite much faster than diamond, therefore leading to diamond growth. Roughly, the reactant gases form C_xH_y radicals and atomic hydrogen at the substrate surface these compounds undergo a series of reactions leading to sp^2 (graphite) and sp^3 -carbon (diamond). The sp^2 bonds are removed by atomic hydrogen, which additionally terminates and stabilizes the sp^3 bonds. The chemical reactions occurring in the gas phase are complex and a comprehensive understanding of the growth mechanism is still needed.

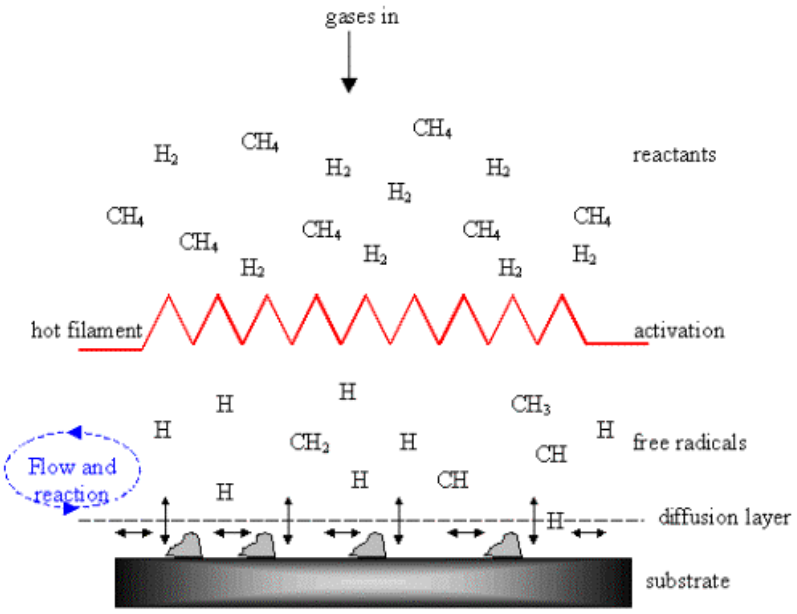

Figure 1.4. Schematic CVD diamond process; the main chemical species are shown.

The H atoms are believed to play a number of crucial roles in the CVD process [14]:

- they undergo H abstraction reactions with stable gas-phase hydrocarbon molecules, producing highly reactive carbon-containing radical species. This is important, since stable hydrocarbon molecules do not react to cause diamond growth. The reactive radicals, especially methyl (CH_3) can diffuse to the substrate surface and react, forming the C-C bond necessary to propagate the diamond lattice;

- H-atoms terminated the dangling carbon bonds on the growing diamond surface and prevent them from cross-linking, thereby reconstructing to a graphite-like surface;
- atomic hydrogen etches both diamond and graphite. As observed, under typical CVD conditions, the rate of diamond growth exceeds its etch rate. This is believed to be the basis for the preferential deposition of diamond rather graphite.

In contrast to HPHT diamond, it is possible to grow CVD diamond under conditions of high purity resulting in fewer defects and impurities. However, plasma-deposited diamond is not a single crystal. It is made up of many individual crystal grains of 1 to 10 μm in diameter that are oriented differently. Plasma-deposited diamond is polycrystalline when grown on a high-purity noncarbon substrate material, usually a Si wafer. Some success was achieved in growing diamond grains with the same crystal orientation on a different substrate (β-SiC), and the resulting films showed promising electronic properties [15]. But β-SiC is also difficult to synthesize, and general progress was impaired by not having available diamond of the required quality. Over the past 2 years there have been renewed grounds for cautious optimism.

High-quality HPHT diamonds in polished form with dimensions of many millimeters have become available, forming suitable substrates on which ultrapure diamond can be grown with a hydrocarbon plasma source [16]. The fusion of the two methods for synthesizing diamond artificially has led to the demonstration of single-crystal diamond layers that approach the quality required for electronic devices [17-19]. Importantly, it has also been possible to control the conductivity of diamond layers by incorporating boron during plasma growth. Therefore, two of the key elements required from a semiconductor material suitable for electronic devices—a high-quality crystal that can be doped—are now achievable in diamond.

In CVD diamond, the (111) octahedral faces are observed at low temperatures and low hydrocarbon concentrations; the (100) cubic faces predominate at high temperatures and high hydrocarbon concentrations. The CVD diamond faces are discussed in more detail in Section 2.1.

1.1.5. Doping diamond

Synthetic and natural diamonds are classified into types according to the amount of certain impurities present within their structure. These can include vacancies and impurity atoms, either interstitial or substitutional. Vacancies occur where a position within the carbon lattice is empty, generally introduced by radiation damage expelling carbon atoms from the structure. Substitutional impurities occur when a carbon atom is replaced by an atom of an element other than carbon, sitting in the same position in the lattice as the atom it replaced. An interstitial impurity, on the other hand, is a foreign atom sitting inside the diamond structure but not sitting at a host lattice site.

As mentioned previously, diamond has a very low concentration of intrinsic charge carriers at temperatures below 1000° C. If a significant room temperature conductivity is desired it is necessary to dope diamond. When a semiconductor is doped with impurity atoms, it becomes extrinsic and impurity energy levels are introduced [20]. Diamond excellent physical properties for electronic applications have led to a concerted effort to model and grow dopants into the diamond lattice in an attempt to create both n-type and p-type diamond for use in a wide variety of devices, especially high power applications not possible using traditional silicon semiconductors due to the higher thermal conductivity of diamond.

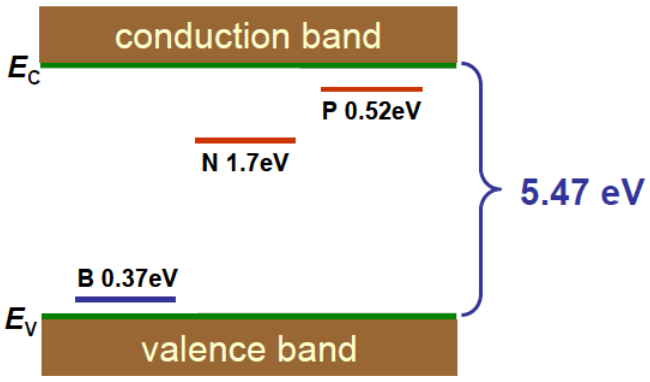

Figure 1.5. Activation energies for some impurities in diamond.

Unfortunately, there are no shallow dopants known for diamond. As shown in Figure 1.5 both for p-type dopant boron (B) and for n-type dopants phosphorus (P) and nitrogen (N) the dopant levels are rather deep and result in low thermal excitation of free charge carriers at room temperature (E_{th} = 1/ 40 eV).

Boron is a substitutional impurity, and due to having one less electron than carbon, it acts as an acceptor and readily accepts electrons thermally excited from the valence band or from donor impurities, as shown in Figure 1.6. Only a very low energy is required for electrons to leave the valence band and substitutional boron induces red light absorption, and so holes are formed in boron doped diamond at room temperature, giving p-type semiconductivity. The activation energy of the boron acceptor is 0.37 eV [21,22]. Although this is quite a shallow acceptor, the activation energy is still quite large compared to k_BT at room temperature and due to this fairly low activation of acceptor sites, high concentrations of boron are required to get good electrical conductivity [23].

Since natural doped diamond (type IIb) is extremely rare and diamond doping through diffusion is not achievable, the first intentional doping of (natural) diamond was done by ion implantation at end of the 1960s [24]. However, with this technique a considerably amount of damage is done to the crystal lattice which cannot be reversed by any annealing.

With the advent of the diamond CVD process in the 1980s it became possible to add the dopants to the gas phase during growth and only a few years later several groups demonstrated p-type boron doping of the diamond films from the gas phase [25–27]. This type of doping can, e.g., be achieved by a diborane B_2H_6 addition to the $H_2/CH_4/Ar$ source gas mixture [28]. This leads to a very homogenous distribution in the bulk and allows rather sharp interfaces (< 1μm) by quickly changing the gas-phase boron concentration during the growth process. Boron uptake is substantially higher in (111) growth sectors compared with (100) growth sectors [29]. Superconductivity has been investigated on super heavily boron doped diamond films [30,31].

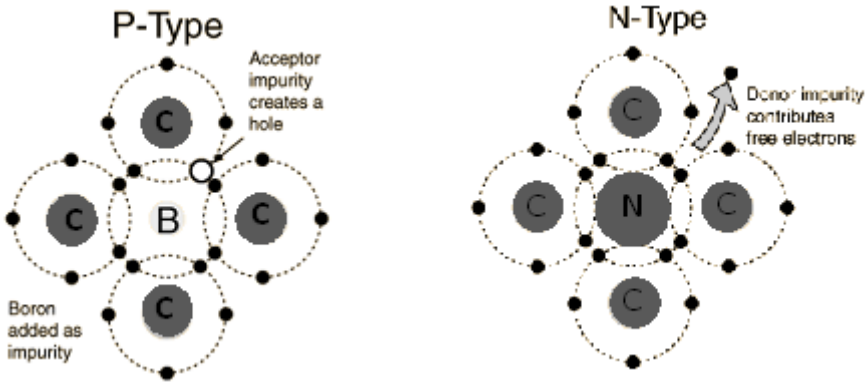

Figure 1.6. P-type doping with boron and n-type doping with nitrogen in diamond

On the other hand, there are many potential n-type dopants in diamond but successful doping to semiconductor device standards has not been as successful as boron has been for p-type material [32]. However, it is also desirable to have efficient n-type diamond doping for electronic applications such as cold cathode electron emitters, UV photodetection and UV light emission diodes.

Nitrogen is the most easily incorporated and is found in most natural diamonds in some quantity, as well as in HPHT and CVD films where nitrogen is present in the gas phase. The next element in the periodic table to carbon, nitrogen incorporates substitutionally into diamond [32]. Although the extra electron in the nitrogen atom compared to carbon forms some n-type behavior (Figure 1.6), the donor level of nitrogen is deep in the band gap, at around 1.7 eV, due to the distortion of the nitrogen atom in the $(\bar{1}\bar{1}\bar{1})$ direction and the preferential formation of the nitrogen's lone pair and dangling bond on one of its four carbon neighbours. This distortion means the unpaired electron is localized closer to the carbon atom in the (111) direction than the nitrogen donor and so is not free to easily conduct [33]. This is sufficient for some interesting luminescence properties and the nitrogen vacancy center is of interest for quantum computing. For electronic applications however the deep donor level provides only low mobilities and for many electronic properties a donor level closer to the conduction band minimum is desired.

Other theoretical n-type dopants include phosphorus, sodium, sulphur, potassium and lithium. Substitutional phosphorus doping of CVD diamond has been reported by a number of groups. The first success to form n-type diamond thin films

by phosphorus doping with PH_3, CH_4, and H_2 gas mixtures during the growth was reported in 1997 [34] and four years later a UV light emission diode with a pn-junction was demonstrated [35]. The breakthrough that made phosphorus doping possible was using epitaxial growth from a (111) oriented HPHT diamond substrate, rather than growing from a (100) oriented substrate. This is due to the stresses caused by the phosphorus inclusion having less of an effect on the higher quality (111) layer [35].

Hall effect studies [36] on phosphorus doped diamond layers show that there is n-type semiconductivity with carrier mobilities above 600 $cm^2V^{-1}s^{-1}$ but the activation energy of the P donor of around 0.6 eV59 is too high for many electrons to occupy states in the conduction band at room temperature, and the resistivity of such films remain high. Mobilities in polycrystalline material is lower than that of epitaxial grown (111) layers.

There are different approaches of how to circumvent the problem of low thermal excitation of free charge carriers for doped diamond at room temperature. One idea is to use two different layers. One layer it very highly doped and thus has a low mobility but a high number of free charge carriers which diffuse into the second (intrinsic) layer. This combines a high number of carriers with the excellent mobility in the intrinsic layer leading to the desired properties. This is called a pulse- or δ-doped structure.

1.2. Diamond structure

Diamond is the four-fold coordinated structure of pure carbon, with four sp^3 hybrid orbitals in a tetrahedral configuration. Carbon atoms in the diamond structure form σ covalent bonds with four neighbouring carbon atoms, as shown in Figure 1.7. The diamond structure is also observed in crystalline silicon and various compound semiconductors. When the structure contains equal amounts of two different elements rather than one element alone it is called the zincblende structure. The stability of the structure yields excellent structural, thermal and electronic behavior.

The crystal structure of diamond is a face-centred cubic (FCC) lattice with a basis of two atoms per lattice point located at (0, 0, 0) and (1/4, 1/4, 1/4) along the unit cell. The conventional unit cell of diamond has a unit cell length a_0 of 3.57 Å at room temperature [37].

In the lattice structure, each carbon atom is tetrahedrally coordinated forming strong bonds to its four neighbors using hybrid sp^3 atomic orbitals, with equal angles of 109 ° to each other, as illustrated on Figure 1.7. The covalent σ bonding between carbon atoms is characterized by a small bond length of 1.545 Å and a high bond energy of 711 $KJmol^{-1}$ [38]. The atomic density is 1.76 $\times 10^{23}$ $atoms/cm^3$, while the diamond's density is 3.52 gcm^{-3}, as shown in Table 1.2. The structure of diamond characterized by a high molar density coupled to the very strong chemical bonding, leads to the aforementioned unique mechanical and elastic properties.

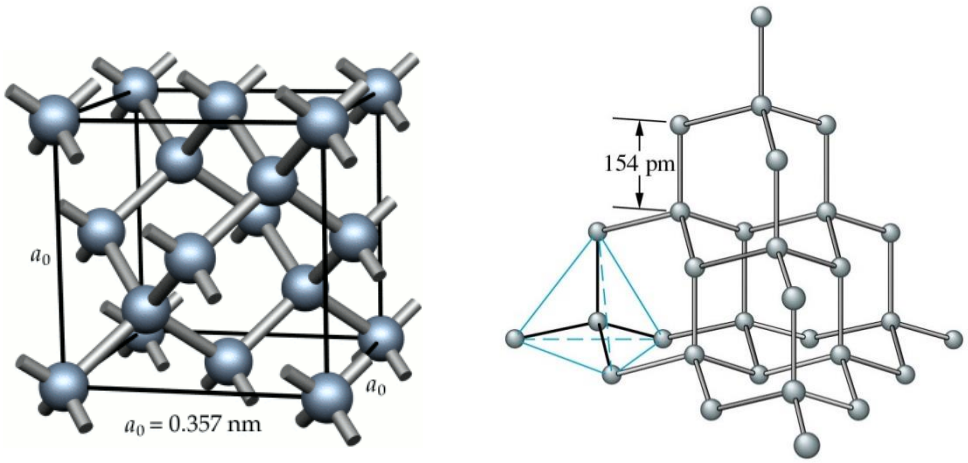

Figure 1.7. Crystal structure of diamond; each carbon atom is tetrahedrally coordinated forming strong bonds to its four neighbors.

1.3. Diamond properties and applications

Recently diamond has attracted attention of many research groups because, compared to other materials, provides an impressive combination of chemical, physical and mechanical properties suitable for several applications.

Table 1.2 lists some of the more notable physical and electronic properties of diamond. The small size of the carbon atom leads to its short bond lengths and

results in low compressibility, resulting in diamond being one of the hardest known materials.

Property	Diamond
Lattice constant (nm)	0.36
Mechanical Hardness (g/mm^2)	5700 - 10400
Bandgap (eV)	5.45
Type	indirect
Work function (eV)	4.81
Electrical resistivity (-/cm)	$> 10^{11}$
Optical transmission	$220\ nm \leq \lambda \geq 2500\ nm$ and $\lambda \geq 6000\ nm$
Biocompatibility	Yes

Table 1.2. Diamond bulk properties [39].

Diamond has a number of other exceptional properties. Phonons are conducted very efficiently through its covalent lattice structure, resulting in diamond possessing the highest room temperature thermal conductivity of any conventional solid, with a thermal conductivity at 300 K of 900 – 2300 $W\ m^{-1}K^{-1}$. Copper by comparison has a thermal conductivity of 400 $W\ m^{-1}K^{-1}$.

The shortness of the carbon bond also leads to a large overlap of the electron orbitals of adjacent carbon atoms and a large separation between the energy of the occupied sp3 bonding orbitals that form the valence band compared to the unoccupied states in the conduction band formed by antibonding orbitals. The result is carbon's very large indirect band gap of 5.47 eV at 300 K, compared to just 1.12 eV for silicon. This allows the doping of a number of different elements within the diamond lattice in order to change the electronic properties of the material. The wide bandgap results also in high transparency in a wide wavelength range, due to the optical transition between free electrons and holes being forbidden. Diamond shows high transmittance from the near ultra-violet (UV) to the far infra-red (IR) region.

In addition to the properties listed in Table 1.1 and 1.2, diamond is chemically and biologically inert and very resistant to radiation damage, which makes it useful for a number of electrochemical devices and also as walls and coatings in fusion systems and high energy particle physics. Also, it exhibits an exceptional wear resistance and a low coefficient of friction.

Turning to electronic properties, as observed diamond is a wide indirect-gap semiconductor. When not doped with impurities it is therefore a highly insulating material showing resistivity up to 10^{15} Ωcm. Diamond possess also a high breakdown electric field of 10 MV/cm, high carrier mobility of 4500 cm^2/Vs and 3800 cm^2/Vs (for electrons and for holes respectively) and low dielectric constant of 5.7. This makes diamond is useful in high power electronics and optoelectronic applications [40-43].

Because of all these outstanding properties, diamond already finds use in many diverse applications besides its appreciation as a gemstone. The most common are:

– Mechanical applications: abrasive and wear-resistant coatings for cutting tools such as drills, saws, knives, glass cutting and wire dies

– Optical applications: lenses, windows for high power lasers and diffractive optical elements

– Thermal applications: heat sinks for power transistors and semiconductor laser arrays

– Detector applications: “solar blind” photodetectors, radiation hard and/or chemically inert detectors, and electrochemical/biochemical sensors

Obviously, given its many unique properties it is possible to imagine numerous other potential applications for diamond as an engineering material, but progress in implementing many such ideas has been constricted by the comparative shortage of (natural) diamond. Most of the electrical applications of diamond are just at the infancy because only since the last couple of years electronic grade SC-CVD diamond became available for device design and development [2].

1.4. Aim of the work

As part of the effort to control the growth of diamond films by chemical vapor deposition, we are studying the adsorption behavior of some foreign atoms on diamond (111) surface. Adsorption of foreign atoms on a surface can play an important role in thin-film growth by affecting for instance; adatom adsorption, nucleation and migration on surfaces. Most common species that terminate diamond surfaces are hydrogen, oxygen and hydroxyl termination. The type of termination can significantly modify physical and chemical properties of diamond surface and thus modify the performance of diamond-based devices. Effects of hydrogen and oxygen to modify diamond surface properties are very attractive for use in electronic applications. However, their behaviors on diamond surfaces seem not to be understood enough.

To understand the correlation between surface structure, electronic properties, and growth chemistry, it is important to investigate the reaction chemistry of hydrogen and oxygen with diamond surfaces. As we discussed in Section 1.2.4, hydrogen plays a critical role in diamond chemical vapor deposition (CVD). The nature of that role is thought to include the maintenance of an sp^3 - bonded surface, creation of surface radical sites by abstraction of adsorbed hydrogen, and preferential etching of graphite [14]. Therefore, characterization of hybrid structures on diamond (111) surfaces is therefore a necessary first step towards understanding the microscopic growth mechanisms.

Oxygen has also been reported to play a significant role in chemical vapor deposition (CVD) diamond synthesis, where it preferentially attacks the graphitic sp^2 bonds [44], and hence improves the diamond film quality as well as having an influence on its texture and morphology [45]. Since the C(111) surface is one of the growth planes in CVD diamond, establishing the stable oxygen configurations would be an important step towards the understanding of their specific role in diamond synthesis, and in other applications too.

Also, we have studied the stepped diamond (111) surface to clarify the effect of the step on adsorption and diffusion of adatoms. Very little is known about the

actual chemistry of the diamond surface near a step. Understanding of the behavior of the steps would be important to determining their role in diamond growth.

This study considered first systematic comparison between neutral H, O atoms and OH group binding on the flat and on the stepped structures of diamond (111). The potential energies for H/O/OH on a flat and stepped diamond (111)-(1×1) surfaces are investigated theoretically by a molecular orbital method based on the density functional theory (DFT).

1.5. Outline of the dissertation

After this introductory chapter, chapter 2 gives the status of diamond faces (100), (110) and (111). Some terminations of diamond surface and their properties are discussed. The most common species that terminate diamond surfaces are hydrogen- (H) and oxygen-related species (e.g., O and OH groups). It has been shown that the type of termination can significantly modify its physical and chemical properties. Previous studies on H-, O- and OH- terminated surfaces are briefly reviewed.

In chapter 3, the theoretical background of this work is explained. The calculations are performed under the quantum chemistry framework. Computational simulations of hydrogen, oxygen and hydroxyl on the surface of diamond were calculated using the density functional theory (DFT) by ORCA program.

Chapter 4 shows the computational details of studying diamond 111 surfaces. Two surface models have been modeled to simulate diamond (111)-(1×1) flat and stepped surfaces. Functions and basis sets employed for the calculations are outlined in this chapter.

Calculation results are introduced in chapters 5, 6 and 7 for flat surface, stepped surface and relaxed stepped surface, respectively. The results of each surface are discussed in the presence of hydrogen adatom, oxygen adatom and hydroxyl group. Finally, concluding remarks are summarized in chapter 8.

References

[1] S. Balmer, I. Friel, S. M. Woollard, C. J. H. Wort, G. A. Scarsbrook, S. E. Coe, H. ElHaji, A. Kaiser, A. Denisenko, E. Kohn, and J. Isberg, Phil. Trans. R. Soc. 366, 251 (2008).

[2] J. Isberg, J. Hammersberg, E. Johansson, T. Wikström, D. J. Twitchen, A. J. Whitehead, S. E. Coe, and G. A. Scarsbrook : Science 297, 1670 (2002).

[3] J. W. Hershey, *Book of diamonds* (Hearthside Press, New York, 1940).

[4] A. W. Phelps, "*Diamond films*," Chapter 42, *Handbook of Materials Selection*, M. Kutz, ed., Wiley, New York, 2002, p. 1287.

[5] Hugh O. Pierson, *Handbook of Carbon, Graphite, Diamonds and Fullerenes: Processing, Properties and Applications*, NOYES PUBLICATIONS, Park Ridge, New Jersey, U.S.A, 1994, P. 43.

[6] G. A. J. Amaratunga, Science 297, 1657 (2002).

[7] M. W. Geis, N. N. Efremow, D. D. Rathman , J. Vac. Sci . A6 , 1953 (1988).

[8] K. Shenai, R. S. Scott, B. J. Baliga: IEEE Trans. Electron. Devices 36, 1811 (1989).

[9] M. B. Kirkley, J. J. Gurney, and A. A. Levinson, Age, origin, and emplacement of diamonds: Scientific advances in the last decade, Gems & Gemology 27 (1), 2 (1991).

[10] H. Liander, *Artificial Diamonds*, ASEA Journal, 28, 97 (1955).

[11] F. P. Bundy, H. T. Hall, H. M. Strong, and Jr. R. H. Wentorf, Man Made Diamonds, Nature, 176, 51 (1955).

[12] S. Matsumoto, Y. Sato, M. Tsutsumi, and N. Setaka, Journal of Materials Science, 17, 3106 (1982).

[13] F. G. Celii and J. E. Bultler, Diamond Chemical Vapor-Deposition, Annual Review of Physical Chemistry, 42, 643 (1991).

[14] H. Umemoto, Chem. Vap. Deposition, 16, 275 (2010).

[15] H. Kawarada et al., Appl. Phys. Lett. 72, 1878 (1998).

[16] H. Okushi, Diamond Relat. Mater. 10, 281 (2001).

[17] B. A. Fox et al., Diamond Relat. Mater. 4, 622 (1995).

[18] A.V.Vescan, P. Gluche,W. Ebert, E. Kohn, IEEE Electron Device Lett. 18, 222 (1997).

[19] H. Taniuchi et al., IEEE Electron Device Lett. 22, 390 (2001).

[20] S. M. Sze, *Semiconductor devices - Physics and Technology* (John Wiley & Sons, Inc., New York, 2002), 2nd edn.

[21] A. Collins, and E. Lightowlers, Physical Review 171, 843 (1968).

[22] A. Collins, and Williams, A. J. Phys. Part C Solid State Phys. 4, 1789 (1971).

[23] G. Scarsbrook, P. Martineau, D. Twitchen, A. Whitehead, M. A. Cooper, and Dorn, B. Patent WO 03052174A2 (2003).

[24] V. S. Vavilov, M. I. Guseva, E. A. Konorova, V. V. Krasnopevtsev, V. F. Sergienko, and V. V. Tutov, Soviet Physics - Solid State 8, 1560 (1966).

[25] N. Fujimori, T. Imai, and A. Doi, Vacuum 36 (1), 99 (1986).

[26] K. Okano, H. Naruki, Y. Akiba, T. Kurosu, M. Iida, and Y. Hirose, Japanese Journal of Applied Physics 27 , L173 (1988).

[27] J. Mort, D. Kuhman, M. Machonkin, M. Morgan, F. Jansen, K. Okumura, Y. M. LeGrice, and R. J. Nemanich, Applied Physics Letters 55, 1121 (1989).

[28] D. J. Twitchen, A. J. Whitehead, S. E. Coe, J. Isberg, J. Hammersberg, T. Wik- strom, and E. Johansson, IEEE Transactions on Electronic Devices 51, 826 (2004).

[29] Ushizawa, K., Watanabe, K., Ando, T., Sakaguchi, I., Nishitani-Gamo, M., Sato, Y., and Kanda, H. Diamond and Related Materials 7, 1719 (1998).

[30] E. Bustarret, J. Kacmarcik, C. Marcenat, E. Gheeraert, C. Cytermann, J. Marcus, and T. Klein, Phys. Rev. Lett. 93, 237005 (2004).

[31] E. Ekimov, V. Sidorov, E. Bauer, N. Mel'nik, N. Curro, J. Thompson, and S. Stishov, Nature 428, 542 (2004).

[32] G. Popovici and M. Prelas, Diamond Relat. Mater. 4, 1305 (1995).

[33] S. Kajihara, A. Antonelli, J. Bernholc, and R. Car, Physical Rev. Lett. 66, 15, (1991).

[34] S. Koizumi, M. Kamo, Y. Sato, H. Ozaki, and T. Inuzuka, Applied Physics Letters 71, 1065 (1997).

[35] S. Koizumi, K. Watanabe, M. Hasegawa, and H. Kanda, Science 292, 1899 (2001).

[36] M. Katagiri, J. S. K. Isoya, and H. Kanda, Appl. Phys. Lett. 85, 6365 (2004).

[37] W. Kaiser and W. L. Bond. Phys. Rev., 115, 857 (1959).

[38] C. Kittel. *Introduction to solid state physics*. Wiley, 1971.

[39] P. W. May, *CVD Diamond - a new Technology for the future?*, Endeavour Magazine 19 , 101 (1995).

[40] T. Sakai, K. S. Song, H. Kanazawa, Y. Nakamura, H. Umezawa, M. Tachiki, and H. Kawarada. *Diam. Relat. Mater.*, 12, 1971 (2003).

[41] T. Kondo, K. Honda, Y. Einaga, D. A. Tryk, and A. Fujishima. Diam. Electrochem., 149, E179 (2002).

[42] G.M. Swain. Semicond. Semimet., 77, 121 (2004).

[43] S. H. P. Serrano, R. C. Mendes de Barros, J. M. S. da Silva, and P. Favero. Reisdorfer. Electroanalyt. Asp. Biol. Signif. Comp., 51, (2006).

[44] K. P. Loh, X. N. Xie, S. W. Wang and J. C. Zheng, J. Phys. Chem. B 106, 5230 (2002).

[45] K. Bobrov, H. Shechter, A. Hoffman and M. Folman, Appl. Surf. Sci. 196, 173 (2002).

CHAPTER 2

CHAPTER 2

Diamond Surfaces

The first few atom layers that constitute a surface are crucial to the behavior and properties of surfaces. These are the atoms that interact with the environment, participate in surface modifications and bond with other materials to form interfaces. These atoms exist in states where they possess surface free energy, a property that makes them susceptible to foreign atom contamination and one that cannot therefore be sustained in the presence of foreign atoms. Foreign atoms may be introduced on surfaces either through alien sources or intentionally.

Diamond exhibits a number of unusual and very useful surface properties depending on the surface dangling bonds saturation by hydrogen or oxygen atoms. The most important crystallographic orientations are (100) and (111) which can be selectively grown by CVD when process parameters are thinly controlled. The crystallographic orientation (110) being is unstable under CVD growth and gas phase etching processes is less frequent [1]. Also, the (111) and (100) surfaces are commonly used as starting materials for homoepitaxial diamond film growth in (CVD).

2.1. The main surfaces of diamond

Under normal growth conditions, the surface of a diamond crystal will become dominated by three principle planes - the (100) plane, the (111) plane and the (110) plane.

Figure 2.1 shows the growth rate of the planes for homoepitaxial CVD diamond with different methane concentrations. The (100) and (111) planes are the slowest to grow [2] so are the most likely to remain, whilst other faster growth planes grow quickly out of a crystal. The (111) plane is the natural cleavage plane for a break in a diamond crystal, which is an additional reason for its predominance.

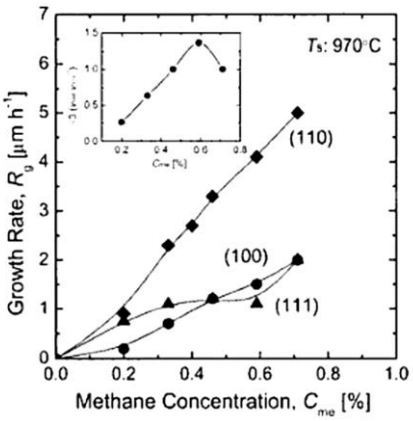

Figure 2.1. Graph showing the growth rate of homoepitaxial diamond films with methane concentration for different crystal orientations [2].

2.1.1. C(100) bare surface

In this case, bare (clean) means with no adsorbates on top of the surface. The clean C(100) surface has two dangling bonds per unterminated surface carbon atom, compared to one dangling bond for the (110) and (111) surfaces. To minimize the surface free energy, in the absence of any suitable terminating species the clean surface experiences a reconstruction where the surface carbon atoms dimerise to form a π-bonded surface structure, which gives rise to a (2×1) symmetry as observed by low electron energy diffraction (LEED). By analogy to the well-studied Si(100) and Ge(100)surfaces, the C(100) surface after reconstruction to the (2×1) structure suggests the formation of dimer bonds between pairs of surface carbon atoms, as illustrated schematically in Figure 2.2 .

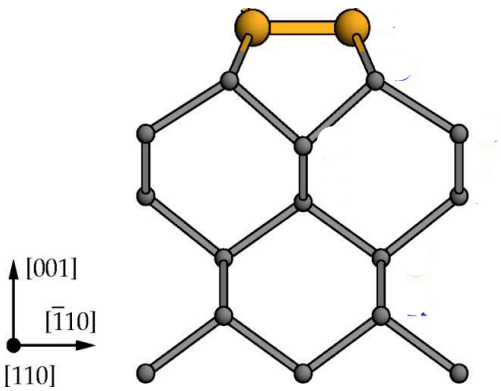

Figure 2.2. Structure of the diamond (100)-(2×1) (side view) [3].

2.1.2. C(110) bare surface

The (110) surface of diamond is less commonly found in CVD diamond, due to faster growth. The clean diamond C(110) surface has been reported to exhibit a (1×1) LEED pattern [4–7] , and even after annealing to 1300 K no reconstruction is observed, unlike the C(100) and C(111) surfaces [8]. However, there has been considerable difficulty in obtaining a high quality (110) surface [9]. The (110) surface is formed by layers of zigzag chains similar to the (2×1) reconstruction on diamond, but the staggered stacking is present throughout the bulk. The C−C bond length of the surface carbon layer is about 1.44 Å, similar to that of graphite. The C(110) − (1×1) surface is displayed in Figure 2.3.

Although the zigzag surface chains are similar in geometry to those of the Pandey chain on the C(111)−(2×1) surface, the zigzag chains on the (110) surface are buckled and tilted out of the surface plane.

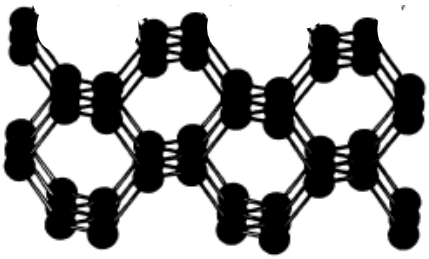

Figure 2.3. Diamond (110)-(1×1) surface (side view) [10].

2.1.3. C(111) bare surface

The (111) surface of diamond is of particular interest because it is the natural cleaving plane of diamond and the formation of atomically flat surfaces has been realized by utilizing a lateral growth mode on the (111) face [11]. C(111) shows one dangling bond per surface atom in its bulk terminated form. The unreconstructed C(111) surface has a (1×1) configuration, but due to the dangling orbitals of the

surface carbons the (1×1) construction is not stable and the lowest energy clean surface is the Pandey chain C(111)−(2×1) reconstruction [12].

In the chain model the surface dimerizes so that the dangling orbitals are closer to their nearest neighbors and so have a stronger interaction, leading to π-bonds in the first upper two layers of the surface. The uppermost C atoms form zigzag chains that run in parallel across the surface. Reconstruction from the ideal (111)−(1×1) bulk terminated structure to the (111)−(2×1) Pandey chain reconstruction has been observed at annealing temperatures above 1000°C [13,14]. The clean reconstructed C(111)−(2×1) Pandey chain surface is shown in Figure 2.4.

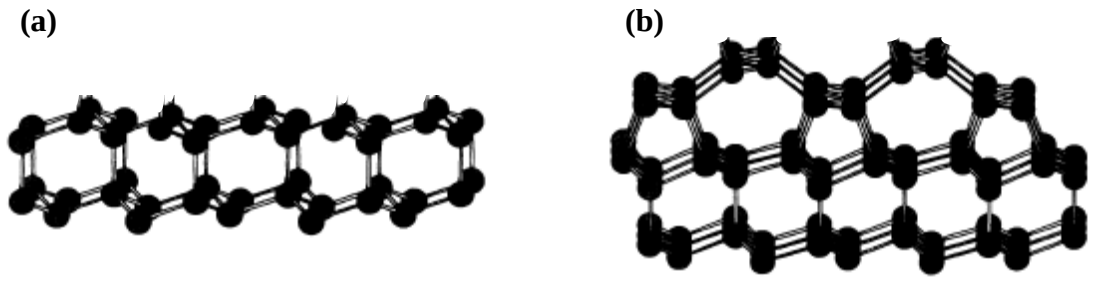

Figure 2.4. Side view of **(a)** the clean ideal (1×1), and **(b)** relaxed π reconstructed (2×1) C(111) surfaces [10].

2.2. Surface termination of diamond

2.2.1. Clean surface

As we mentioned in the previous section, the term clean (bare) surface means with no adsorbates on top of the surface. It refers to the diamond surface after the sample has been heated high enough so that all adsorbates have desorbed. This creates a large number of dangling bonds and surface stabilizes itself by reconstruction of the bonds of the upper atoms. In surfaces such as the Si(111)−(7×7) reconstructed surface, atoms several monolayers from the surface rearrange their position and bonding.

Clean (111) diamond surfaces are known to possess positive electron affinities [15, 16] due to the surface dipoles associated with the dangling bonds and this will be discussed later in Section 2.2.4.

2.2.2. Hydrogenated surface

Hydrogen termination on diamond has been increasingly studied over recent decades, in part because of its interesting properties and also due to its ease of preparation and ubiquity in the advent of chemical vapor deposition (CVD) processes. The adsorption of hydrogen on diamond surfaces, however, is still not clearly understood. All the as-grown CVD diamond films present a hydrogenated surface because hydrogen is usually introduced in the reactor at the end. The critical role played by hydrogen in diamond chemical vapor deposition (CVD) is well established [17] and discussed in Section 1.2.4. The nature of that role is thought to include the maintenance of an sp^3 -bonded surface, creation of surface radical sites by abstraction of adsorbed hydrogen, and preferential etching of graphite [8]. Therefore, characterization of hybrid structures on diamond (111) surfaces is therefore a necessary first step towards understanding the microscopic growth mechanisms.

Exposure to even a few minutes of hydrogen plasma replaces any existing termination with hydrogen on the majority of surface carbons and exposure to a hydrogen plasma has been shown to reproducibly induce a hydrogen termination on the C(100), C(111) and C(110) surfaces [18]. On the C(100) surface the monohydride surface has two hydrogen atoms per surface unit cell, whereas on the C(111) surface the adsorption of hydrogen breaks the (2 × 1) structure. Hydrogen termination of the (111) surface displays a monohydride surface where each dangling bond of (111)-(1×1) is terminated by one hydrogen atom, as pictured in Figure 2.5.

The principle advantage to hydrogen terminating a diamond surface is that it induces a negative electron affinity [4,19-22], which puts it at the forefront of field emission and thermionic devices using diamond, as well as for tuning the interfaces between diamond and other materials for microelectronics.

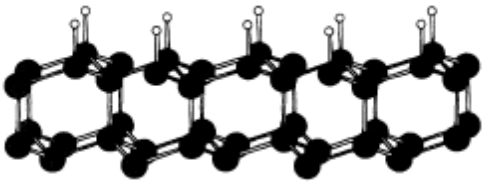

Figure 2.5. Hydrogenated ideal (1×1) diamond (111) surface (side view) [10].

In addition to the advantages to electron emission given by the negative electron affinity, under the presence of adsorbates on the surface, hydrogen terminated diamond displays a p-type conductivity layer from the surface to some 10 nm below the diamond surface [1,23]. This surface transfer doping behaviour is highly advantageous for devices such as field effect transistors. Also, adsorbed hydrogen atoms on diamond surfaces have also been known to make them hydrophobic [24].

2.2.3. Oxygenated surface

The behavior of hydrogen on diamond is perhaps best illuminated when compared with the oxygen-terminated surface. The study of the interaction of oxygen with diamond surfaces is also important from the perspective of understanding the effects of oxygen on the low-temperature growth of diamond [25,26] as well as controlling its surface electronic and chemical properties by varying the surface functional groups [27,28]. The addition of oxygen into the CVD plasmas has been found to lower the growth temperatures and enhance the crystalline quality of chemical vapor deposited diamond [25,26]. This may come about from the enhanced surface etching of non-diamond sp^2 phases by atomic O, or through the higher regeneration of surface radical sites by O ion abstraction of surface H during CVD, although the detailed mechanism is not understood. Establishing the stable oxygen configurations, their coverages and sites as the oxygen coverage increases progressively would be an important step towards the understanding of their specific role in diamond synthesis, and in other applications too.

The surface electronic properties of diamond may be tuned by creating spatially resolved domains of oxygen or hydrogen, which can produce opposing influences on its electron affinity and surface conductivity, the latter two properties being the most critical in the applications of diamond as electron emitters and transistors [27,28].

Oxygen has been reported to bond in several configurations with diamond carbon atoms. P. E. Perhsson *et al*. [29] reported observing carbonyl C–O (where the oxygens lie vertically above each surface carbon atom), bridge-bonded C–O–C (in which the oxygen atom is shared between two of the surface carbon atoms) and hydroxyl groups C–OH on diamond surfaces, as illustrated in Fig 2.6. It can created intentionally using a number of methods including washing in concentrated strong acids, exposure to an oxygen plasma and exposure to ozone (O_3) under an ultraviolet light.

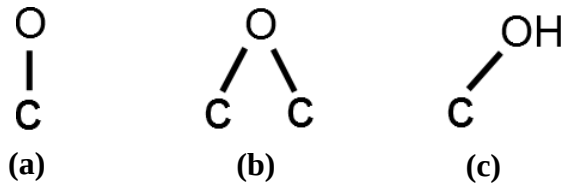

Figure 2.6. Schematic illustration of possible oxide species on diamond surface **(a)** carbonyl, **(b)** bridge-bonded, and **(c)** hydroxyl group.

Thoms et al. exposed the diamond (100) surfaces to molecular oxygen activated over a hot iridium filament and reported that atomic O could convert the reconstructed (2×1) surface into the (1×1) phase [30]. R. Klauser *et al.* applied a microwave plasma source to prepare an oxygenated diamond (111) surface [31]. They reported that the surface reconstruction on C(111)−(2×1) is not affected by O adsorption and that atomic H can replace the adsorbed O readily to convert the surface structure to (2×1), while atomic O cannot do the same to pre-adsorbed H. It is not known whether this result is specific to the C(111) surface, since both theoretical and experimental studies have shown that the adsorption of O proceed

more readily on the pre-hydrogenated H:C (100)−(2×1) than on the clean surface [32,33].

Loh *et al.* [34, 35] reported recently that oxygen chemisorption on the C(111) plane depends on coverage, and at low coverages (0.5 monolayers (ML)), epoxy-like (bridge) oxygen adsorbs, while at higher coverages, the carbonyl on-top chemisorption dominates. The results of Derry *et al.* [36] and Rebuli *et al.* [37], revealed that under ultrahigh vacuum (UHV) conditions the optimum oxygen coverage on the C(111) surface was 1⁄3 ML. Rebuli *et al.* [37] went further to show that oxygen adsorption on diamond surfaces depends on the vacuum level, and hence the environment under which the surfaces are prepared or exposed becomes an integral part of the observed coverage. While this possibility has not been explored fully starting from the low to higher coverages, it has already been known for some time that diamond surfaces prepared in air are always terminated with oxygen atoms among other adsorbates [36], exhibiting different oxidation states.

It has already been shown that adsorbed oxygen atoms have the ability of altering the surface properties of diamond in a way that makes them quite attractive for various technological applications. Unlike the hydrogenated surface, oxygen-terminated diamond does not display a negative electron affinity. In particular, they are able to change the electron affinity of different diamond surfaces to a positive electron affinity in relation to that of a clean surface [15, 38], a property that has major implications for electronic applications. Adsorbed oxygen atoms on diamond surfaces have also been known to make them hydrophilic and this means that these surfaces were found to experience a high reactivity towards water molecules in an attached atmospheric adlayer.

Oxygen-terminated surfaces are particularly important because of their specific optical and electrical properties [27,28] therefore, a deeper understanding of various oxygen-termination reactions at diamond surfaces is of major importance. The presence of oxygen on the diamond surface can significantly affect the chemical reactivity [39,40], electrical conductivity [4,42], field emission [43,44] and Schottky barrier height.

2.3.4. Hydroxylated surface

It was found that CVD (polished) diamond surfaces are always terminated with hydrogen [4,42,43]. Therefore, the investigation of hydrogen and oxygen coexistence on the diamond surfaces could also be important. Also, as mentioned in previous section, Hydroxyl group is one of oxygen bond configurations with diamond carbon atoms.

The presence of the hydroxyl species on diamond surfaces has been demonstrated by organic chemical reactions wetting angle measurements and by XPS [44]. Rebuli *et al.* [45] studied the oxygenated diamond (111) and (100) surfaces in the presence of hydrogen. They found that, as hydrogen termination has been well established, the most probable form of the oxygen is a hydroxyl (–OH) group on the (111) surface and C–O–C bridges or C=O groups on the (100) surface. Using the density-functional theory (DFT), Larsson [46] reexamined these surfaces. His results confirmed that the hydroxylated structures are indeed stable. Pehrsson reported the observation of hydroxyl groups following the oxidation of the hydrogenated (100) surface and attributed that to oxygen insertion into C-H bonds on the surface [47,48]. The recent X-ray scattering study of the C(111) surface following high-pressure oxygen-water oxidative etching by Theije *et al*. suggested that the surface was terminated by a full monolayer of OH instead of carbonyl or ether species [49].

Previous studies have established that the diamond surface terminated with OH exhibits a negative electron affinity, while the clean surface and those terminated with oxygen atoms possess a positive electron affinity [15, 50]. Negative electron affinity is a phenomenon that has only been observed previously with H adsorption. This has been attributed to the changes occurring in the surface's work function, which alters the levels of the conduction band minimum and the vacuum level, thereby making it easy to extract electrons from such surfaces. This makes the material potentially useful in a number of applications, such as photocathodes and cold cathode emitters [51, 52]. Nonetheless, in spite of its obvious importance, the adsorption of OH on diamond is still not well understood, especially in conditions

other than ultrahigh vacuum (UHV), where the surface is in contact with the atmosphere.

2.2.5. Properties of terminated surfaces

2.2.5.a. Electron affinity (E_A)

Electrons in the conduction band are generally prevented from escaping into vacuum by the electron affinity barrier χ. The electron affinity of a semiconductor is defined as the energy difference between the conduction band minimum E_{CBm} and the vacuum level E_0. For most materials the vacuum level lies above the conduction band minimum, corresponding to a positive electron affinity. Surfaces of wide bandgap semiconductors like diamond have the potential of exhibiting a negative electron affinity (NEA) since the conduction band minimum lies near the vacuum level to begin with. Electrons present in the conduction band have sufficient energy to overcome the work function of a NEA surface and can be emitted into the vacuum.

Indeed, different surface terminations can shift the position of the bands with respect to the vacuum level and, therefore, induce a NEA or remove it. These changes have been found to be due to surface adsorbates because generally they generate to heteropolar bonds. Different surface adsorbates result in changes of the surface dipole. Changing the surface dipole can lead to an increase or decrease in the electron affinity. For example hydrogen has been reported to induce a NEA on the diamond (111) and (100) surfaces. Whereas oxygen leads to a dipole such that a positive electron affinity (PEA) is observed on these surfaces [4,19,53–55].

As-loaded diamond C(111) samples have been reported to be at least partially covered with a monohydride. The monohydride terminated surfaces show a (1×1) unreconstructed LEED pattern. Also a NEA was detected for these samples experimentally by ultraviolet photoemission spectroscopy (UPS) [4,19,53–55]. Annealing these surfaces to above 950°C leads to a (2×1) reconstruction, and a positive electron affinity is observed. These changes are attributed to the removal of

hydrogen. An Ar plasma clean was found to have the same effects on the electron affinity [55].

The variation in electron affinity (E_A) can be understood in term of surface electric dipoles arising from differences in the electronegativities of the terminating species. We can imagine two classes of surface dipole: $C^{+\delta}$–$X^{-\delta}$ and $C^{-\delta}$–$X^{+\delta}$, where δ is the partial charge on the atom,8 and X the adsorbate. $C^{-\delta}$–$X^{+\delta}$ dipoles bend the bands upward with respect to the vacuum level, while $C^{+\delta}$–$X^{-\delta}$ dipoles cause a downward band bending. Experimentally [21], $C^{-\delta}$–$H^{+\delta}$ dipoles yield an NEA of -1.3 eV, while $C^{+\delta}$–$O^{-\delta}$ dipoles result in a PEA of 1.70 eV.

2.2.5.b. Surface conductivity

Undoped diamond with a band gap of 5.5 eV is commonly considered an electrical insulator or sometimes a semiconductor with a wide band gap. Surprisingly a surface conduction of the as-grown (on both single crystals and thin films samples) hydrogenated diamond surface was observed by Landstrass and Ravi [56] in 1989. Later the presence of a conductive layer was confirmed, using the Seebeck effect, and identified as p-type by Maki *et al*. [57].

During the last years many other experiments have shown the same behavior on H-terminated diamonds. The surface conductivity (SC) of hydrogenated diamond films is of the order of 10^{-4} to 10^{-5} Ω/□ at room temperature, i.e., 4 –5 orders of magnitude larger than that of the undoped diamond [25,55,58,59]. This unique feature of the HD is found to disappear after dehydrogenation or oxidation of the surface. This observation led to the assumption by Maier *et al.* [23] that hydrogen plays a key role in the establishment of the high conductivity of the hydrogenated diamond.

The mechanism of surface conduction is still puzzling, but it is definitely ascertained that the conduction is related to hydrogen. So SC is associated to surface band bending due to hydrogen termination [60], hydrogen incorporation [61] and deep level passivation [62]. Since surface wet-chemical oxidation drastically change the p-type semiconducting nature to the intrinsic insulating behavior of diamond,

there is thus general agreement that the carriers are holes residing in an accumulation layer at the surface.

Despite the exceptional nature of SC on diamond, there is no clear understanding of the nature of the doping mechanism that leads to the surface-near hole layer. Such an understanding is, however, highly desirable in order to be able to exploit fully considerable potential of SC for applications.

References

[1] J. Ristein. Surf. Sci., 600, 3677 (2006).

[2] S. Koizumi, C. Nebel, and M. Nesladek, *Physics and Applications of CVD Diamond*,Wiley- VCH, (2008).

[3] Michael Sternberg, Peter Zapol, and Larry A. Curtiss, Physical Review B 68, 205330 (2003).

[4] B.B. Pate, Surf. Sci. 165, 83 (1986).

[5] P.G. Lurie, J.M. Wilson, Surf. Sci. 65, 453 (1977).

[6] B.B. Pate, J. Woicik, J. Hwang, J. Wu, in: S. Saito, O. Fukunaga, M. Yoshikawa, Science and Technology of New Diamond, vol. 345, KTK Scientific Publishers, Tokyo, 1990.

[7] B.B. Pate, L.S. Pan, D.R. Kania, Diamond: Electronic Properties and Applications, vol. 35, Kluwer Academic, Boston, 1995.

[8] P. G. Lurie and J. M. Wilsson, Surf. Sci. 65, 453 (1977).

[9] J. Wilks, E. Wilks, *Properties and Applications of diamond*, Butterworth-Heinemann, Oxford, UK, 1992, p. 192.

[10] B. N. Davidson and W. E. Pickett, Physical Review B, 49, 16 (1994).

[11] N. Tokuda, T. Makino, T. Inokuma and S. Yamasaki: Jpn. J. Appl. Phys. 51, 090107 (2012).

[12] K. Pandey, Phys. Rev. B 25, 4338 (1982).

[13] S. Tong Lee and G. Apai, Phys. Rev. B. 48, 2684 (1993).

[14] A.Hamza, G. Kubiak, and R. Stulen, Surf. Sci. Lett. 206(35), L833-L844 (1988).

[15] M. J. Rutter and J. Robertson, *Phys. Rev.* B 57, 9241 (1998).

[16] G. Kern, J. Hafner and G. Kresse, *Surf. Sci.* 366, 445 (1996).

[17] (a) J. C. Angus and C. C. Hayman, Science 241, 913 (1988); (b) W. A. Yarbrough and R. Messier, Science 247, 688 (1990); (c) F. G. Celii and J. E. Butler, Annu. Rev. Phys. Chem. 42, 643 (1991).

[18] L. Diederich, P. Aebi, O. Küttel, and L. Schlapback, Surface Science 424, L314 (1999).

[19] F.J. Himpsel, J. A. Knapp, J. A. Van Vechten, and A. E. Eastman. Phys. Rev. B, 20, 624, (1979).

[20] J. Van der Weide, Z. Zhang, P. K. Baumann, M. G. Wensell, J. Bernholc, and R. J. Nemanich. *Phys. Rev. B*, 50, 5803, (1994).

[21] F. Maier, J. Ristein, and L. Ley. *Phys. Rev. B*, 64, 165411, (2001).

[22] Daisuke Takeuchi *et al., Appl. Phys. Express* 3, 041301 (2010).

[23] F. Maier, M. Riedel, B. Mantel, J. Ristein, and L. Ley, Physical Review Letters , 85, 3472 (2000).

[24] L. Ostrovskaya, V. Perevertailo, V. Ralchenko, A. Dementjev, and O. Loginova. *Diam. Relat. Mater*, 11, 845 (2002).

[25] M. Yoshimoto, M. Furusawa, N. Nakajima, M. Takakura, Y. Hishitani, *Diamond Relat. Mater*., *10*, 295 (2001).

[26] I. Sakaguchi, M. N. Gamo, K. P. Loh, S. Hishita, H. Haneda, T. Ando, *Appl*. *Phys*. *Lett*. *73*, 2675 (1998).

[27] M. Tachiki, T. Fukuda, K. Sugata, H. Seo, H. Umezawa, H. Kawarada, *Appl*. *Surf*. *Sci*., *159*, 578 (2000).

[28] P. Gluche, A. Aleksor, A. Vescan, W. Eberl, E. Kohn, *IEEE Electron De*V. *Letts*., *18*, 547 (1997).

[29] P. E. Perhsson and Thomas W. Mercer, Surf. Sci. 460, 49 (2000).

[30] R. E. Thomas, R. A. Rudder, R. J. Markunas, J. Vac. Sci. Technol. A., 10, 2451 (1992).

[31] R. Klauser, J. Chen, T. Chuang, L. Chen, M. Shih, J. Lin, Surf. Sci., 356, L410 (1996).

[32] H. Tamura, K. Sugisako, Y. Yokoi, S. Takami, M. Kubo, K. Teraishi, A. Miyamoto, Phys. Rev. B., 61, 11025 (2000).

[33] J. S. Foord, L. C. Hian, R. B. Jackman, Diamond Relat. Mater., 10, 701 (2001).

[34] K. P. Loh, X. N. Xie, S. W. Wang, J. S. Pan and P. Wu, Diamond Relat. Mater. 11 1379 (2002).

[35] K. P. Loh, X. N. Xie, S. W. Wang and J. C. Zheng, J. Phys. Chem. B 106 5230 (2002).

[36] T. E. Derry, J. O. Hansen, P. E. Harris, R. G. Copperthwaite and J. P. F. Sellschop, ICSOSII: The Structure of Surfaces II: Proc. 2nd Int. Conf. on the Structure of Surfaces (Amsterdam, June 1987) (Springer Series in Surface Sciences vol 11) ed J. F. Van der Veen and H A Van Hove (Berlin: Springer) p 384 (1988).

[37] D. B. Rebuli, T. E. Derry, E. Sideras-Haddad, B. P. Doyle, R. D. Maclear, S. H. Connell and J. P. F. Sellschop, Diamond Relat. Mater 8 1620 (1999).

[38] P. K. Baumann and R. J. Nemanich Surf. Sci. 409, 320 (1998).

[39] J.I.B. Wilson, J.S. Walton, G. Beamson, J. Electron, Spectrosc. Relat. Phenom. 121, 183 (2001).

[40] C. Saby, P. Muret, Diam. Relat. Mater. 11, 851 (1996).

[41] H. Kawarada, *Surf. Sci. Rep.* 26, 205 (1996).

[42] T. Tachibana, J. T. Glass and R. J. Nemanich, *J. Appl. Phys.*73, 835 (1993).

[43] N. W. Makau and T. E. Derry, *Surf. Rev. Lett.* 10, 295 (2003).

[44] R. Boukherroub, X. Wallart, S. Szunerits, B. Marcus, P. Bouvier, M. Mermoux, Electrochem. Commun. 7, 937 (2005).

[45] D. R. Rebuli, J. E. Butler, P. Aggerholm, S. H. Connell, T. E. Derry, B. P. Doyle, E. Sideras-Haddad and J. F. P. Sellschop, *Nucl. Instrum. Methods* B 158, 701 (1999).

[46] K. Larsson, New Diamond and Frontier Carbon , 15, 229 (2005).

[47] P. E. Pehrsson, T. W. Mercer, Surf. Sci., 460, 49 (2000).

[48] P. E. Pehrsson, T. W. Mercer, Surf. Sci., 460, 74 (2000).

[49] F. K. de Theije, M. F. Reedijik, J. Arsic, W. J. P. van Enckevort, E. Vlieg, Phys. ReV. B, 64, 85403 (2001).

[50] M. J. Rutter and J. Robertson, *Comput. Mater. Sci.* 10, 330 (1998).

[51] M. W. Geis, J. C. Twichell, J. Macaulay, and K. Okano, Appl. Phys. Lett. 67, 9 (1995).

[52] A. Breskin, R. Chechik, E. Shefer, D. Becon, Y. Avigal, R. Kalish, and Y. Lifshitz, Appl. Phys. Lett. 70, 3446 (1997).

[53] F.J. Himpsel, D.E. Eastman, P. Heimann, J.F. van der Veen, Phys. Rev. B 24, 7270 (1981).

[54] B.B. Pate, M.H. Hecht, C. Binns, I. Lindau, W.E. Spicer, J. Vac. Sci. Technol., 21, 364 (1982).

[55] J. van der Weide, R.J. Nemanich, Appl. Phys. Lett., 62, 1878 (1993).

[56] M. I. Landstrass and K. V. Ravi, Appl. Phys. Lett. , 55, 975 (1989).

[57] T. Maki, S. Shikama, M. Komori, Y. Sakuta, and T. Kobayashi., Jpn. J. Appl. Phys., 31, 1446 (1992).

[58] H. Kawarada, H. Sasaki, and A. Sato, Phys. Rev. B 52, 11 351 (1995).

[59] M. I. Landstrass and K. V. Ravi, Appl. Phys. Lett. 55, 1391 (1989).

[60] T. Sugino, Y. Sakamoto, A. Furuya, and J. Shirafuji. Mater. Res. Soc. Symp. Proc., 339, 45 (1994).

[61] K. Hayashi, S. Yamanaka, H. Okushi, and K. Kajimura. Appl. Phys. Lett., 68, 376 (1996).

[62] S. Albin and L. Watkins. Appl. Phys. Lett., 56, 1454 (1990).

CHAPTER 3

CHAPTER 3

Computational Theory

Computational simulations of hydrogen, oxygen and hydroxyl on the surface of diamond were calculated using the density functional theory (DFT) by ORCA program on a Linux cluster. As the theoretical background behind the operation of DFT is important for the interpretation of the results presented herein, the theoretical assumptions and techniques used during the computational work of this thesis are discussed in this chapter.

3.1. Crystal notation

A material can be represented in three-dimensional space by a unit cell, a volume of the material's crystal lattice that can be repeated to reproduce the crystal as a whole. A primitive cell is the smallest unit cell that can be repeated to represent the full lattice, although for many materials it is preferable to pick a unit cell larger than this for more convenient lattice transformations. The structure of an ideal crystal without defects can be described by an infinitely repeating unit cell, and this periodicity allows a simplified description of the structure by defining a base repeatable unit cell. There are fourteen basic 3D lattices with unique symmetries, known as the Bravais lattices, which can be broken down into seven crystal systems (Cubic, Tetragonal, Orthorhombic, Hexagonal, Trigonal, Monoclinic and Triclinic). There are numerous arrangements of atoms within each Bravais lattice that define the structure of a wide variety of materials. Diamond, for instance, has a face-centered cubic unit cell, where each lattice point contains a basis of two atoms at (0,0,0) and $(\frac{1}{4},\frac{1}{4},\frac{1}{4})$.

The unit cell can be described by three unit vectors, **a**, **b** and **c**, and thus any lattice point in the crystal can be described by the vector

$$r = n_1\boldsymbol{a} + n_2\boldsymbol{b} + n_3\boldsymbol{c} \tag{3.1}$$

where n_1, n_2 and n_3 are integers. As surfaces are important for many properties of a material, it is useful to have a system to describe the planes that intersect the *x*, *y* and *z* axes of the lattice. In the case of the plane shown in Figure 3.1, the intercepts of the *y* and *z* lattices are infinite as the plane is parallel to those axes. Thus, using the real-space intercepts creates problems for a mathematical description of the plane.

Instead the reciprocals of the intercepts of the three axes are used, multiplied by their lowest common denominator to obtain integers. So a plane intersecting the *x*, *y* and *z* axes at 3, 4 and 1 would have reciprocal intercepts of $\frac{1}{3}, \frac{1}{4}$ and 1, which when multiplied by the lowest common denominator would give (4, 3, 12). These integers are known as the Miller indices of the plane (*hkl*) and are a useful tool for describing a crystal. Figure 3.1 shows the (100), (111) and (110) planes, for example. Any atom intersecting the (110) plane would be significant for interactions and properties of the (110) surface. Any plane parallel to the one shown will have the same Miller indices and are equivalent. A reciprocal lattice vector $g_{(hkl)}$ is defined as:

$$g_{hkl} = ha^* + kb^* + lc^* \tag{3.2}$$

where a*, b* and c* are the reciprocal lattice vectors. Just as the unit cell allows the lattice structure of a crystal in real space to be simplified to a small repeatable unit, a similar approach to the reciprocal lattice yields the Brillouin zone. The first Brillouin zone is defined as the volume enclosed by the Wigner-Seitz cell within reciprocal space. The Wigner-Seitz cell is a primitive unit cell that contains all the symmetry of the entire lattice.

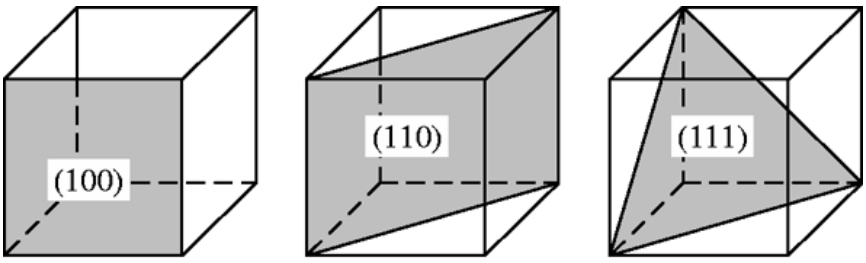

Figure 3.1. The 100, 110 and 111 planes of an arbitrary unit cell [1].

3.2. Band structure of crystals

3.2.1. Multi-atom systems

For the purposes of this thesis we need to cover the behavior of an electron in a crystal of many atoms, such as the crystal lattice of diamond and other semiconductors. To do this we need to consider the effect on the electronic behavior, particularly that of the valence electrons, when an atom is in close proximity to other atoms.

When two atoms are close together, the probability density functions $|\psi(x)|^2$ overlap, as shown in Figure 3.3. This means that some identical states could be possible in both atoms, which the Pauli Exclusion Principle states cannot happen. When two overlapping states possess the same quantum numbers, the energy levels in each atom split to slightly different energies so that the electrons are in unique states.

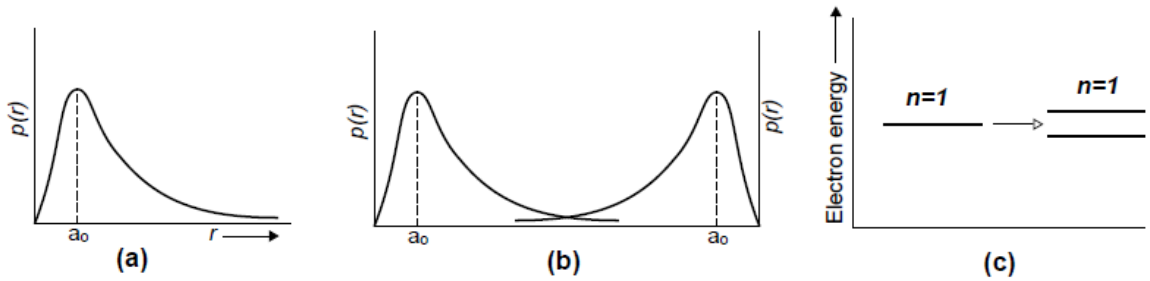

Figure 3.3. (a) shows the probability density for an electron within one atom, **(b)** shows the overlap of two probability densities when two atoms draw close to each other, and **(c)** shows the splitting caused by this overlap that splits the energy levels into two discrete and separate levels. [2].

As the number of atoms with overlapping states increases, this behavior continues, such that what would be a single quantized energy level in the case of an electron in a single atom is split or 'perturbed' many times into a band of states all with slightly different energies. The Pauli Exclusion Principle demanding that no states should have the same quantum numbers extends across the entire electronic system independent of the system's size, with the result that as the system grows larger the band continues to extend into a large number of discrete energy levels

with infinitesimally different but still distinct energies. For large systems with 10^{20} electrons or more, the gaps between each state become so small as to make the band essentially continuous for many purposes, but it is important to remember that no matter how small the difference between the levels the states of each electron remain discrete.

An important effect of this splitting of energy levels into bands is observable for the valence electron shell. For the core electrons, the individual states split across a small energy range, but do not overlap significantly with neighboring shells, since the electrons are tightly bound to the ionic core. For the valence electrons, especially those in the part-filled valence shell which are only weakly bound to the ionic core, it is possible that when they split into bands several overlapping shells can contribute, as shown in Figure 3.4 which shows the electronic shells of a single carbon atom and the result after the orbitals split into bands. The four valence electrons in carbon lie in the *2s* and *2p* states corresponding to $n = 2$, $l = 0$ and $n = 2$, $l = 1$ respectively. In a single atom of carbon, the *2s* state holds two electrons and the *2p* state holds two electrons of the total of six it could hold. As carbon atoms come closer together, the 2*s* and 2*p* states overlap and split, but with a degree of mixing between the two states. As a result, instead of two bands of two and six electronic states, the two states overlap such that they form two separate bands, one at lower energy with four states and the other higher with the other four electronic states.

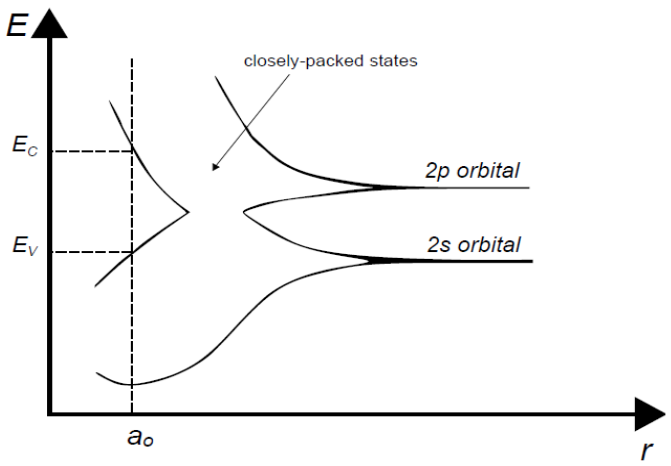

Figure 3.4. The behavior of the valence electrons in carbon as a carbon atom is in free space and as multiple carbon atoms are brought close together so that overlapping of the *2s* and *2p* states occurs. [1]

This splitting and overlapping is important, as it introduces an energy gap into the bands of the material. At low temperatures, only the bottom (or valence) band of four states is filled, whilst the top (or conduction) band remains empty, with a so-called 'band gap' between the two bands. It is this band gap that produces much of the interesting behavior of semiconductors like diamond and silicon.

3.3. Density functional theory

3.3.1. First principles of computational modelling

In order to calculate the electronic and physical structure of materials, a computationally accurate method of determining the wavefunction of the electrons in a material is needed. The ground-state behavior can be described in a more refined way with a first-principles approach than the more empirical models shown in the previous section. The most important advantage of a first-principles approach is the inclusion of electron-electron interactions.

A number of different computational methods for solving the Schrödinger equation for systems with many atoms have been developed. Fundamental to this study is Density Functional Theory (DFT), although several other methods will be briefly discussed as part of the derivation of the DFT equations used in this study.

3.3.2. Born-Oppenheimer approximation

One of the main approximations used to simplify the many-body wavefunction, first proposed by Born and Oppenheimer [3], is that the wavefunctions of the electrons and nuclei can be decoupled. The mass of the electron is approximately two thousand times less than that of the nucleus so the electron responds much more quickly to forces than the nucleus that the change in the electron wavefunction in response to changes in the atomic nuclei can be assumed to be instantaneous and adiabatic. This means the wavefunction $\psi(r;R)$ for the degrees of freedom for nuclei and electrons can be rewritten as the multiple

of two independent wavefunctions, one for the nuclei $\chi(R)$ and one for the electrons $\psi R(r)$:

$$\psi(r;R) = \chi(R)\,\psi R(r) \tag{3.3}$$

The separation of the nuclear and electronic charge is very useful as it means that the two systems can be decoupled such that:

$$\left[\hat{T}_n + \hat{V}_{n-n}\right]\chi(R) = E_n\chi(R) \tag{3.4}$$

$$\left[\hat{T}_e + \hat{V}_{e-e} + \hat{T}_{e-n}\right]\psi(R) = E_e\psi(R) \tag{3.5}$$

where the subscript *e* refers to electronic terms and the subscript *n* to the nuclear terms, with $\hat{T}$ and $\hat{V}$ referring to the kinetic and potential energy respectively. Using the energy eigenvalues E_n and E_e and the Born-Oppenheimer approximation in Equation 3.3 we can rewrite the Schrödinger equation for the complete system:

$$\hat{H}\chi(R)\psi_R(r) = (E_n + E_e)\chi(R)\psi_R(r)$$
$$-\sum_{\alpha}^{N_n}\frac{1}{2M_\alpha}[\chi(R)\nabla_\alpha^2\psi_R(r) + 2\nabla_\alpha\psi_R(r)\nabla_\alpha\chi(R)] \tag{3.6}$$

where α refers to the α^{th} atomic nucleus. If the electron-nuclear coupling is weak, then the second term on the right of Equation 3.6 may be negligible due to the large mass of the nucleus, and the electronic and nuclear terms can be considered completely independent of each other, so that if the atomic positions of the nuclei remain fixed, the system's properties can be calculated using only the electronic wavefunction .

3.3.3. Bloch's theorem

Bloch's theorem states that an electron's wavefunction $\psi_{(j,k)}$ in a periodic potential can be written as the multiple of two parts - one contributed by the periodic lattice $u_j(r)$ and the other representing the wavelike part of the wavefunction $e^{ik.r}$:

$$\psi_{(j,k)}(r) = u_j(r)e^{ik.r} \tag{3.7}$$

where k is a wave vector within the first Brillouin zone of the reciprocal lattice and the band index is indicated by the subscript j. The periodicity of $u_j(r)$ is identical to the direct lattice, allowing it to be rewritten into a discrete plane-wave basis set where its wave vectors G are reciprocal lattice vectors within the crystal structure with lattice vectors r and plane wave coefficients $c_{j,G}$:

$$U_j(r) = \sum_G c_{j,G} e^{iG.r} \tag{3.8}$$

where $G.R = 2\pi m$ and m is an integer, when R are the crystal lattice vectors. By substituting this into Equation 2.7 the electron wavefunction can be expanded to

$$\psi_{(j,k)}(r) = \sum_G c_{(j,k+G)} e^{i(k+G).r} \tag{3.9}$$

written in this way, the wavefunction is a linear combination of plane-waves, making manipulation easier, independent of the type of crystal and behaving the same across all space, unlike Gaussian and other localized functions, which are dependent on position.

3.3.4. Hartree-Fock theory

Although the free-electron model is useful in showing the basic electronic structure of atoms and in grasping the concepts of band structure, it neglects the interactions between electrons. The simplest approximation of the electron-electron interaction is the Hartree approximation [4]. The Hartree approximation is also known as the self-consistent field (SCF) method as each time the calculation is made; the wavefunction is estimated and used for the subsequent iteration, so that one cycle is consistent with the next estimate. Calculating the wavefunction of a many-electron system is complicated due to the electron-electron interactions, and as a result the Hamiltonian is dependent on the positions of all the electrons $H = H(r_1, r_2 \ldots)$, making calculation of the true wavefunction virtually impossible. The Hartree approximation simplifies this calculation by assuming that the interaction between an electron and all other electrons can be described by an averaged

potential energy and each electron is then treated separately, so that the Hamiltonian depends only on the sum of single-electron terms:

$$H(r_1, r_2 \ldots) = H(r_1) + H(r_2) + \ldots \tag{3.10}$$

The assumption that electrons are independent is only a good approximation due to the screening of the electron-electron interaction by the remaining electrons. The many-body wavefunction becomes the product of the individual one-electron terms:

$$x_i(r_1, r_2 \ldots) = x_i(r_1) \times x_i(r_2) \times \ldots \tag{3.11}$$

Hartree's first formulation of the approximation was designed to create a solution to the time-independent many-body Schrödinger equation using *ab initio* fundamental methods. The initial Hartree Method did not contain all of the information required to describe the behavior of fermions; it did not include the requirement for two electrons to have antisymmetric wavefunctions such that:

$$\psi(x_1, x_2 \ldots x_j, \ldots x_i \ldots x_N) = -\psi(x_1, x_2 \ldots x_j, \ldots x_i \ldots x_N) \tag{3.12}$$

Following work from Slater and Fock [5,6], the Hartree method was adjusted to use a determinant of single-particle orbitals to represent the wavefunction, as it allows an exact inclusion of electron exchange, which was not included in the original method. The Hartree-Fock method approximates the complicated true many-body wavefunction to a single Slater determinant of *N* spin-orbitals:

$$\Psi = \begin{vmatrix} \psi_1(x_1) & \psi_1(x_2) & \ldots & \psi_1(x_N) \\ \psi_2(x_1) & \ldots & & \\ \vdots & & & \\ \psi_N(x_1) & \psi_N(x_2) & \ldots & \psi_N(x_N) \end{vmatrix} \tag{3.13}$$

This Slater determinant can be inserted into the Schrödinger equation to derive an expression for the total energy of the system. The wavefunction is normalized using a Lagrange multiplier e_i so that the value of the determinant is left unchanged by non-singular linear transformations:

$$\frac{\delta}{\delta\psi}[< \hat{H} > - \sum_j \epsilon_j] \int |\psi_j|^2 \, dr = 0 \tag{3.14}$$

This greatly simplifies the electron orbital wavefunctions to a set of one-electron wavefunctions, with the full Hartree-Fock equations for $E_i\ \psi_i(r)$ given by

$$E_i\ \psi_i(r) = \left(-\frac{1}{2}\nabla^2 + V_{ion}(r)\right)\ \psi_i(r) + \sum_j \int dr'(\frac{\left|\psi_j(r')\right|^2}{|r-r'|}\ \psi_i(r) - \sum_j \delta_{\sigma_i\sigma_j} \int \frac{\psi_j^*(r')\ \psi_i(r')}{|r-r'|}\ \psi_j(r)dr' \quad (3.15)$$

The first and second terms in the right hand side of the Hartree-Fock equation describe the kinetic energy and the potential energy of the interaction between the electron and the ion. The third term, known as the Hartree term, is the potential energy of the electron-electron interactions, in this case approximated by the electrostatic potential between an electron and the average charge distribution of *N* electrons in the system. The final term derives from the Pauli Exclusion Principle stating that two electrons cannot be in the same state and includes a delta-function for the behavior when $j = i$, so that it cancels the effect of the third term having an unphysical self-interaction when $j = i$ but is zero when $j \neq i$.

The Hartree-Fock equation captures a lot of the physical detail required to solve the Hamiltonian accurately, with certain caveats. Hartree-Fock algorithms ignore relativistic effects, for example. The biggest weakness to the Hartree-Fock method is the lack of any consideration to electron correlation. The Hartree-Fock method considers all electron interactions as the interaction between a single electron and the average electric field produced by the remaining electrons in the system, whereas in a real system there are other types of electron-electron interactions such as Pauli repulsions that also contribute. Without consideration of the electron correlation, the total energy of the system calculated using Hartree-Fock is always higher than the actual energy of the system, with the difference between the two known as the correlation energy.

3.3.5. Density functional theory

Whilst Hartree-Fock is still in use for computational simulations, an alternative theory, density functional theory (DFT), has come to be just as important

a tool for *ab initio* modelling. Significantly, density functional theory accounts for both exchange and correlation energies, where the Hartree-Fock algorithm only includes the former without additional modifications [7].

Density Functional Theory was developed from a series of important papers from Hohenberg, Kohn and Sham [8,9] that proposed that the total density of electrons *n(r)* would be used rather than the many-body Schrödinger equation used in the Hartree and Hartree-Fock methods. This simplifies calculations substantially as the many-body wavefunction does not need to be explicitly calculated. In density functional theory the electron charge density determines all the electronic behavior of the system, so long as they are in the ground state. In their seminal 1964 paper, Hohenberg and Kohn proposed that the ground-state energy of an interacting electron gas can be defined as a unique functional of the charge density *n(r)*. Calculations using density functional theory use a variational principle to find the ground-state energy, which is at its minimum when the charge density *n(r)* is identical to the true ground-state charge density *ρ(r)*. The Kohn-Sham ground state energy functional is

$$E[\rho(r)] = T[\rho(r)] + \int [\rho(r)]\phi_N(r)dr + \frac{1}{2}\int \rho(r)\phi_H(r)dr + E_{xc}[\rho(r)] \qquad (3.16)$$

As in the Hartree-Fock equation (shown in Equation 3.15), the first term in Equation 3.16 corresponds to the kinetic energy, whilst the second represents the energy due to the interaction between the electronic charge q_i and the ionic potential, with

$$\phi_N(r) = \sum_i \frac{q_i}{4\pi\epsilon_0|r - R_i|} \qquad (3.17)$$

where R_i is the position of the *i*th nucleus. The third (or Hartree) term describes the energy of an electron moving through the electrostatic field of all other electrons in the system, with the Hartree potential $\phi_H(r)$ given by

$$\phi_H(r) = \int \frac{\rho(r')}{4\pi\epsilon_0|r - r'|}dr' \qquad (3.18)$$

Similarly to the Hartree-Fock method, this Hartree term overestimates the Coulomb repulsion between electrons, and neglects the effect of exchange-correlation hole. Due to the Pauli Exclusion Principle, the chances of finding an electron close to an electron is much reduced, as electrons with parallel spins will repel, and this repulsion is not considered in the Hartree term. The fourth term in the ground-state energy functional compensates this overestimation of energy in the Hartree term. The exact exchange-correlation energy is defined by

$$E_{xc}[n] = \frac{1}{2}\int\int n(r)\frac{n_{xc}(r,r')}{|r-r'|}dr\,dr' \tag{3.19}$$

In practice this exchange-correlation function is not known exactly and so an approximation must be used. Density functional theory calculations often use forms of the local density approximation (LDA) or the generalized gradient approximation (GGA) to estimate the exchange-correlation energy. The various approximations for the exchange-correlation energy will be discussed in Section 3.3.8.

The effect of the exchange-correlation hole allows the electrons to be treated as if they were independent, with no electron-electron Coulomb interactions. This leads to the Kohn-Sham equations transforming the *N* electron system into a *N* single-electron equations.

3.3.6. Kohn-Sham equations

As detailed in the previous section, the Kohn-Sham ground-state energy functional is given by Equation 3.16. The contribution of the exchange-correlation whole energy due to Pauli Exclusion effects means that the electrons can be treated as non-interacting independent particles that contribute the same charge density as a system of interacting particles. Subject to the number of electrons *N* being conserved, each *i*th electron can have its own Kohn-Sham time-independent Schrödinger equation such that

$$-\frac{h^2}{(8\pi^2 m_e)}\nabla^2\boldsymbol{\psi}_i(r) + V_{\text{eff}}(r)\boldsymbol{\psi}_i(r) = E_i^{KS}\boldsymbol{\psi}_i(r) \tag{3.20}$$

where the effective Kohn-Sham potential $V_{\text{eff}}(r)$ is the combination of the Hartree potential $V_H(r)$, the potential due to the ion cores of the atoms in the system $V_N(r)$ and the potential due to the exchange-correlation hole $V_{XC}(r)$:

$$V_{\text{eff}}(r) = V_H(r) + V_N(r) + V_{XC}(r) \tag{3.21}$$

The key component of this approach is the electron density *ρ(r)*, since the Hartree term is dependent on *ρ(r)* and the exchange-correlation potential is equal to the derivative of the exchange-correlation energy E_{XC} with density - $\frac{\delta E_{XC}[\rho(r)]}{\delta \rho(r)}$. In a density functional theory calculation for a periodic system (rather than a single molecule), the Kohn-Sham equations (Equation 3.20) are expanded in terms of a plane wave basis set using Bloch's Theorem and in terms of the reciprocal lattice vectors of the crystal. After the wavefunction $\boldsymbol{\psi}_i(r)$ has been estimated, the density *ρ(r)* can be found by

$$\rho(r) = \sum_{i \ occupied} \boldsymbol{\psi}_i(r)\boldsymbol{\psi}_i^*(r) \tag{3.22}$$

Once the density has been found it can be used to recalculate the potentials in the Kohn-Sham equations, allowing a new wavefunction to be calculated and a new density, which leads to a new wavefunction and so on. This process is repeated until the energy is minimized and self-consistency is achieved. This `self-consistency cycle' comprises the basic approach of density functional theory, which has been used to simulate the electronic and structural properties of many systems to good agreement with experimental results. Whilst the Kohn-Sham orbitals themselves lack true physical meaning, they can be a useful tool in observing the density and localization of electrons within a crystal.

Once the self-consistent charge density has been calculated, geometry optimization can be performed to reach a more accurate structural configuration of the atoms. The forces on each atom can be calculated from the total energy, as

$$F_a = -\nabla_a E. \tag{3.23}$$

The atoms are then moved in the direction of this force. The process then starts again, with the total energy and force on each atom is calculated, and the atom

is moved again. The process repeats until the force on each atom falls below a certain tolerance level.

3.3.7. Convergence criteria

It is easy to perform calculations using density functional theory methods that produce structural and electronic information about a system. However, because of the many variables in such a calculation, the result may not give physically realistic values unless these variables are properly calibrated first.

To ensure that the final calculations are providing realistic results, the various parameters are varied independently on a test case supercell. As the value of the parameter changes, the total energy of the simulated system should converge to a constant value, usually at the cost of additional computational time. For each variable, the computational cost versus accuracy is weighed up and a value chosen that gives the best compromise between the two. The most critical parameters for convergence are typically the cut-off energy and the density of *k*-points used in a Monkhorst-Pack grid to sample the Brillouin Zone.

3.3.8. Exchange-correlation functionals

The accuracy of a DFT calculation depends on the approximation for the exchange-correlation energy, as it is the one feature that cannot be calculated exactly. There are a number of different approximations that can be used, which each have their advantages and disadvantages and may be more or less suitable depending on the nature of the system being studied.

The local density approximation (known as the local spin-density approximation for the case of systems with non-zero total spin) is one of the more simple ways to approximate the exchange-correlation energy, as it depends only on a single variable, the electron density.

$$E_{xc}^{LDA}[N(r)] = \int N(r)\epsilon_{xc}^{hom}[n(r)]\,dr \tag{3.24}$$

Generally the LDA falls short of being able to model the complexity of many systems due to its singular variable, but it can be an effective tool for modelling simple covalent and metallic systems. For more complicated materials such as molecules and systems with widely varying electron densities, the more advanced generalized gradient approximate (GGA) is used instead.

The generalized gradient approximation takes the local density approximation and adds a second variable to improve the accuracy of the approximation. In addition to the density, the GGA also depends on the gradient of the density.

$$E_{xc}^{GGA}[n(r)] = \int n(r)\epsilon_{xc}^{GGA}[n(r), \nabla n(r)]\, dr \qquad (3.25)$$

Because of the additional variable in the GGA compared to the LDA, the GGA can produce a more accurate wavefunction with a faster convergence than the LDA. Some examples of GGA functionals include the Perdew and Wang PW91 functional [10], the original and revised PBE functionals [11,12] and the WC functional [13]. PW91 was the first reliable GGA and has been used to characterize a large number of materials, whilst the PBE, RPBE and WC functionals contain a mix of the features of the LDA and the PW91 functionals.

3.3.9. Potential Energy surface (PES)

Information about the Potential Energy Surface (PES) has improved enormously in recent years, both from the analysis of experimental data and from ab initio calculations. However it is still a major task to gather available information to construct a functional representation which can be used for dynamical calculations. In general, different experiments experience different parts of the surface and highly accurate calculations are expensive to perform. Therefore, it is only by using chemical judgement that one can combine information from different sources to produce a satisfactory function for the whole surface.

Potential energy surface is the potential interaction energy of nuclei in a molecular system. It is a function of the nuclei internal coordinates (bonds, angles,

and dihedral angels). If a molecular has N atoms, it has 3 degrees of freedom for translational motions of the whole molecule and 2 or 3 overall rotational motions if it has a linear or non-linear structure, respectively. Thus, the potential energy surface has a (3N – 5) or (3N - 6) dimensions. The simplest potential energy surface is the potential curve of a diatomic molecule that is a function of only the bond distance. Figure 3.5 is an illustration of a potential energy surface with identifications of its topological features.

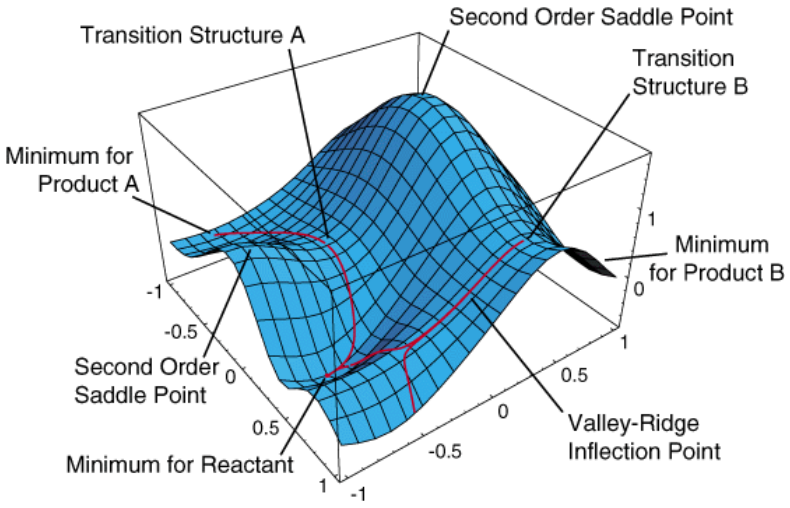

Figure 3.5. The potential energy surface with identifications of its topological features.

A local minimum corresponds to a stable structure or conformer. A saddle point indicated by either the transition structure A or B has only one direction going downhill while other directions going uphill. Saddle point is important for elucidating reaction mechanism and chemical kinetics. Higher-order transition states have more than one direction going downhill and often is not important is chemistry. Reaction path is defined by the steepest descent path connecting a saddel point to its nearest local minima on both sides as shown by the red curve connecting minimum from Reactant to transition structure A and minimum for Product A.

Potential energy surface is calculated by solving the Schrodinger equation using the Born-Oppenheimer approximation which assumes the electron motions can be separated from the nuclear motions for a large number of geometrical

structures. Generate a complete PES quantum mechanically is computationally very expensive procedure since it has (3N-6) or (3N - 5) dimensions. To elucidate reaction mechanism often one only needs to identify minima that correspond to the reactant and product of interest and the saddle point connecting them. Reaction path is often calculated to confirm the saddle point actually connecting the reactant and product of interest but not to other local minima. Since the Schrodinger equation can only be solved approximately for multi-electron systems, depending on the level of approximation (method/basis set) used locations of these stationary points (miminum or transition state) may vary from their 'true' structures. Thus, comparisons between predicted structures with those from experimental observations provide an indication on the accuracy of the method used.

3.3.10. ORCA software

ORCA can perform most semi-empirical, DFT and *ab initio* calculation. The ORCA program can be used to calculate wavefunctions for electrons in molecules by solving the time-independent Schrödinger equation in an approximate way. At the basic level, these are so-called `self- consistent-field' (SCF) calculations, or, in the limit of an infinite (complete) basis set, Hartree-Fock (HF) calculations. Other levels of approximation are also available in this software, both higher and lower.

Among all the different formalisms of electronic structure theory, Kohn–Sham density functional theory [14,15] achieves so far the best compromise between accuracy and efficiency, and has become the most widely used electronic structure model for condensed matter systems. Kohn–Sham density functional theory gives rise to a nonlinear eigenvalue problem, which is commonly solved using the self-consistent field iteration method [16]. In each iteration, the Kohn–Sham Hamiltonian is constructed from a trial electron density and is discretized into a finite dimensional matrix. The electron density is then obtained from the low-lying eigenfunctions, called Kohn–Sham orbitals, of the discretized Hamiltonian. The resulting electron density and the trial electron density are then mixed and form a new trial electron density. The loop continues until self-consistency of the electron

density is reached. An efficient algorithm therefore contains three phases: discretization of the Hamiltonian; evaluation of the electron density from the discretized Hamiltonian; and self-consistent iteration.

References

[1] S. Elliott, *The Physics and Chemistry of Solids*. Wiley, Chichester, UK, (1998).

[2] D. Naemen, *Semiconductor Physics and Devices* 3rd edition. McGraw-Hill, New York, NY, USA, (2002).

[3] M. Born, and R. Oppenheimer, Annalen der Physik 84, 457 (1927).

[4] D. Hartree, Proc. Cambridge Phil. Soc 24, 89 (1927).

[5] Slater, J. Phys. Rev. 34, 1293 (1929).

[6] V. Z. Fock, Physik 61, 126 (1930).

[7] E. Kaxiras, *Atomic and Electronic Structure of Solids*. Cambridge University Press, (2003).

[8] P. Hohenberg, and W. Kohn, Phys. Rev. 136, B864 (1964).

[9] W. Kohn, and L. Sham, Phys. Rev. 140, A1133 (1965).

[10] J. Perdew, and Y. Wang, Phys. Rev. B 45, 13244 (1992).

[11] J. Perdew, K. Burke, and M. Ernzerhof, Phys. Rev. Lett. 77, 3865 (1996).

[12] B. Hammer, L.Hansen, and J. Norskov, Phys. Rev. B. 59, 7413 (1999).

[13] Z. Wu, and R. Cohen, Phys. Rev. B. 73, 235116 (2006).

[14] P. Hohenberg, W. Kohn, Phys. Rev. 136, B864–B871 (1964).

[15] W. Kohn, L. Sham, Phys. Rev. 140, A1133–A1138 (1965).

[16] R. Martin, *Electronic structure: basic theory and practical methods*, Cambridge Univ. Press, Cambridge, 2004.

CHAPTER 4

CHAPTER 4

Calculation Details of Studying Diamond (111)−(1×1) Surfaces

4.1. Cluster Model

Diamond structure is based on tetrahedrally coordinated carbon atoms, which are linked with each other through pure covalent bonding forces. All six-membered carbon rings, analogous to those in cyclohexene in chair conformation, are formed by the overlap of sp^3 hybridization. The diamond (111) surface is important because, unlike the (110) and (100) surfaces, it does not allow reconstruction. Furthermore, the diamond (111) surface has a sufficient number of ideal sites for adsorption of adatoms. The ideal C(111)-(1×1) surface was determined to have the bulk-terminated C(111) structure as indicated by LEED and He scattering experiments [1-3]. The surface structure of the bulk-terminated C(111)surface has atoms that are threefold coordinated with atoms on the subsurface layer, and contains dangling bonds normal to the surface plane.

Flat and stepped diamond (111) surfaces were modeled by $C_{46}H_{39}$ and $C_{68}H_{47}$ clusters, respectively, whose C-atom networks have a lattice structure of diamond. In Figure 4.1, those clusters are depicted by ball-and-stick models. The $C_{46}H_{39}$ cluster as a model for flat surface consists of two (111) bilayers, and the $C_{68}H_{47}$ cluster as a model for the stepped surface consists of three (111) bilayers with a monoatomic height step, as shown in Figure 4.1.

Both clusters have a bare (111) surface on the top face. Bottom and side faces in both models were then terminated by H atoms to saturate the dangling bonds and to maintain the tetrahedral coordination of C atoms. The C atoms denoted by black circles in Figure 4.1 construct the topmost layer of diamond (111) flat (terrace) surface, where we define $\boldsymbol{z}$ = 0 Å.

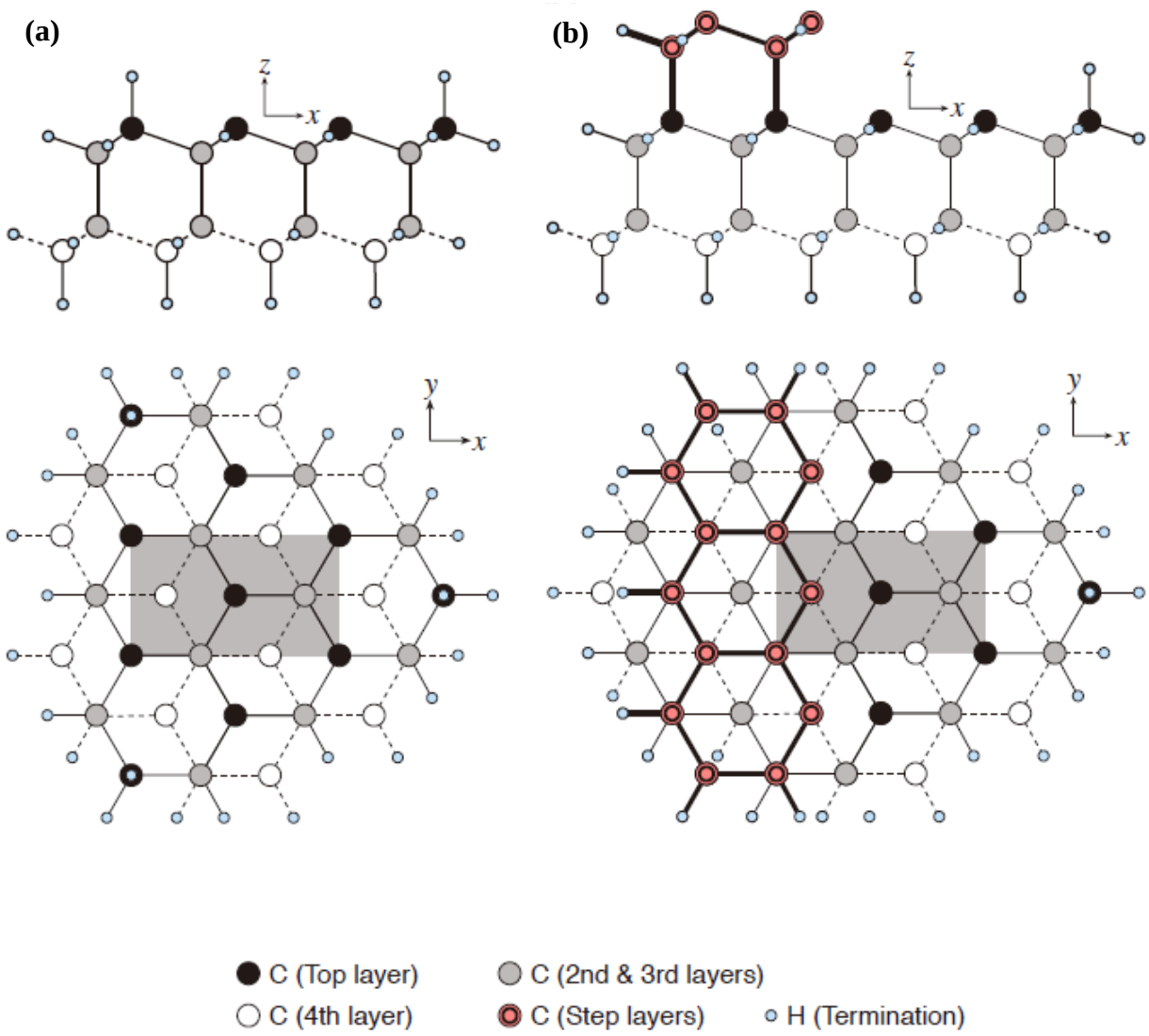

Figure 4.1. Side view (upper) and top view (lower) of **(a)** $C_{46}H_{39}$ cluster used for the calculation in a flat (111) surface and **(b)** $C_{68}H_{47}$ cluster used for the calculation in a stepped (111) surface. Gray-colored area indicates the area that potential energy was calculated.

Diamond models used in this study were constructed on the basis of information found in the literature [4-7]: the interatomic C-C distances were set at 1.54 Å and bond angles at 109.5° in accordance with the tetrahedrally coordinated structure. The C-H distance was 1.07 Å. All layers of C atoms plus H termination layer were fixed for the subsequent computations, unless noted otherwise. The potential for the H and O atoms were evaluated by placing an H/O adatom above the (111) bare surface of the cluster, and by calculating the self-consistent-field total energy as a function of the position of the H/O atom.

4.1.1. Cluster size

A cluster is an aggregate of a few to several thousands atoms. The surface energy of any system must depend on its structure. It was found that the calculated potential energy surface varies with the cluster size. Also, it was found that the convergence of potential energy depends on the cluster size. As the cluster size increases, it becomes more computationally difficult.

In this work, the surface model here was designed to be as large as possible, while remaining computationally feasible. Also, the surface must contain a sufficient number of atoms to minimize interaction effects originating from the periodic boundary condition. Edge effects of the cluster calculations are minimized by using a portion of the wave function to simulate connection of the cluster to a more extended solid.

To be sure that our model is large enough and has sufficient number of atoms, we performed a test on flat model where the cluster size in the vertical and horizontal directions was separately extended. Then, we had two extended flat models (vertically and horizontally extended), which were used to perform same calculation as that will be described in next chapter with presence of H adatom on the surface.

The basic physical characteristics of the cluster such as the potential energy surface contours and energy barrier (as explained in details in Chapter 5) estimated from our calculations on these two tested models were compared with that of the

original cluster shown in Figure 4.1(a). It was found that the results change negligibly. By this way, we proved that the “first guess” cluster size that represents the minimum cluster size and depicted in Figure 4.1(a) is quite enough to satisfy accurate results with exhibiting much faster computational time.

4.2. Computational Method

The calculations were performed with the ORCA software package (version 2.8) developed by Neese [8] on a linux cluster. Spin-polarized DFT calculations employed the Becke-Perdew BP86 exchange-correlation functionals with generalized gradient approximation [9,10]. Basis sets are essential input data for calculations. The Ahlrichs’ split-valence basis set called def2-SVP [11,12], which includes polarization functions for all kind of atoms, was used. It is a split-valence double-ζ basis set with one set of polarization functions on all non-hydrogen atoms.

The total energy of the cluster/adatom system was self-consistently (SCF) determined by the spin-unrestricted Kohn-Sham method (UKS) [13]. All electrons in the system were treated in the same nonrelativistic nature because the atoms involved were light (C, H, and O). The Resolution of the Identity approximation in Density Functional Theory improves the computational efficiency of large-scale calculations but requires the use of a second, or "auxiliary" basis set. The resolution of the identity (RI) approximation [14,15] was used in conjunction with the def2-SVP/C auxiliary basis set.

The coordinates obtained from the crystal structure of ideal C (111)-(1×1) surface clusters (flat and stepped models) described in previous section were used as the starting input structure. Edge effects of the cluster calculations are minimized by using a portion of the wave function to simulate connection of the cluster to a more extended solid. The potential energies for the H, O adatoms and OH group were evaluated by placing the adatom above the (111) bare surface of the cluster, and by calculating the self-consistent-field total energy as a function of the position of the adatom, and then is plotted as a contour map.

First, the calculation was preliminarily carried out to obtain the potential

energy surface (PES) of diffusion of H/ O/ OH on flat and stepped surface, and the height of the atom from the surface (***z***) was roughly estimated. After that, the calculation was applied to obtain a more accurate potential energy surface. The result of the PES relevant for diffusion of the adatom on the diamond (111) is plotted as a contour map consists of 104 calculated points by using Octave software.

References

[1] P.G. Lurie and J.M. Wilson, Surf. Sci. 65, 453 (1977).

[2] A.V. Hamza, G.D. Kubiak and R.H. Stulen, Surf. Sci. Lett. 206, L833 (1988).

[3] G. Vidali and D.R. Frankl, Phys. Rev. B 37, 2480 (1983).

[4] H.-D. Jakubke and H. Jeschkeit, Concise Encyclopedia Chemistry (Walter de Gruyter & Co., Berlin, 1993).

[5] J. D. Lee, Concise Inorganic Chemistry (Blackwell Science Ltd., Oxford, U.K., 1996) 5th ed..

[6] R. J. Borg and G. J. Dienes, The Physical Chemistry of Solids (Academic Press: San Diego, CA, 1992).

[7] W. Parrish, Acta Cryst. 13, 838 (1960).

[8] F. Neese, *ORCA - An ab initio, Density Functional and Semi-empirical Program Package, version 2.8*; University of Bonn: Bonn, Germany, 2010.

[9] A. D. Becke, J. Chem. Phys. 84, 4524 (1986).

[10] J. P. Perdew, Phys. Rev. B 33, 8822 (1986).

[11] A. Schafer, H. Horn and R. Ahlrichs, J. Chem. Phys. 97, 2571 (1992).

[12] F. Weigend and R. Ahlrichs, Phys. Chem. Chem. Phys. 7, 3297 (2005).

[13] W. Kohn and L. J. Sham, Phys. Rev. A 140, 1133 (1965).

[14] F. Weigend and M. Haser, Theor. Chem. Acc. 97, 331 (1997).

[15] F. Weigend, M. Haser, H. Petzelt and R. Ahlrichs, Chem. Phys. Lett. 294, 143 (1998).

CHAPTER 5

CHAPTER 5

Study of the Flat (111)-(1×1) Surface

(111) Surface is the natural cleaving plane of diamond and shows one dangling bond per surface atom in its bulk terminated form as shown in Figure 5.1. In the present work, we consider the adsorption of a H/O/OH on a flat diamond (111) surface as the first step. A $C_{46}H_{39}$ cluster was used to calculate PES for flat diamond (111) surface. As we mentioned before, the plane of $\boldsymbol{z}$ = 0 Å was defined at the topmost layer of diamond (111) surface. We have performed DFT calculations to map out the total energy of the structure as a function of adatom position *E(x,y)*.

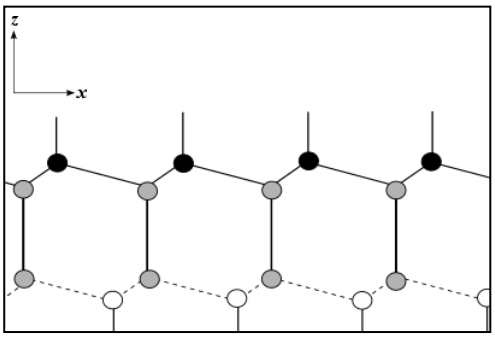

Figure 5.1. Diamond (111)-(1×1) surface with one dangling bond per surface carbon atom (side view).

5.1. Adsorption of Hydrogen atom

Numerous studies have suggested that one of the roles of the H atoms (which are present during typical CVD diamond growth) is to destabilize sp^2 bonding configuration on the growing diamond surface [1-3]. Hydrogen is capable of forming a single bond with a carbon atom in the sp^3 configuration on a diamond

(111) surface. This single bond results from σ overlap between the surface dangling bond perpendicular to the surface and a corresponding orbital of the adsorbent.

Figure 5.2 shows the contour plot of the potential energy variation *E(x,y)*, which is obtained by moving an H atom within the planes of z = 1.11 Å on the flat (111) surface. This value of z corresponds to the length of C–H bond, with the C–H bond pointing normal to the surface plane. The z value was determined by the calculations searching equilibrium bond lengths. These calculations will be discussed in section 5.1.1.

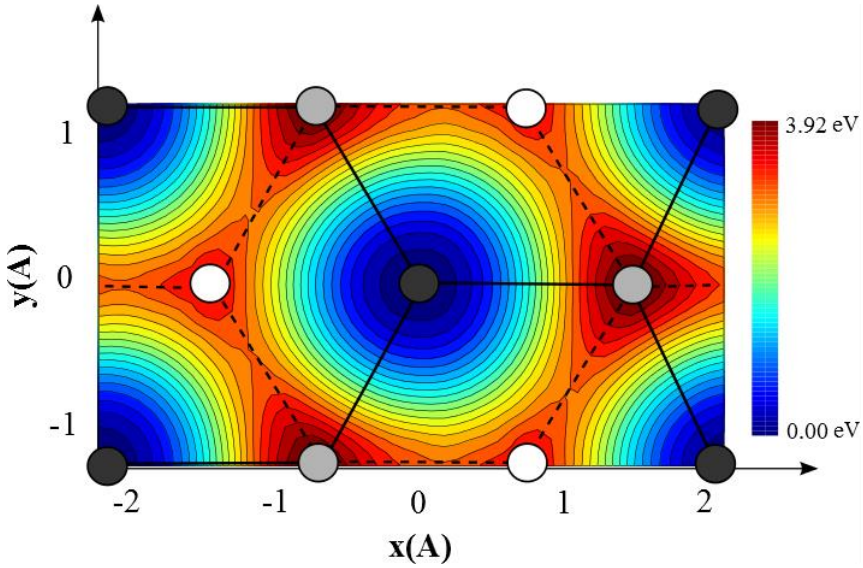

Figure 5.2. Contour map of dependence of the total energy on the position of the H adatom on flat surface at z= 1.11 Å. The represented area corresponds to the gray rectangle shown in Figure 4.1(a). The values of energy are relative ones.

The C–H bond length obtained in this study agrees with the value of 1.12 Å by Zhu and Louie [4] and 1.1255 Å from Stumpf and Marcus [5]. As shown in Figure 5.1, the energy minima (the most stable adsorption site) were obtained when the H adatom was located just above the topmost threefold C atoms that have dangling bonds, as shown schematically in Figure 5.3. This site called On-top site.

Since surface radical sites can be produced by hydrogen migration, such processes could be important. In fact, hydrogen migration plays an important role in the growth mechanism. H atoms were then found to migrate with energy dependent

on the path between neighboring sites, as well as dependent on different directions on the surface.

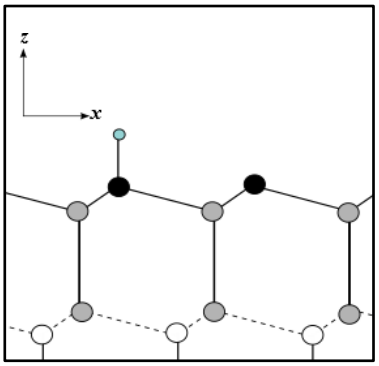

Figure 5.3. Diamond (111)–(1×1) surface with H adatom bonded to the topmost threefold C atom, the on-top site (side view).

From the result shown in Figure 5.2, the energy barrier heights E_A for migrating between adjacent threefold C atoms were calculated to be 2.98 eV for H atom. This value of E_A was evaluated as the difference between the energy at the site of minimum energy and the energy at the saddle point between the adjacent topmost C sites. This means that; for a hydrogen atom initially bonded to threefold carbon atom, the minimum energy profile for migration path obtained by computing the potential energy from on-top site to an adjacent radical site (the nearest potential minimum). This migration path has the lowest energy barrier of 2.98 eV.

The migration of an H atom on a diamond (111) surface has investigated theoretically by Chang *et al* [6] and Larsson *et al* [7]. The migration path with the lowest energy barrier obtained by Chang and co-workers for a migration between two adjacent carbon radical sites, by using classical variational theory, was 3.29 eV. Furthermore, Larsson *et al*. calculated migration barrier of H atoms to be 2.8 eV (270 kJ/mol) by *ab initio* calculations with second order Møller−Plesset (MP2) perturbation theory. The value of E_A for H atoms in the present work agrees fairly well with the results obtained in those previous studies.

5.1.1. Determination of (*z*) value for H adatom

The value of ***z*** was determined by some calculations searching equilibrium bond length:

1- First, by varying one reaction coordinate (***z***) in subsequent calculations, while the rest of the coordinates (*x*,*y*) for the adatom were changed freely in each calculation. Then, the height of the adatom from the surface (***z***) was roughly estimated to be ***z*** ≈ 1.1 Å. We have performed DFT calculations to map out the total energy of the structure as a function of adatom position *E(x,y)* at ***z*** = 1.1 Å, 1.5 Å, 1.7 Å and 2.0 Å. Figure 5.4 Shows contour maps of the total energy variation with the position of the H adatom on flat surface at these different values of ***z***.

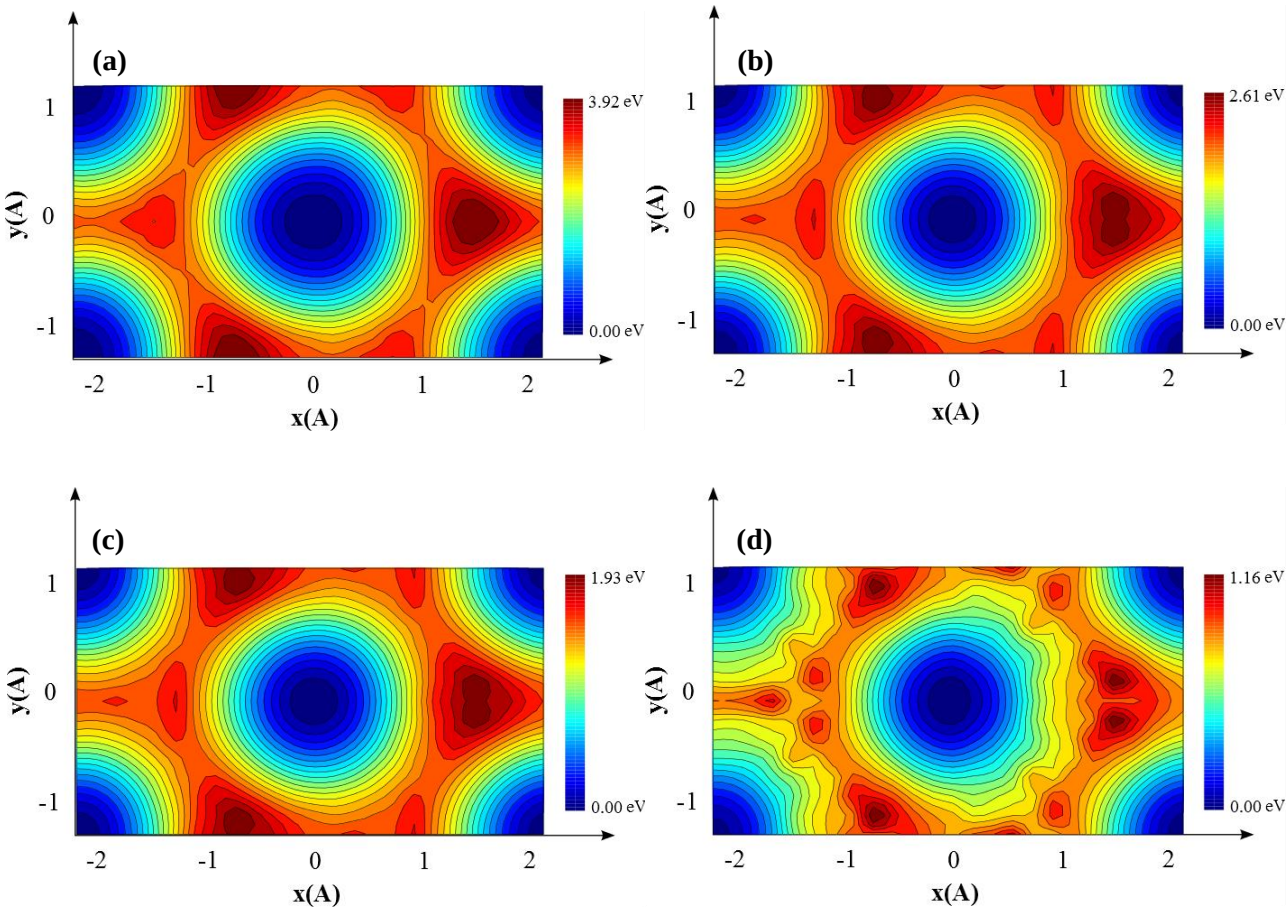

Figure 5.4. Contour map of dependence of the total energy on the position of the H adatom on flat surface at **(a)** ***z***= 1.1 Å, **(b)** ***z***= 1.5 Å, **(c)** ***z***= 1.7 Å, **(d)** ***z***= 2.00 Å. The represented area corresponds to the gray rectangle shown in Figure 4.1(a). The values of energy are relative ones.

It is evident from these contour maps for different values of ***z*** that the energy minima were obtained when the H adatom was located just above the topmost threefold C atoms that have dangling bonds (on-top site). By studying the variation of total energy at this site with respect to the height ***z*** of the H adatom from the surface, the optimal height of the adatom from the surface (***z***) was roughly estimated to be about ***z*** ≈ 1.1 Å, as shown in Figure 5.5.

2- Second, the more exact height ***z*** of H adatom on diamond surface (the equilibrium bond length) was obtained by performing optimization calculation for flat diamond cluster with H adatom on the bare surface. All atomic layers were allowed to relax, except the last three layers (including H-terminating layer) were fixed at their bulk position. The minimum energy configuration of H atom diffusion on flat diamond (111) surface was found to be at *z* = 1.11Å.

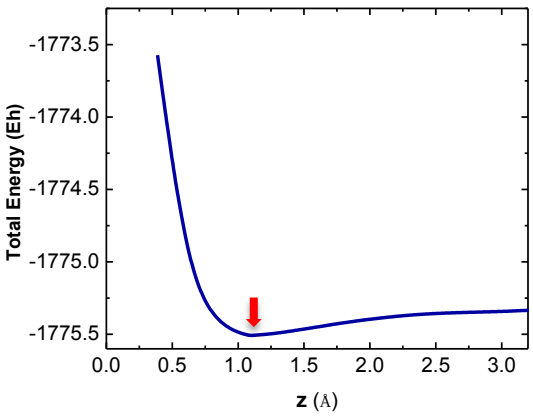

Figure 5.5. Energy variation with respect to height ***z*** of H adatom at the on-top site on flat (111) surface.

5.2. Adsorption of Oxygen atom

For O atom, same procedure was done to calculate the potential energy surface of its diffusion on flat diamond (111)-(1×1) surface. Figure 5.4 shows the contour plot of the potential energy variation, which is obtained by moving an O atom within the planes of ***z*** = 1.33 Å on the flat (111) surface. This value of ***z***

corresponds to the length of C–O bond, and was determined by the same procedure of calculations searching equilibrium bond lengths as in H adatom case.

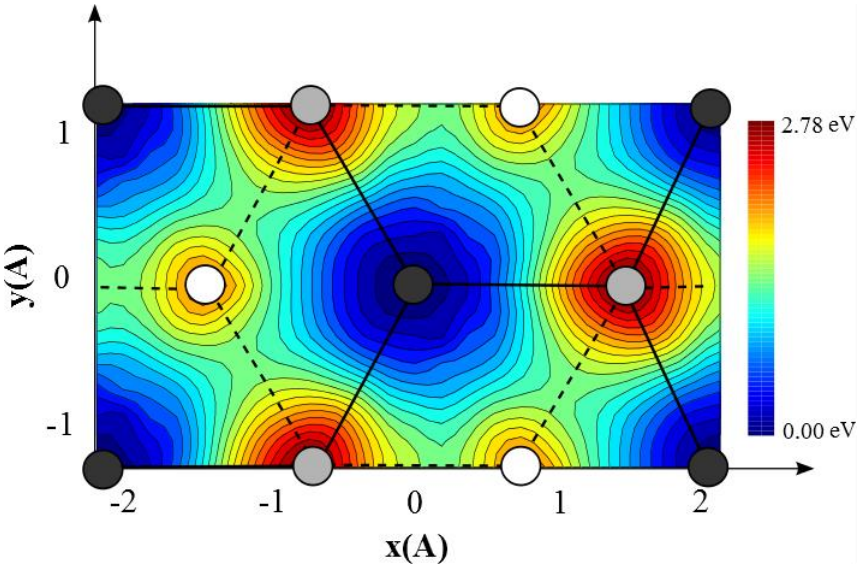

Figure 5.6. Contour map of dependence of the total energy on the position of the O adatom on flat surface at ***z***= 1.33 Å. The represented area corresponds to the gray rectangle shown in Figure 4.1(a). The values of energy are relative ones.

The C–O bond length of 1.33 Å is slightly shorter than the experimental value of 1.36 Å reported by Lide *et al.* [8] for paraffinic compounds, but considered to be reasonable enough. Also, it was found that the most stable adsorption site (energy minima) of atomic O is the On-top site, where the O adatom located just above the topmost threefold C atoms. This is in good agreement with a periodic DFT calculations carried out by Loh *et al.* [9] which had investigated the interaction of atomic O and C (111)-oriented diamond. Their theoretical results suggest that the on-top site for the 1 × 1 surface is the local energy minima and the C-O bond lengths were determined to be 1.326 Å. Also, Zheng *et al.* [10] reported that the C-O bond length of the optimized (1×1) on-top geometry is determined by using the SLAB-MINDO molecular orbital method to be 1.34 Å. Recently, Derry and co-workers [11] studied O adsorption on the (1×1) C(111)surface by using a molecular dynamics simulation. They reported that, the C–O bond of 1.304 Å on the (1 × 1) surface occurs for the 1/3 ML-on-top site and of 1.324 Å occurs for the full ML-on-top site. They found that, generally, the on-top site was found to be the most stable bonding site for O atoms on the (1 × 1) surface.

From the contour map shown in Figure 5.6, the energy barrier heights E_A for migrating of O adatom between adjacent threefold C atoms were calculated to be 1.42 eV. The value of E_A was also evaluated as the difference between the energy at the site of minimum energy and the energy at the saddle point between the adjacent topmost C sites. As for O adatom, the energy barrier heights for surface migration seem to be scarcely reported yet with respect to O adatoms on the diamond (111) surface.

5.2.1. Determination of (*z*) value for O adatom

The value of ***z*** for O adatom was determined by same calculations, as in H adatom case, searching equilibrium bond length:

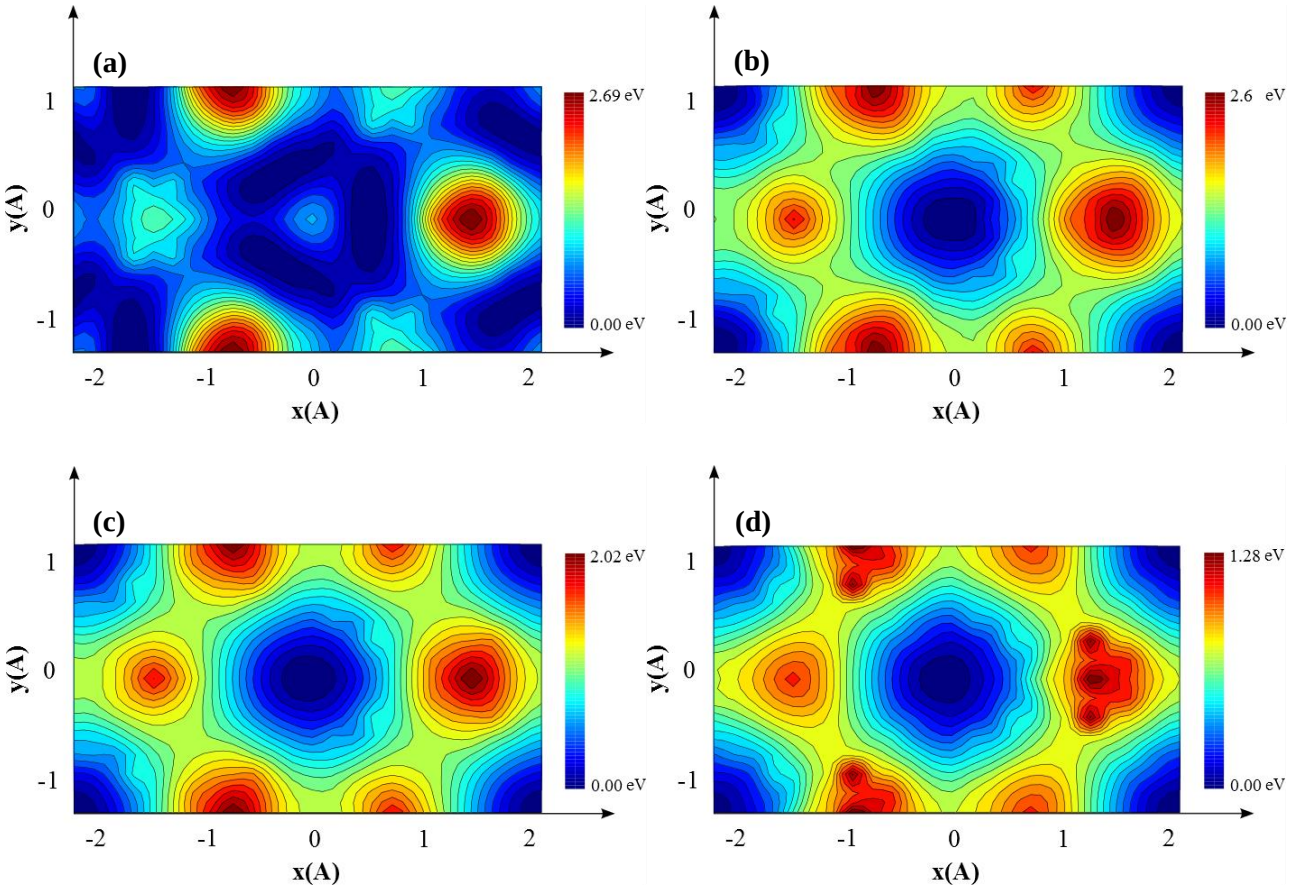

Figure 5.7. Contour map of dependence of the total energy on the position of the O adatom on flat surface at **(a)** ***z***= 1.1 Å, **(b)** ***z***= 1.5 Å, **(c)** ***z***= 1.7 Å, **(d)** ***z***= 2.00 Å. The represented area corresponds to the gray rectangle shown in Figure 4.1(a). The values of energy are relative ones.

1- First, by varying one reaction coordinate (***z***) in subsequent calculations, while the rest of the coordinates (*x*,*y*) for the adatom were changed freely in each calculation. The height of the adatom from the surface (***z***) was roughly estimated to be ***z*** ≈ 1.38 Å. We have performed DFT calculations to map out the total energy of the structure as a function of O adatom position *E(x,y)* at ***z*** = 1.1 Å, 1.5 Å, 1.7 Å and 2.0 Å. Figure 5.7 Shows contour map of the total energy variation with the position of the O adatom on flat surface at these values of ***z***.

These contour maps for different values of ***z*** in Figure 5.7 show that the energy minima were obtained when the O adatom was located just above the topmost threefold C atoms that have dangling bonds (on-top site). By plotting the variation of total energy at on-top site with respect to the height ***z*** of the O adatom from the surface, the optimal height of the adatom from the surface (***z***) was roughly estimated to be about ***z*** ≈ 1.38 Å, as shown in Figure 5.8.

2- Second, optimization calculation was performed for flat diamond cluster with O adatom on the bare surface to estimate the equilibrium bond length (the exact height ***z***) of O adatom on diamond surface. All atomic layers were allowed to relax, except the last three layers (including H-terminating layer) were fixed at their bulk position. The minimum energy configuration of O atom diffusion on flat diamond (111) surface was found to be at ***z*** = 1.33 Å.

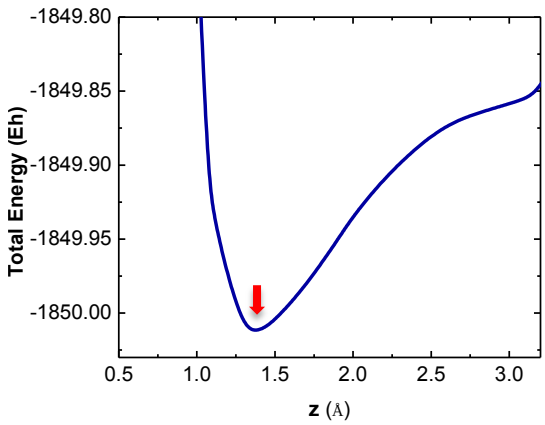

Figure 5.8. Energy variation with respect to height ***z*** of O adatom at the on-top site on flat (111) surface.

5.3. Comparison between Hydrogen and Oxygen adsorption

5.3.1. Energy barrier

The value of energy barrier E_A = 1.42 eV for O adatom obtained in the present study was considerably lower than that for H adatom which was E_A = 2.98 eV. We consider that these results are due to the divalent nature of neutral O atom. This can be explained through analysis of the volumetric data of spin density distribution which is provided in the next section.

5.3.2. Spin density distribution

After a careful analysis of the volumetric data of spin density distribution, it was found that the O adatom at the midpoint (bridging position) of two C dangling bond sites terminates the two dangling bonds almost completely, as shown in Figure 5.9.(f). Whereas, the H adatom at the same position does not cancel the C dangling bonds so efficiently because of its monovalent nature (Figure 5.9.(c)).

In general, since the unpaired electrons of dangling bonds have higher energy than bonding electrons, the total energy of the system should be lowered. Therefore, it could be concluded that the O adatom lowers the energy barrier E_A through the efficient termination of the two C dangling bonds in their migrating pathways.

5.3.3. Surface diffusion coefficient

In principle, the energy surface *E(x,y)* contains all the important physics of surface diffusion. A simple analysis of such an energy surface yields the surface diffusion activation energies. Once determined, the activation energies can serve as input data for calculating surface diffusion coefficient. Based on the potential barrier heights of H and O adatom for migrating between adjacent threefold C atoms on the flat surface, surface diffusion coefficients *D* by thermal activation can be calculated from this equation:

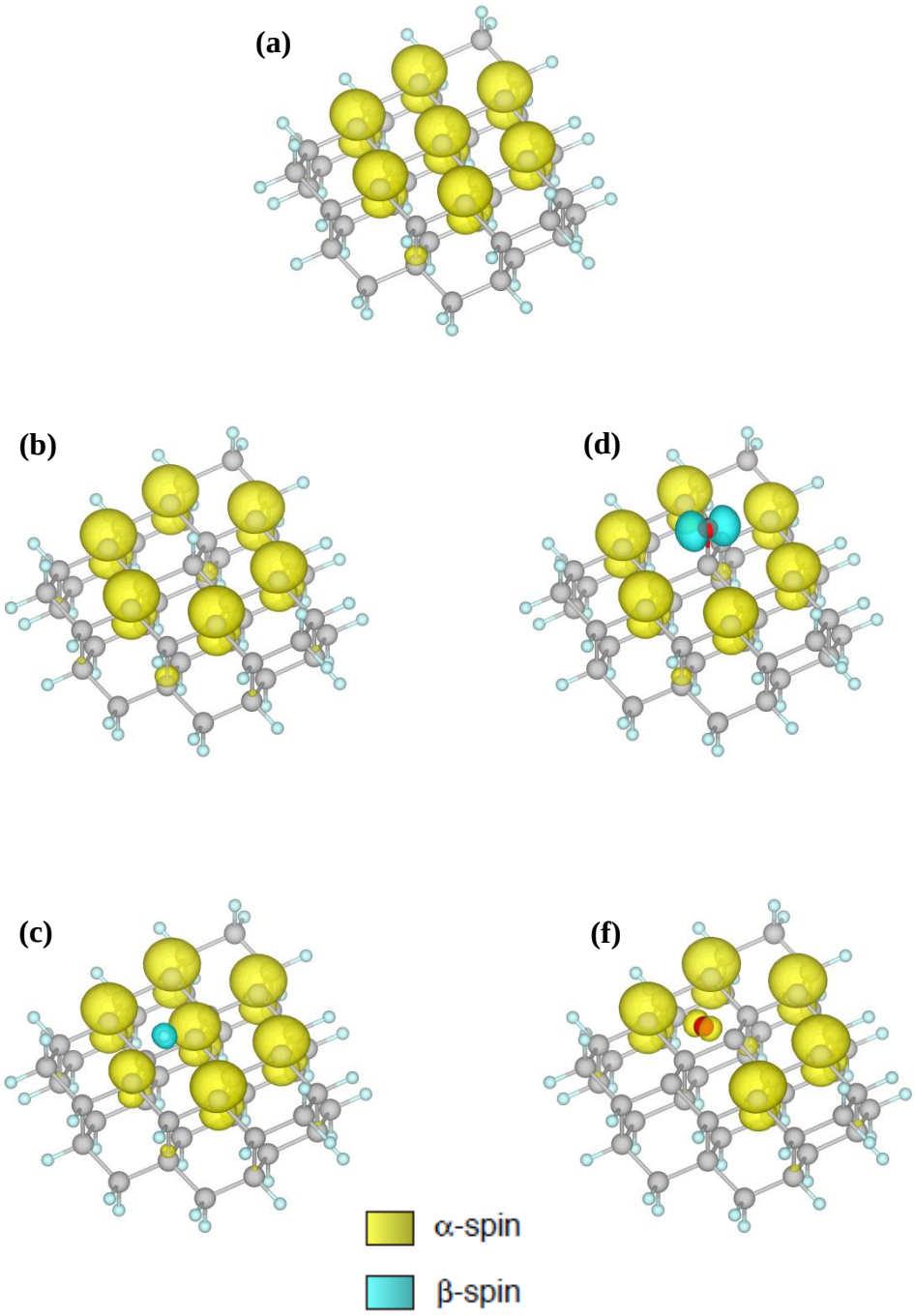

Figure 5.9. Spin density distribution of (111)-(1×1) surface **(a)** bare surface with one dangling bond for each threefold C atom, **(b)** H adatom on the surface at the on-top site (C atom with one dangling bond), **(c)** H adatom on the surface at the midpoint between two C dangling bond sites, **(d)** O adatom on the surface at the on-top site (C atom with one dangling bond), and **(f)** O adatom on the surface at the midpoint between two C dangling bond sites.

$$D = \frac{a^2}{2\tau} \tag{5.1}$$

where,

$$\tau^{-1} = f = Z\,\nu\,exp(-\frac{E_A}{k_B T}) \tag{5.2}$$

a is the inter-site distance (a = 2.52 Å), τ is hopping rate, f is frequency factor, ν is the frequency of trial, Z is the number of hopping sites (Z = 6), E_A is the activation energy, T is the temperature and k_B is Boltzmann constant. As the frequency ν, we adopt the frequency of bending modes of C–H and C–O bonds, calculated also by ORCA.

The calculated values of D are shown in Table 5.1. At 900K, the values of D were estimated to be $3.9\text{x}10^{-19}$ cm^2/s and $6.4\text{x}10^{-11}$ cm^2/s for H and O atoms, respectively. This result suggest that O adatom migrate more easily than H adatom on flat C (111) surface.

		Hydrogen	Oxygen
Vibration Frequency (C-X bending mode)		$\sim 10^{13}\ s^{-1}$	$\sim 3\times10^{12}\ s^{-1}$
Activation Energy E_A		2.98 eV	1.42 eV
Frequency Factor f	(300K)	$5.2\times10^{-37}\ s^{-1}$	$2.5\times10^{-11}\ s^{-1}$
	(900K)	$1.2\times10^{-3}\ s^{-1}$	$2.0\times10^{5}\ s^{-1}$
Diffusion Coefficient D	(300K)	1.7×10^{-52} cm²/s	8.0×10^{-27} cm²/s
	(900K)	3.9×10^{-19} cm²/s	6.4×10^{-11} cm²/s
Diffusion Length per second	(300K)	1.8×10^{-19} nm/s	1.3×10^{-6} nm/s
	(900K)	8.8×10–3 nm/s	1.1×102 nm/s

Table 5.1. Vibration frequency, activation energy, frequency factor, diffusion coefficient, and diffusion length, $\sqrt{2Dt}$, evaluated for the H and O adatoms on the diamond (111) surface at 300 K and 900 K.

5.4. Adsorption of Hydroxyl group

Same procedure was done to calculate the potential energy surface of OH group diffusion on flat diamond (111)-(1×1) surface. Figure 5.10 shows the contour plot of the potential energy variation, which is obtained by moving an OH group within the planes of ***z*** = 1.42 on the flat (111) surface. This value of ***z*** corresponds to the length of C–OH bond, and was determined by the same procedure of calculations searching equilibrium bond lengths as in H/O adatom cases. The C–OH bond length obtained in this study agrees with the value of 1.41 Å by Petrini and Larsson [12].

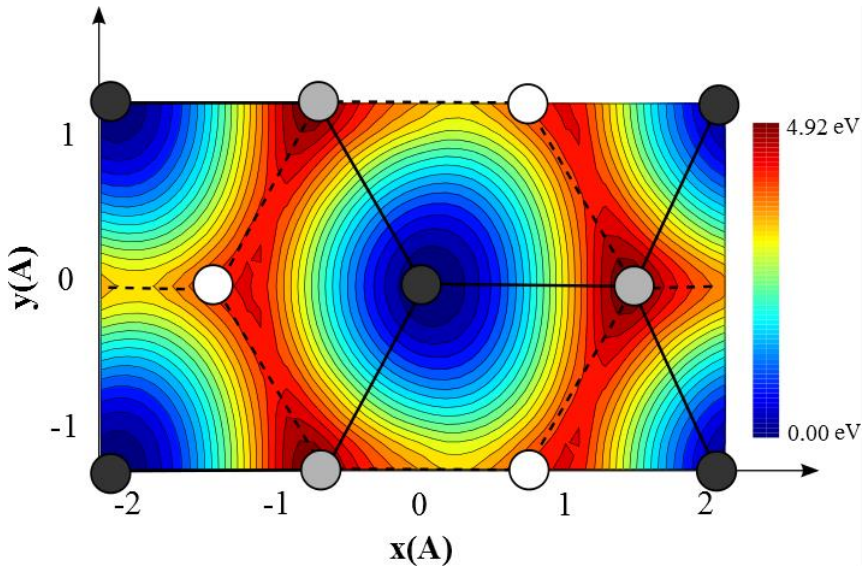

Figure 5.10. Contour map of dependence of the total energy on the position of the OH group on flat surface at ***z***= 1.42 Å. The represented area corresponds to the gray rectangle shown in Figure 4.1(a). The values of energy are relative ones.

Figure 5.10 shows that the energy minima (the most stable adsorption site) were obtained when the OH group was located just above the topmost threefold C atoms (on-top site). This is in agreement with first principle DFT calculations of Stampfl *et al.* [13]. They reported that the on-top site is the most stable for OH on the C(111)–(1 × 1) for all converges. C–OH bond lengths average from 1.422 Å to 1.43 Å for different converges. Larsson [14] examined this surface by using the density-functional theory (DFT). His calculations showed that there was

energetically no probability for a gaseous OH species to be chemisorbed at a final bridge site. The OH species started to migrate from the initial bridge positions to a neighboring on-top position during the geometry optimization procedure.

From the result shown in Figure 5.10, the energy barrier heights E_A for migrating between adjacent threefold C atoms were calculated to be 4.09 eV for OH group. This value of E_A was evaluated as the difference between the energy at the site of minimum energy and the energy at the saddle point between the adjacent topmost C sites.

Figure 5.11 shows the orientation direction of OH group adsorbed at on-top site on flat (111)-(1×1) surface after optimization. For the optimized structure, the C–O–H angle was 105.8 º. This agrees well with the results of Stampfl *et al.* [13] who investigate the adsorption of OH group on C(111) surface. They reported that the orientation of the C–OH bond changes with different coverages on (111) surface to in order to accommodate the repulsive Coulombic effects. They also notice that the OH groups are oriented differently on the different atom rows on both the (2 × 1) surface and the (1 × 1) surface.

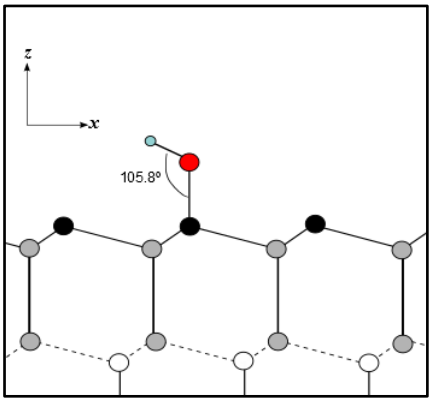

Figure 5.11. Side view of the optimized diamond (111)-(1×1) surface with OH group adsorbed at the on-top site (the topmost threefold C atom).

5.4.1. Determination of (*z*) value for OH group

The value of ***z*** for OH adspices was determined by same calculations as that for H/O adatoms, searching equilibrium bond length:

1- First, varying one reaction coordinate (***z***) in subsequent calculations, while the rest of the coordinates (*x*,*y*) for the adatom were changed freely in each calculation. The height of the adatom from the surface (***z***) was roughly estimated to be ***z*** ≈ 1.5 Å. We have performed DFT calculations to map out the total energy of the structure as a function of OH group position *E(x,y)* at ***z*** = 1.1 Å, 1.5 Å, 1.7 Å and 2.0 Å. Figure 5.12 Shows contour map of the total energy variation with the position of the OH group on flat surface at these values of ***z***.

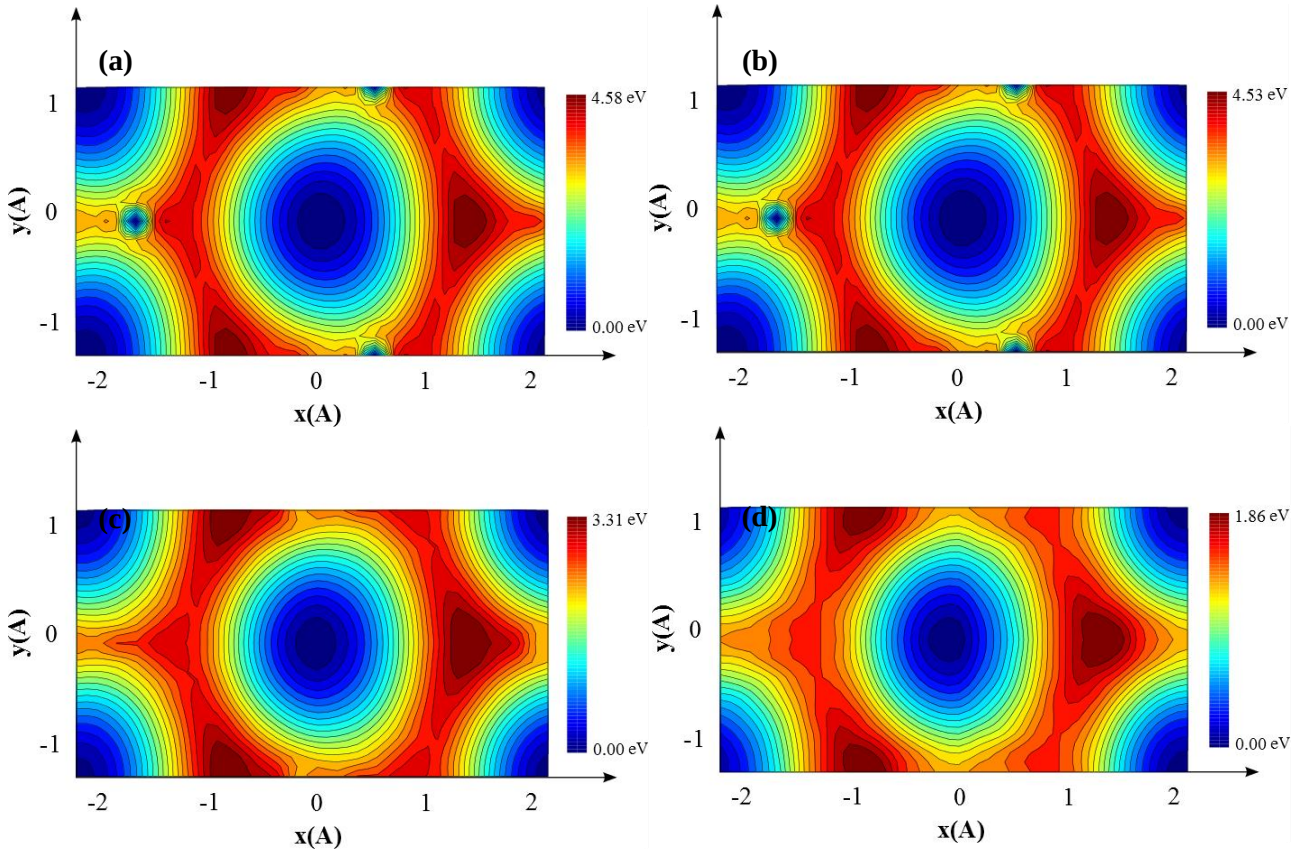

Figure 5.12. Contour map of dependence of the total energy on the position of the OH group on flat surface at **(a)** ***z***= 1.1 Å, **(b)** ***z***= 1.5 Å, **(c)** ***z***= 1.7 Å, **(d)** ***z***= 2.00 Å. The represented area corresponds to the gray rectangle shown in Figure 4.1(a). The values of energy are relative ones.

These contour maps for different values of ***z*** in Figure 5.12 show that the energy minima were obtained when the OH group was located just above the topmost threefold C atoms that have dangling bonds (on-top site). By plotting the variation of total energy at on-top site with respect to the height ***z***

of the O adatom from the surface, the optimal height of the adatom from the surface (***z***) was roughly estimated to be about ***z*** ≈ 1.5 Å, as shown in Figure 5.13.

2- Second, optimization calculation was performed for flat diamond cluster with OH group on the bare surface to estimate the equilibrium bond length (the exact height ***z***) of OH group on diamond surface. All atomic layers were allowed to relax, except the last three layers (including H-terminating layer) were fixed at their bulk position. The equilibrium bond length of OH group diffusion on flat diamond (111) surface was found to be ***z*** = 1.42 Å.

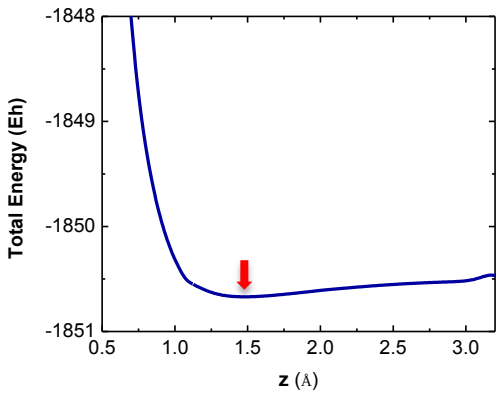

Figure 5.8. Energy variation with respect to height ***z*** of OH group at the on-top site on flat (111) surface.

References

[1] R. E. Clausing, L. L. Hostou, J. C. Angus, and P. Koidl, *Diamond and Diamond Like Films and Coatings*, (Plenum, New York, 1991).

[2] J. P. Dismukes and K. V. Ravi, *Proceedings of the Third International Symposium on Diamond Materials*, (The Electrochemical Society, New Jersey, 1993), Vol. 93, p. 17.

[3] F.G. Celii and J.E. Butler, Ann. Rev. Phys. Chem. 42, 643 (1991).

[4] X. Zhu and S.G. Louie, Phys. Rev. B 45, 3940 (1992) .

[5] R. Stumpf and P.M. Marcus, Phys. Rev. B 47, 16016 (1993).

[6] X. Y. Chang, D. L. Thompson, and L. M. Raff, J. Chem. Phys. 100, 1765 (1994).

[7] K. Larsson and J.-O. Carlsson, Phys. Rev. B 59, 8315 (1999).

[8] D. R. Lide, *CRC Handbook of Chemistry and Physics* (CRC Press, Boston, MA, 1992) 71st ed.

[9] K. P. Loh, X. N. Xie, S. W. Yang and J. C. Zheng, J. Phys. Chem. B 106, 5230 (2002).

[10] X. M. Zheng and P. W. Smith, *Surf. Sci.* 262, 219 (1992).

[11] T. E. Derry, N.W. Makau and C. Stampfl, J. Phys.: Condens. Matter 22, 265007 (2010).

[12] D. Petrini and K. Larsson, *J. Phys. Chem. C 112*, 3018 (2008).

[13] C. Stampfl, T. E. Derry and N. W. Makau, J. Phys., Condens. Matter 22, 475005 (2010).

[14] K. Larsson, New Diamond and Frontier Carbon (Special Issue: Surface Related Physics and Applications of Diamond") 15, 229 (2005).

CHAPTER 6

CHAPTER 6

Study of the Stepped (111)-(1×1) Surface

For stepped surface, we present an ab initio molecular orbital calculation of monoatomic height step on a C (111) surface with ideal, bulk terminated bond lengths and angles. $C_{68}H_{47}$ cluster model (shown in Figure 4.1) was used in the calculations of the stepped surface. The carbon atoms at the edge of the step have two dangling bonds. ***z*** = 0 Å plane was defined at the topmost layer of the lower terrace of diamond (111) surface.

In order to compare the stepped surface with flat surface, the heights of H, O adatoms and OH group on stepped surface were fixed to 1.1 Å, 1.33 Å and 1.42 Å, respectively, that is, the same ***z*** value as those of the calculations for the flat surface.

6.1. Adsorption of Hydrogen atom

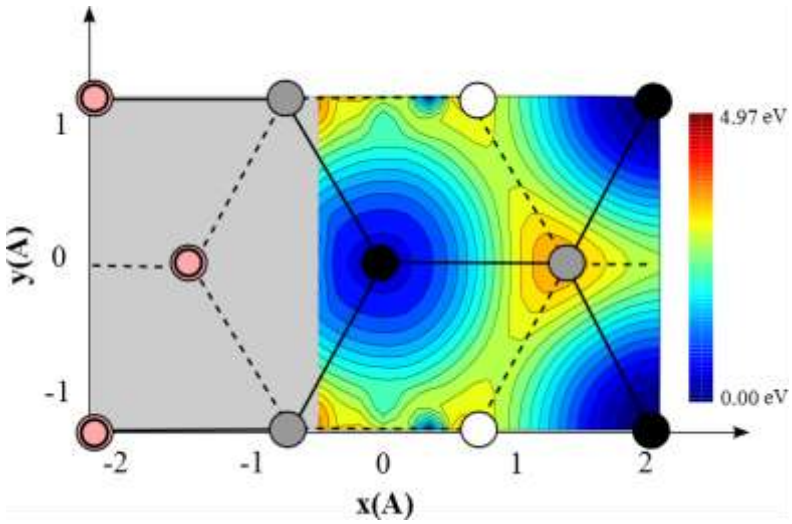

Figure 6.1. Contour map of dependence of the total energy on the position of the H adatom on stepped surface at ***z***= 1.11 Å. The represented area corresponds to the gray rectangle shown in Figure 4.1(b). The values of energy are relative ones.

For H adatom, the contour plots of the potential energy near the step edge were shown in Figure 6.1. This figure shows the potential energy of H adatom as a function of position on the lower terrace of the step within the planes of z = 1.11 Å on the (111) surface. It was found that the minima of the potential energy appear in the vicinity of the position just above the threefold C atom, same as in the flat surface case.

6.2. Adsorption of Oxygen atom

Figure 6.2 shows the potential energy of O adatom as a function of position on the lower terrace of the step within the planes of z = 1.33 Å on the (111) surface near the step edge. The minima of the potential energy appear in the vicinity of the position just above the threefold C atom (on-top site), as well as for the flat surface.

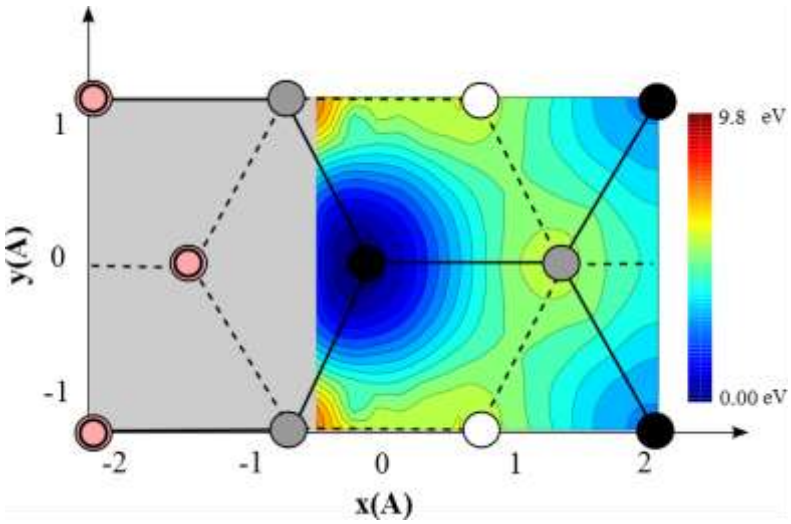

Figure 6.2. Contour map of dependence of the total energy on the position of the O adatom on stepped surface at z= 1.33 Å. The represented area corresponds to the gray rectangle shown in Figure 4.1(b). The values of energy are relative ones.

6.3. Adsorption of Hydroxyl group

For OH group, the contour plot of the potential energy near the step edge as a function of position on the lower terrace of the step within the planes of z = 1.42 Å

on the (111) surface are shown in Figure 6.3. This figure shows that the minima of the potential energy appear in the vicinity of the position just above the threefold C atom, as in the case of flat surface with OH group.

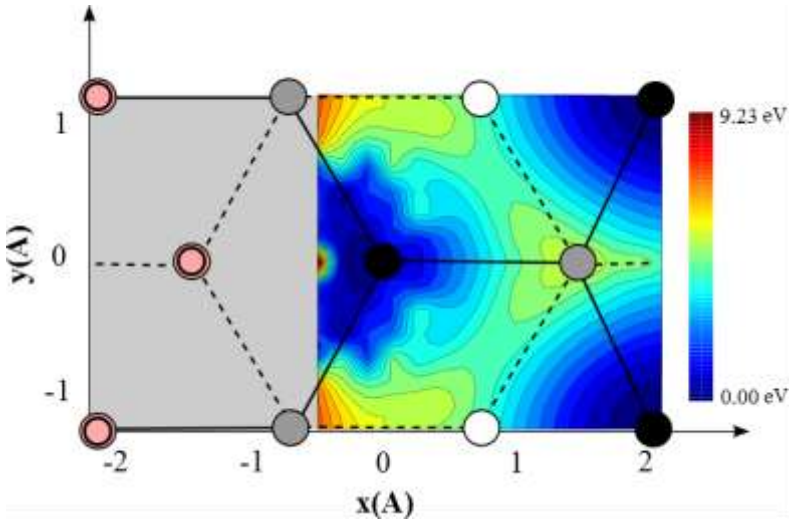

Figure 6.3. Contour map of dependence of the total energy on the position of the OH group on stepped surface at ***z***= 1.42 Å. The represented area corresponds to the gray rectangle shown in Figure 4.1(b). The values of energy are relative ones.

6.4. Comparison between flat and stepped 111 surface

To compare the stepped surface with flat surface, we will call Figures 5.2, 5.4, 5.6 for PES contour map of H/O/OH on flat surface besides Figures 6.1, 6.2, 6.3 for H/O/OH on stepped surface (all are collected in Figure 6.6 for comparison).

Figure 6.4 shows the variation of potential energy for H ,O adatoms and OH group with respect to their position along *x* axis at *y* = 0.0 Å for flat and stepped (111) surfaces. Each curve in Figure 6.4 was conformed in the side far from the step edge in order to clarify the difference near the step.

At stepped (111) surface, the potential energy above threefold C site close to the step increases by ~0.7 eV for the H adatom, whereas it decreases by ~2.6 eV for the O adatom, in comparison with those in the flat surface. This means that the O adatom adsorbed on diamond (111) surface favor to be trapped near an atomic step

after migration at high temperatures. In the case of OH group, there is not much difference between flat surface and near the step. The potential energy above threefold C site close to the step decreases by ~0.17 eV in comparison with those in the flat surface.

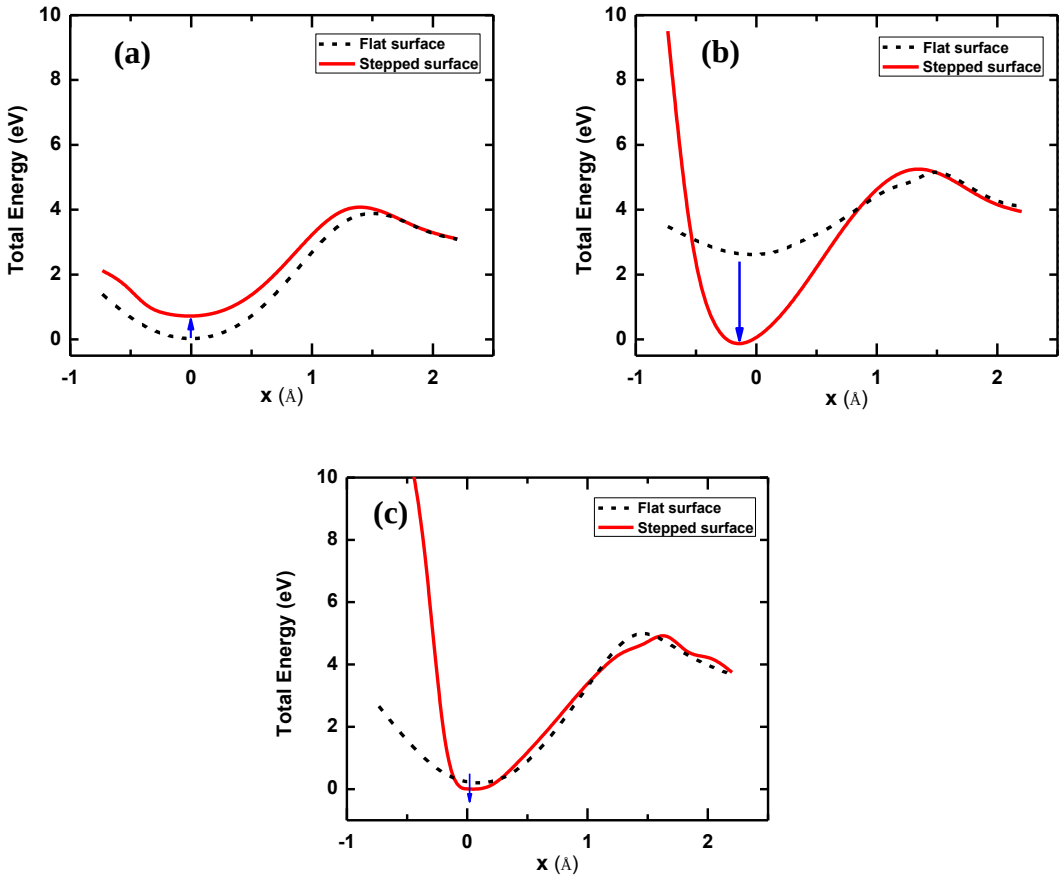

Figure 6.4. Energy dependence along *x* axis at *y*=0.0 Å for **(a)** H adatom at ***z*** = 1.11 Å, **(b)** O adatom at ***z*** = 1.33 Å, **(a)** OH group at ***z*** = 1.42 Å, on flat and stepped (111) surface.

These differences in behavior between the H and O adatoms can be understood from the viewpoint of their valencies. The divalent O atom located near the step edge interacts with not only the C dangling bonds on the lower terrace but also that protruded from the step edge. In Figure 6.5, it is shown that the atomic arrangement which decreases the lowest total energy for oxygen adatom near an atomic step and increases it for hydrogen. The oxygen atom is in a bridging position between two carbon atoms. As for H adatom, the C dangling bond at the step edge

would bring about a repulsive Coulomb force that increases the total energy of the system.

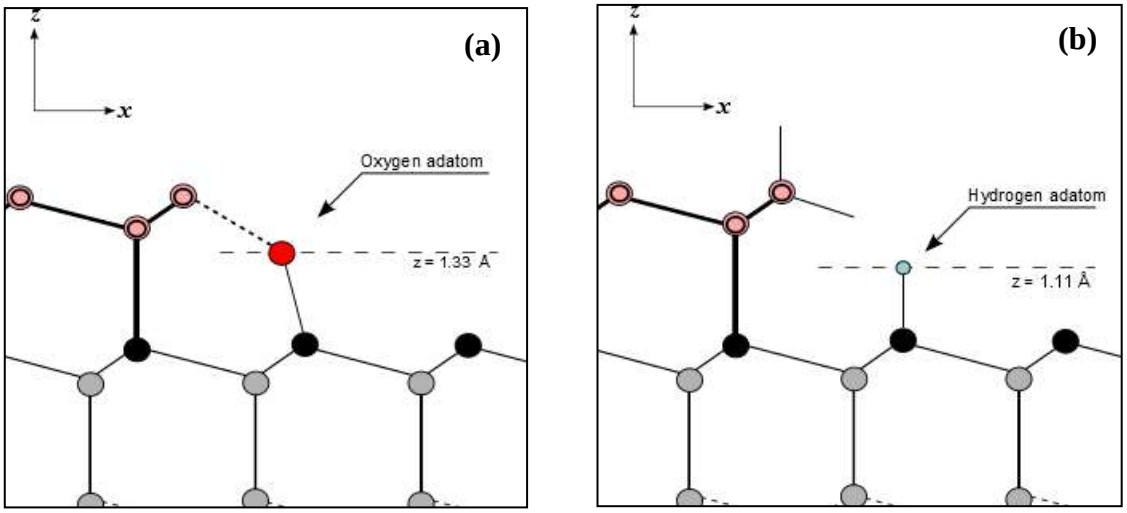

Figure 6.5. Cross sectional view in *x*-*z* plane for the atomic arrangement which **(a)** decrease the lowest total energy for oxygen adatom near an atomic step in Figure 6.4(b), and **(b)** increase lowest total energy for hydrogen in Figure 6.4(a).

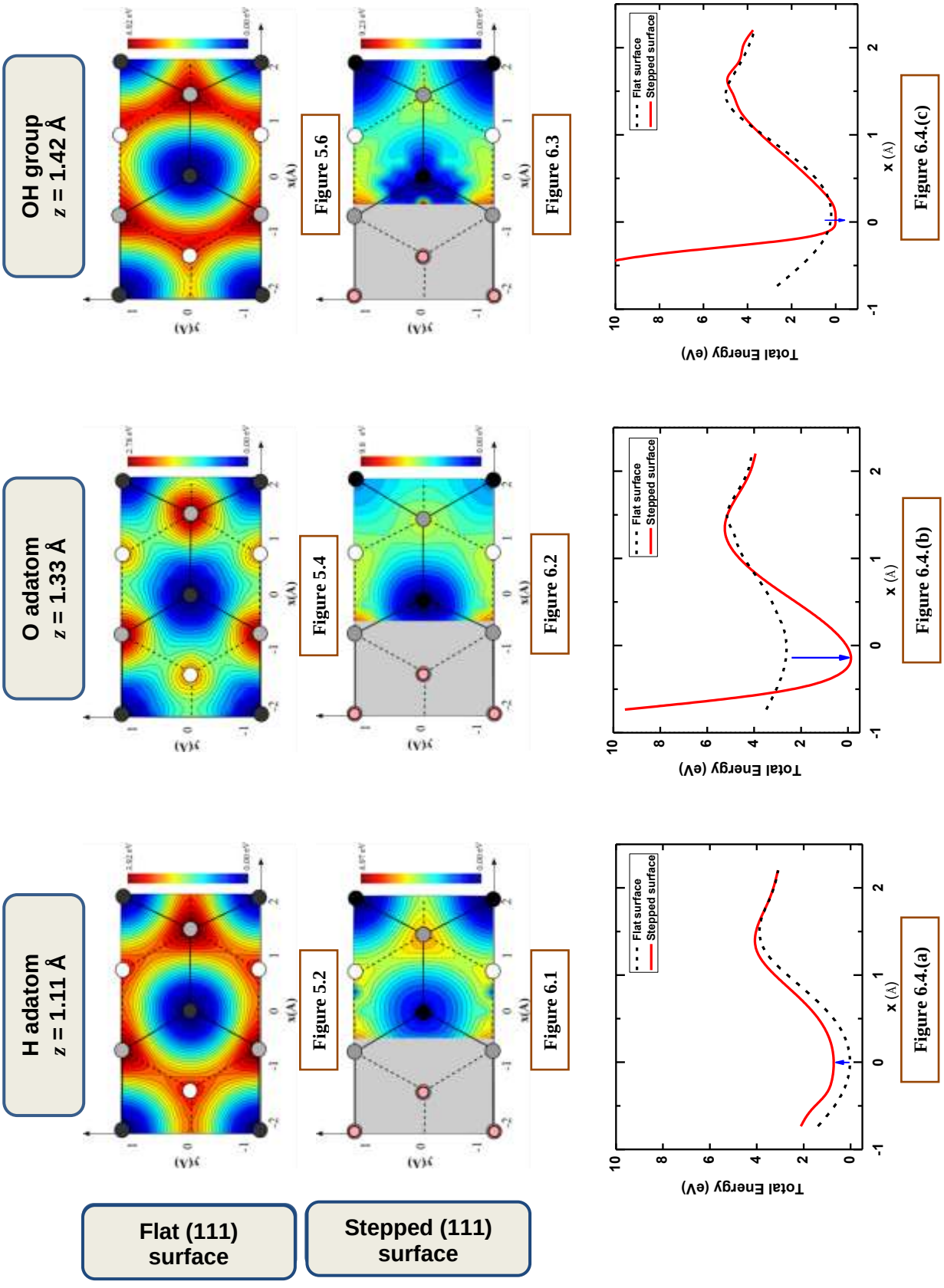

Figure 6.6. Summery for comparison between flat and stepped (111) surface by recalling Figures 5.2, 5.4, 5.6,6.1,6.2 and 6.3, as well as Figure 6.4.

CHAPTER 7

CHAPTER 7

Study of Relaxation in Stepped (111)–(1×1) Surface

We have performed optimization calculation for stepped diamond cluster with presence of H/O/OH on diamond (111)–(1×1) surface in order to study the relaxed stepped surface. All atomic layers were allowed to relax, except the highlighted layers shown in Figure 7.1 were kept fixed at their bulk positions in order to hold the characteristics of the crystal.

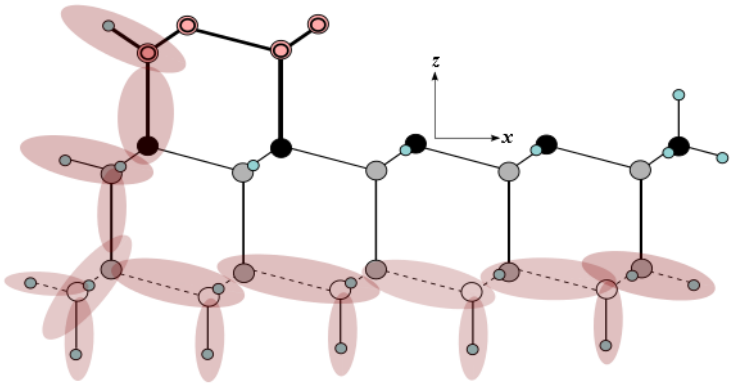

Figure 7.1. Side view of $C_{68}H_{47}$ cluster used for the calculation in a stepped (111) surface. The highlighted atoms and bonds were kept fixed at their bulk positions during optimization calculations.

7.1. Adsorption of Hydrogen atom

For H atom, we have examined it on relaxed stepped diamond (111) surface. After relaxation, the minimum energy configuration was found to be at $\boldsymbol{z}$ = 2.79 Å. It was found that the most stable site for H atom on stepped model is point X, as shown in Figure 7.2, where carbon atom is located at the step edge. This site called step-edge site. C-H bond length was 1.104 Å which was a little shorter than that at

relaxed flat surface (1.11 Å). C−H angle was about 113.7º. Hydrogen atoms interact with the stepped surface carbon atoms to form single C–H bonds.

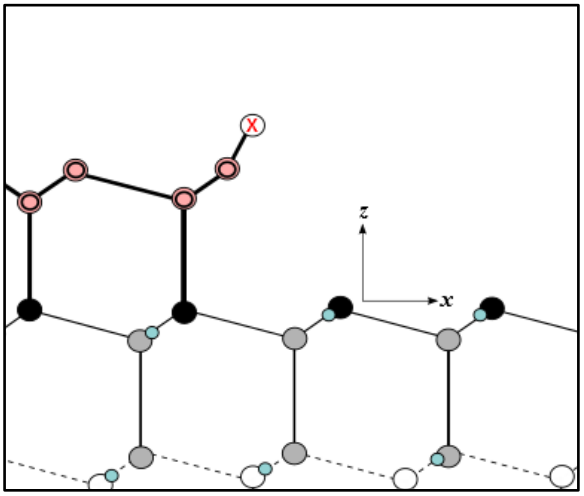

Figure 7.2. Diamond (111)–(1×1) stepped surface with adatom at site X, bonded to step-edge C atom (side view).

Alfonso *et al* [1] has found that atomic H adsorption on all the step surfaces is energetically favorable with respect to the unhydrogenated substrate. Davison and Pickett [2] have applied a tight binding calculation to a C (111) surface step. According to their analysis, the surface H bond at the step is the strongest H bond. The weaker H bonds, which would be more likely to break, are the ones attached to terrace atoms. They also reported that the terrace H bonds were 1.126 Å and the step H bonds were slightly shorter at 1.124 Å. Also, Frenklach [3] has reported that all C-H bond lengths are 1.11 Å for flat C (111)–(1×1) and on the step they are 0.005 Å shorter than on the flat part. In this work by Frenklach, a diamond surface covered by radical and diradical sites was studied by a Monte Carlo kinetic method. Two gas-surface reactions were then assumed to govern the formation of surface radicals: abstraction of a surface hydrogen atom by an impinging hydrogen atom, and the addition of a gaseous hydrogen atom to the surface radical formed. The results showed that there is a large probability for a surface radical on a diamond (111) surface to have an adjacent radical site. In our investigation it will be assumed that the stepped morphology of the diamond (111) surface is also activated through reactions with atomic hydrogen from the gas phase, resulting in the formation of

diradical surface sites at the step. Energy barrier E_A for H migration on stepped C(111) surface to an adjacent diradical site (a step-edge site) was calculated to be 2.48 eV. This value of E_A was evaluated as the difference between the energy at the site of minimum energy and the energy at the saddle point between the adjacent step-edge sites.

Hydrogen adsorption is an exothermic process since the energy gained by forming an extra C-H bond at the edge is higher than the step-formation energy [4]. However, only on adsorption of atomic hydrogen will the energy difference be high enough to overcome an eventual barrier. Therefore, only atomic H will induce step formation on the C (111) surface as observed by Pate [5]. So, exposure of C (111) to atomic hydrogen can lead to a roughening of the surface.

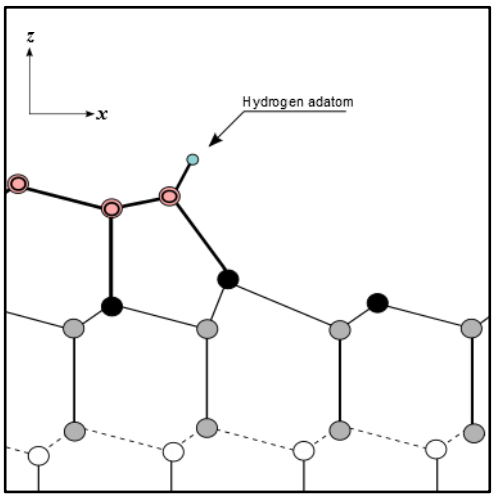

Figure 7.3. Relaxed step surface with H adatom (side view).

It was observed in the relaxed cluster that the carbon atom at the step edge, which is bonded to H adatom, is reconstructed to lower the surface energy and numbers of dangling bonds on the surface, and forms a downward slope in the $(11\bar{2})$ direction as shown in Figure 7.3. By this way, stepped diamond (111) surface become more stable against hydrogen plasma etching because it became monohydrided surface. This is consisting with experimental observation by Sasaki and Kawarada [6] and by Tokuda *et al.* [7]. Tokuda *et al.* also reported reconstruction of H-terminated stepped (111) surface.

7.2. Adsorption of Oxygen atom

We have also examined relaxation of stepped diamond (111)–(1×1) surface with presence of O adatom on the bare surface. The minimum configuration of O atom diffusion on stepped C (111) surface after relaxation was found at ***z*** = 3.16 Å. The most stable site for O atom is located also at the step edge, X site (Figure 7.2). Because carbon atom at the edge of step has two dangling bonds, O atom forms double bond with carbon atom at the step edge. C=O bond length was 1.22 Å (little shorter than C−O bond length at relaxed flat surface which was 1.33 Å) and C=O angle was 123.1 º.

Energy barrier for O migration on stepped C (111) surface was found to be 3.83 eV. The high barrier for migration prevents an adsorbed O atom to move more or less freely over the surface. This high barrier can be explained by the increase in C=O bond degree (double bond) compared to C−O bond degree (single bond) on flat surface. Hence, this result indicate an almost identical probability for desorption and migration of O atom to occur when energy is supplied to the system, for example, in the form of an increased temperature.

For the relaxed stepped (111) surface with O adatom, it was observed that there is no reconstruction as that occurs in the case of stepped surface with H adatom. This is because O adatom forms double bond with it and saturates its dangling bonds as illustrated in Figure 7.4.

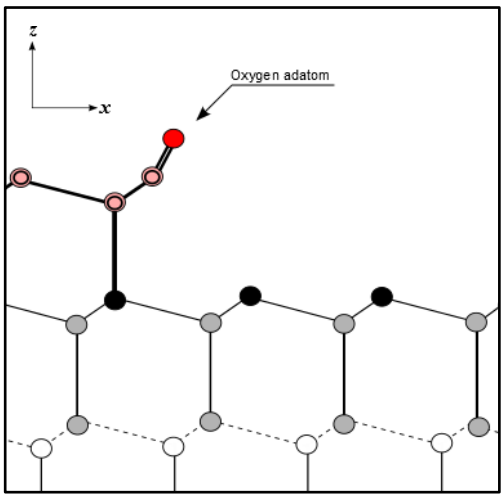

Figure 7.3. Relaxed step surface with O adatom (side view).

7.3. Adsorption of Hydroxyl group

Also, relaxed stepped surface with OH group was investigated. The minimum energy configuration of OH group diffusion on stepped C (111) surface after relaxation was found at $\boldsymbol{z}$ = 2.85 Å and the most stable site for OH is located also at the step-edge site, same as H/O adatoms. C−OH bond length was 1.39 Å which was a little shorter than that at relaxed flat surface (1.42 Å). C−OH angle was about 113.9º. Hydroxyl group interacts with the stepped surface carbon atoms to form single C–OH bonds. Energy barrier for OH migration on stepped C (111) surface was found to be 4.16 eV.

Figure 7.4 shows the relaxed stepped surface with presence of OH group at the step-edge site. The carbon atom at the step edge bonded to OH group has been found to reconstruct and form a downward slope in the $(11\bar{2})$ direction to lower the surface energy and numbers of dangling bonds on the surface, same as in the case of H adatom adsorbed at step-edge. Also, we should notice that the orientation direction of OH changed on the relaxed stepped surface than that at flat surface in Section 5.4.

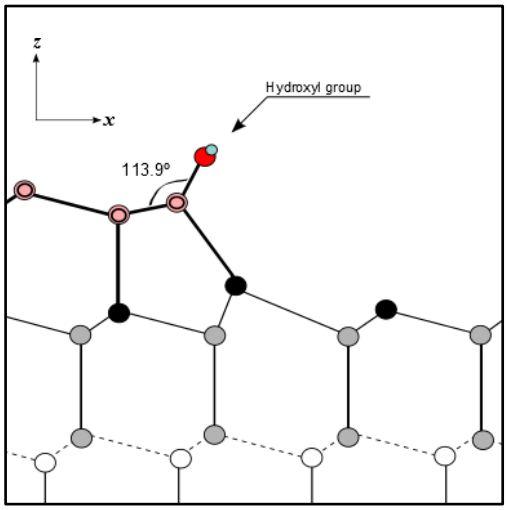

Figure 7.4. Relaxed step surface with OH group (side view).

References

[1] Dominic Alfonso, David Drabold and Sergio Ulloa, J. Phys.: Condens. Matter 8, 641 (1996).

[2] B. N. Davidson and W. E. Pickett, Phys. Rev. B 49(20), 14770 (1994).

[3] G. Kern and J. Hafner, Phys. Rev. B 58, 2161 (1998).

[4] B. B. Pate, Surf. Sci. 165, 83 (1986).

[5] M. Frenklach, Phys. Rev. B 45, 9455 (1992).

[6] H. Sasaki and H. Kawarada, Jpn. J. Appl. Phys. 32, L1771 (1993).

[7] N. Tokuda , M. Ogura, S. Yamasaki and T. Inokuma: under review.

CHAPTER 8

CHAPTER 8

Conclusions

We have employed molecular orbital method based on the density functional theory to study adsorption and diffusion of H, O adatoms and OH adgroup. Flat and stepped diamond (111)-(1×1) surfaces were modeled to be used in calculation which were performed by using ORCA software.

We have calculated the potential energy for these adspecies on diamond (111)-(1×1) flat and stepped (monoatomic step) surfaces. Two-dimensional profiles of the potential energy for hydrogen, oxygen atoms and hydroxyl group are presented. The behaviors of surface diffusion and the influence of atomic steps are discussed.

For flat surface, the most stable site was found to be the on-top site for H atom, O atom and OH group. For stepped surface, the most stable site was step-edge site.

The H adatom diffuses on flat surface by migrating from On-top site to another and reaches the step region. The total energy of the system becomes lower near the step. The H adatom can diffuse easily along the edge of the step. Therefore, atomic H can induce step formation on the C (111) surface.

The O adatom can diffuse on flat surface more easily than H adatom (even at 300K) with a lower activation barrier and reaches near the step region. Also, the total energy of the system is lower near the step. But, the O adatom is much more likely to fall into the well at on-top site near the step, than to continue to the edge of the step.

We consider that these differences in behavior between H adatom and O adatom are due to the difference in their valencies. This could be concluded by analyzing the volumetric data of spin density distribution.

For OH group, it is difficult to diffuse on flat surface by migrating from On-top site to another because of the high energy barrier. The orientation of the C–OH bond changes on stepped surface than that on flat surface. OH termination is found to be the most stable structure on the oxygen adsorption flat (111)-(1×1) surface.

Also, we have studied the relaxed stepped surface in the presence of H, O adatoms and OH group on diamond (111)-(1×1) surface. It was found that the stepped surface with H adatom and OH group is reconstructed and forms a downward slope in the $11\bar{2}$ direction to lower the surface energy and numbers of dangling bonds on the surface. This can lead to that stepped diamond (111) surface become more stable against hydrogen plasma etching because it became monohydrided surface.

APPENDIX

APPENDIX: Orca Input Files

1- Adsorption of Hydrogen on Flat Surface

```
#-----------------------------------------
# Diamond (111) cluster KS scan H `new unit cell`
#-----------------------------------------
#
! UKS BP86 Def2-SVP Def2-SVP/C RI PAL4
%scf
  Convergence    Normal
  MaxIter  500
  Autostart false
  end
%method
  SwitchToSOSCF  false
  ScanGuess Hueckel
  end
#%geom
#  MaxIter  300
#  end
%output
  PrintLevel           mini
#  Print[P_MOs]  1
  end
%MaxCore 6000
%coords
  CTyp           XYZ
  Charge          0
  Mult           3
  pardef
    xH = 0.0, 2.202, 13;    # atom 1 to 2
    yH = -1.2706, 0.0, 8;   # atom 2 to 1
    end
  coords
  C       0.000000     -0.000000      0.000000
  C       2.201960     -1.270643      0.004005
  C      -2.201743     -1.272600      0.002261
  C       2.198990      1.275699      0.004271
  C      -2.204719      1.267566      0.002552
  C      -0.001593      2.543295      0.003763
  C       0.004302     -2.543256      0.003237
  C      -2.197042      3.794879      0.018674
  C      -2.188281     -3.799916      0.017800
  C       4.383666      0.005079      0.019640
  C      -0.732485     -1.271863     -0.484918
  C       1.466906      0.001800     -0.483822
  C      -0.735466      1.270437     -0.484626
  C      -2.914779     -2.548249     -0.494278
  C      -2.920695      2.541770     -0.493750
  C      -0.741311     -3.800124     -0.493710
```

```
C       3.662761     -1.250027     -0.492409
C      -0.750115      3.798610     -0.492923
C       3.659810      1.258660     -0.492134
C      -2.910780     -0.003243     -0.501209
C       1.457541     -2.519499     -0.499808
C       1.451672      2.523041     -0.499289
C      -2.926617     -2.526545     -2.039206
C      -2.932539      2.520305     -2.038659
C      -0.717430     -3.799319     -2.038596
C       3.649741     -1.270801     -2.037307
C      -0.726269      3.798164     -2.037841
C       3.646772      1.279661     -2.037049
C      -0.733173     -1.272018     -2.048961
C      -0.736159      1.270823     -2.048690
C       1.466628      0.001924     -2.047805
C       1.471757     -2.545136     -2.051530
C      -2.940449     -0.003139     -2.053027
C       1.465843      2.549011     -2.051023
C       0.733414     -1.268600     -2.536305
C      -1.466506     -0.001321     -2.537467
C       0.730448      1.271014     -2.535994
C      -1.467334     -2.546749     -2.539209
C       2.937340      0.003724     -2.537260
C      -1.473290      2.544115     -2.538694
C      -3.645959     -1.272726     -2.551766
C      -3.648918      1.264967     -2.551474
C       0.727490     -3.792196     -2.550836
C       2.923706     -2.520489     -2.550077
C       2.917841      2.527878     -2.549519
C       0.718681      3.794507     -2.550056
H       0.731077      3.815400     -3.654652   newgto "SV" end
H       2.930498      2.548784     -3.654431   newgto "SV" end
H       0.739823     -3.812944     -3.655434   newgto "SV" end
H       2.936279     -2.541123     -3.655003   newgto "SV" end
H      -3.670393     -1.272850     -3.656675   newgto "SV" end
H      -3.673445      1.265177     -3.656384   newgto "SV" end
H       0.729207      1.267580     -3.645904   newgto "SV" end
H      -1.462034     -0.001339     -3.647327   newgto "SV" end
H       0.732152     -1.265221     -3.646213   newgto "SV" end
H      -1.471517      2.541289     -3.646149   newgto "SV" end
H       2.934605      0.003751     -3.644850   newgto "SV" end
H      -1.465581     -2.543958     -3.646671   newgto "SV" end
H      -1.238595     -4.701277     -2.408616   newgto "SV" end
H      -3.445331     -3.429648     -2.409044   newgto "SV" end
H      -3.453315      3.422315     -2.408291   newgto "SV" end
H       4.691173     -1.268054     -2.407283   newgto "SV" end
H       4.688228      1.279676     -2.406970   newgto "SV" end
H      -1.249393      4.699159     -2.407486   newgto "SV" end
H       1.247032      4.703413     -2.208261   newgto "SV" end
H       3.446324     -3.432670     -2.208627   newgto "SV  end
H       1.257992     -4.699920     -2.209199   newgto "SV" end
H       3.438392      3.441101     -2.207725   newgto "SV" end
H      -4.696564     -1.269260     -2.209885   newgto "SV" end
H      -4.699511      1.258851     -2.209583   newgto "SV" end
H      -2.712053     -4.709455     -0.325419   newgto "SV" end
H       5.432702      0.006440     -0.323311   newgto "SV" end
```

```
  H      -2.722978      4.703445     -0.323809   newgto "SV" end
  H      -3.955308     -0.004572     -0.131943   newgto "SV" end
  H       1.980635     -3.423401     -0.130645   newgto "SV" end
  H       1.972778      3.427957     -0.129857   newgto "SV" end
  H      -3.956250     -2.544207     -0.124926   newgto "SV" end
  H      -0.215167     -4.699295     -0.124398   newgto "SV" end
  H      -0.226037      4.698906     -0.123468   newgto "SV" end
  H       4.175170      2.163696     -0.122879   newgto "SV" end
  H      -3.962141      2.535116     -0.124361   newgto "SV" end
  H       4.180185     -2.153973     -0.123344   newgto "SV" end
  H       4.407367      0.004983      1.123455   newgto "SV" end
  H      -2.208992      3.814798      1.122262   newgto "SV" end
  H      -2.200418     -3.820490      1.121354   newgto "SV" end
# H       0.002185      2.539246      1.111356
# H       0.008038     -2.539234      1.110822
# H       2.193703      1.277207      1.111889
# H       2.196652     -1.272163      1.111617
# H      -2.204093      1.261993      1.110260
# H      -2.201124     -1.267167      1.109972
# H      -0.000690      0.000016      1.110291
  H        {xH}          {yH}        +1.11
  end
end
```

2- Adsorption of Oxygen on Flat Surface

```
#-----------------------------------------
# Diamond (111) cluster KS scan O `new unit cell`
#-----------------------------------------
#
! UKS BP86 Def2-SVP Def2-SVP/C RI PAL4
%scf
  Convergence    Normal
  MaxIter  500
  Autostart false
  end
%method
  SwitchToSOSCF  false
  ScanGuess Hueckel
  end
#%geom
#  MaxIter  300
#  end
%output
  PrintLevel           mini
#  Print[P_MOs]  1
  end
%MaxCore 6000
%coords
  CTyp           XYZ
  Charge          0
  Mult            4
  pardef
```

```
  xO = 0.0, 2.202, 13;    # atom 1 to 2
  yO = -1.2706, 0.0, 8;   # atom 2 to 1
  end
coords
C       0.000000     -0.000000      0.000000
C       2.201960     -1.270643      0.004005
C      -2.201743     -1.272600      0.002261
C       2.198990      1.275699      0.004271
C      -2.204719      1.267566      0.002552
C      -0.001593      2.543295      0.003763
C       0.004302     -2.543256      0.003237
C      -2.197042      3.794879      0.018674
C      -2.188281     -3.799916      0.017800
C       4.383666      0.005079      0.019640
C      -0.732485     -1.271863     -0.484918
C       1.466906      0.001800     -0.483822
C      -0.735466      1.270437     -0.484626
C      -2.914779     -2.548249     -0.494278
C      -2.920695      2.541770     -0.493750
C      -0.741311     -3.800124     -0.493710
C       3.662761     -1.250027     -0.492409
C      -0.750115      3.798610     -0.492923
C       3.659810      1.258660     -0.492134
C      -2.910780     -0.003243     -0.501209
C       1.457541     -2.519499     -0.499808
C       1.451672      2.523041     -0.499289
C      -2.926617     -2.526545     -2.039206
C      -2.932539      2.520305     -2.038659
C      -0.717430     -3.799319     -2.038596
C       3.649741     -1.270801     -2.037307
C      -0.726269      3.798164     -2.037841
C       3.646772      1.279661     -2.037049
C      -0.733173     -1.272018     -2.048961
C      -0.736159      1.270823     -2.048690
C       1.466628      0.001924     -2.047805
C       1.471757     -2.545136     -2.051530
C      -2.940449     -0.003139     -2.053027
C       1.465843      2.549011     -2.051023
C       0.733414     -1.268600     -2.536305
C      -1.466506     -0.001321     -2.537467
C       0.730448      1.271014     -2.535994
C      -1.467334     -2.546749     -2.539209
C       2.937340      0.003724     -2.537260
C      -1.473290      2.544115     -2.538694
C      -3.645959     -1.272726     -2.551766
C      -3.648918      1.264967     -2.551474
C       0.727490     -3.792196     -2.550836
C       2.923706     -2.520489     -2.550077
C       2.917841      2.527878     -2.549519
C       0.718681      3.794507     -2.550056
H       0.731077      3.815400     -3.654652   newgto "SV" end
H       2.930498      2.548784     -3.654431   newgto "SV" end
H       0.739823     -3.812944     -3.655434   newgto "SV" end
H       2.936279     -2.541123     -3.655003   newgto "SV" end
H      -3.670393     -1.272850     -3.656675   newgto "SV" end
H      -3.673445      1.265177     -3.656384   newgto "SV" end
```

```
  H       0.729207      1.267580     -3.645904   newgto "SV" end
  H      -1.462034     -0.001339     -3.647327   newgto "SV" end
  H       0.732152     -1.265221     -3.646213   newgto "SV" end
  H      -1.471517      2.541289     -3.646149   newgto "SV" end
  H       2.934605      0.003751     -3.644850   newgto "SV" end
  H      -1.465581     -2.543958     -3.646671   newgto "SV" end
  H      -1.238595     -4.701277     -2.408616   newgto "SV" end
  H      -3.445331     -3.429648     -2.409044   newgto "SV" end
  H      -3.453315      3.422315     -2.408291   newgto "SV" end
  H       4.691173     -1.268054     -2.407283   newgto "SV" end
  H       4.688228      1.279676     -2.406970   newgto "SV" end
  H      -1.249393      4.699159     -2.407486   newgto "SV" end
  H       1.247032      4.703413     -2.208261   newgto "SV" end
  H       3.446324     -3.432670     -2.208627   newgto "SV" end
  H       1.257992     -4.699920     -2.209199   newgto "SV" end
  H       3.438392      3.441101     -2.207725   newgto "SV" end
  H      -4.696564     -1.269260     -2.209885   newgto "SV" end
  H      -4.699511      1.258851     -2.209583   newgto "SV" end
  H      -2.712053     -4.709455     -0.325419   newgto "SV" end
  H       5.432702      0.006440     -0.323311   newgto "SV" end
  H      -2.722978      4.703445     -0.323809   newgto "SV" end
  H      -3.955308     -0.004572     -0.131943   newgto "SV" end
  H       1.980635     -3.423401     -0.130645   newgto "SV" end
  H       1.972778      3.427957     -0.129857   newgto "SV" end
  H      -3.956250     -2.544207     -0.124926   newgto "SV" end
  H      -0.215167     -4.699295     -0.124398   newgto "SV" end
  H      -0.226037      4.698906     -0.123468   newgto "SV" end
  H       4.175170      2.163696     -0.122879   newgto "SV" end
  H      -3.962141      2.535116     -0.124361   newgto "SV" end
  H       4.180185     -2.153973     -0.123344   newgto "SV" end
  H       4.407367      0.004983      1.123455   newgto "SV" end
  H      -2.208992      3.814798      1.122262   newgto "SV" end
  H      -2.200418     -3.820490      1.121354   newgto "SV" end
# H       0.002185      2.539246      1.111356
# H       0.008038     -2.539234      1.110822
# H       2.193703      1.277207      1.111889
# H       2.196652     -1.272163      1.111617
# H      -2.204093      1.261993      1.110260
# H      -2.201124     -1.267167      1.109972
# H      -0.000690      0.000016      1.110291
  O        {xO}          {yO}         +1.33
  end
end
```

3- Adsorption of Hydroxyl on Flat Surface

```
#-----------------------------------------
# Diamond (111) cluster KS scan OH `new unit cell`
#-----------------------------------------
#
! UKS BP86 Def2-SVP Def2-SVP/C RI PAL4
! Opt
%scf
```

```
  Convergence    Normal
  MaxIter  500
  Autostart false
  end
%method
  SwitchToSOSCF  false
  ScanGuess Hueckel
  end
#%geom
#  MaxIter  300
#  end
%output
  PrintLevel           mini
#  Print[P_MOs]  1
  end
%MaxCore 6000
%coords
  CTyp           XYZ
  Charge          0
  Mult           3
  pardef
    xO = 0.0, 2.202, 13;    # atom 1 to 2
    yO = -1.2706, 0.0, 8;   # atom 2 to 1
    end
  coords
  C       0.000000     -0.000000      0.000000
  C       2.201960     -1.270643      0.004005
  C      -2.201743     -1.272600      0.002261
  C       2.198990      1.275699      0.004271
  C      -2.204719      1.267566      0.002552
  C      -0.001593      2.543295      0.003763
  C       0.004302     -2.543256      0.003237
  C      -2.197042      3.794879      0.018674
  C      -2.188281     -3.799916      0.017800
  C       4.383666      0.005079      0.019640
  C      -0.732485     -1.271863     -0.484918
  C       1.466906      0.001800     -0.483822
  C      -0.735466      1.270437     -0.484626
  C      -2.914779     -2.548249     -0.494278
  C      -2.920695      2.541770     -0.493750
  C      -0.741311     -3.800124     -0.493710
  C       3.662761     -1.250027     -0.492409
  C      -0.750115      3.798610     -0.492923
  C       3.659810      1.258660     -0.492134
  C      -2.910780     -0.003243     -0.501209
  C       1.457541     -2.519499     -0.499808
  C       1.451672      2.523041     -0.499289
  C      -2.926617     -2.526545     -2.039206
  C      -2.932539      2.520305     -2.038659
  C      -0.717430     -3.799319     -2.038596
  C       3.649741     -1.270801     -2.037307
  C      -0.726269      3.798164     -2.037841
  C       3.646772      1.279661     -2.037049
  C      -0.733173     -1.272018     -2.048961
  C      -0.736159      1.270823     -2.048690
  C       1.466628      0.001924     -2.047805
```

```
  C       1.471757     -2.545136     -2.051530
  C      -2.940449     -0.003139     -2.053027
  C       1.465843      2.549011     -2.051023
  C       0.733414     -1.268600     -2.536305
  C      -1.466506     -0.001321     -2.537467
  C       0.730448      1.271014     -2.535994
  C      -1.467334     -2.546749     -2.539209
  C       2.937340      0.003724     -2.537260
  C      -1.473290      2.544115     -2.538694
  C      -3.645959     -1.272726     -2.551766
  C      -3.648918      1.264967     -2.551474
  C       0.727490     -3.792196     -2.550836
  C       2.923706     -2.520489     -2.550077
  C       2.917841      2.527878     -2.549519
  C       0.718681      3.794507     -2.550056
  H       0.731077      3.815400     -3.654652   newgto "SV" end
  H       2.930498      2.548784     -3.654431   newgto "SV" end
  H       0.739823     -3.812944     -3.655434   newgto "SV" end
  H       2.936279     -2.541123     -3.655003   newgto "SV" end
  H      -3.670393     -1.272850     -3.656675   newgto "SV" end
  H      -3.673445      1.265177     -3.656384   newgto "SV" end
  H       0.729207      1.267580     -3.645904   newgto "SV" end
  H      -1.462034     -0.001339     -3.647327   newgto "SV" end
  H       0.732152     -1.265221     -3.646213   newgto "SV" end
  H      -1.471517      2.541289     -3.646149   newgto "SV" end
  H       2.934605      0.003751     -3.644850   newgto "SV" end
  H      -1.465581     -2.543958     -3.646671   newgto "SV" end
  H      -1.238595     -4.701277     -2.408616   newgto "SV" end
  H      -3.445331     -3.429648     -2.409044   newgto "SV" end
  H      -3.453315      3.422315     -2.408291   newgto "SV" end
  H       4.691173     -1.268054     -2.407283   newgto "SV" end
  H       4.688228      1.279676     -2.406970   newgto "SV" end
  H      -1.249393      4.699159     -2.407486   newgto "SV" end
  H       1.247032      4.703413     -2.208261   newgto "SV" end
  H       3.446324     -3.432670     -2.208627   newgto "SV" end
  H       1.257992     -4.699920     -2.209199   newgto "SV" end
  H       3.438392      3.441101     -2.207725   newgto "SV" end
  H      -4.696564     -1.269260     -2.209885   newgto "SV" end
  H      -4.699511      1.258851     -2.209583   newgto "SV" end
  H      -2.712053     -4.709455     -0.325419   newgto "SV" end
  H       5.432702      0.006440     -0.323311   newgto "SV" end
  H      -2.722978      4.703445     -0.323809   newgto "SV" end
  H      -3.955308     -0.004572     -0.131943   newgto "SV" end
  H       1.980635     -3.423401     -0.130645   newgto "SV" end
  H       1.972778      3.427957     -0.129857   newgto "SV" end
  H      -3.956250     -2.544207     -0.124926   newgto "SV" end
  H      -0.215167     -4.699295     -0.124398   newgto "SV" end
  H      -0.226037      4.698906     -0.123468   newgto "SV" end
  H       4.175170      2.163696     -0.122879   newgto "SV" end
  H      -3.962141      2.535116     -0.124361   newgto "SV" end
  H       4.180185     -2.153973     -0.123344   newgto "SV" end
  H       4.407367      0.004983      1.123455   newgto "SV" end
  H      -2.208992      3.814798      1.122262   newgto "SV" end
  H      -2.200418     -3.820490      1.121354   newgto "SV" end
# H       0.002185      2.539246      1.111356
# H       0.008038     -2.539234      1.110822
```

```
# H       2.193703      1.277207      1.111889
# H       2.196652     -1.272163      1.111617
# H      -2.204093      1.261993      1.110260
# H      -2.201124     -1.267167      1.109972
# H      -0.000690      0.000016      1.110291
  O        {xO}          {yO}         +1.42
  H        {xO-0.91465}  {yO-0.00112}  1.82298
  end
end
```

4- Adsorption of Hydrogen on Stepped Surface

A) First half of unit cell

```
#----------------------------------------------
# Diamond (111) cluster KS scan back-step H1
#----------------------------------------------
#
! UKS BP86 Def2-SVP Def2-SVP/C RI PAL4
%scf
  Convergence    Normal
  MaxIter  500
  Autostart false
  end
%method
  SwitchToSOSCF  false
  ScanGuess Hueckel
  end
#%geom
#  MaxIter   300
#  end
%output
  PrintLevel     mini
#  Print[P_MOs]  1
  end
%MaxCore 6000
%coords
  CTyp           XYZ
  Charge          0
  Mult            7
  pardef
    xH = -2.2032, 0.00, 13;    # atom 5 to 1
    yH =  0.00, 1.2701, 8;     # atom 1 to 5
    end
  coords
  C      +0.000000     +0.000000     +0.000000
  C      +2.200482     -1.273153     -0.011447
  C      -2.203181     -1.270089     +0.006556
  C      +2.200464     +1.273163     +0.000000
  C      -2.203216     +1.270057     +0.017996
```

C	+0.001374	+2.543259	+0.014918
C	+0.001367	-2.543253	-0.007930
C	-2.192535	+3.797262	+0.045162
C	-2.192580	-3.797466	+0.010954
C	+4.383717	+0.000000	-0.000000
C	-0.736129	-1.268884	-0.487201
C	+1.464729	+0.002253	-0.490382
C	-0.736161	+1.273392	-0.475752
C	-2.919916	-2.542734	-0.492369
C	-2.919925	+2.547238	-0.469496
C	-0.747918	-3.797069	-0.507036
C	+3.659066	-1.252028	-0.514309
C	-0.747908	+3.801589	-0.472891
C	+3.659025	+1.256638	-0.503017
C	-2.912998	+0.002276	-0.488159
C	+1.452365	-2.518941	-0.517384
C	+1.452341	+2.523552	-0.494729
C	-2.938653	-2.514239	-2.037121
C	-2.938722	+2.532573	-2.014417
C	-0.730958	-3.789515	-2.052000
C	+3.639101	-1.266002	-2.059212
C	-0.730991	+3.807893	-2.017890
C	+3.639087	+1.284434	-2.047756
C	-0.743816	-1.262178	-2.051208
C	-0.743858	+1.280638	-2.039776
C	+1.457442	+0.009238	-2.054330
C	+1.459604	-2.537785	-2.069250
C	-2.949620	+0.009221	-2.039815
C	+1.459589	+2.556317	-2.046379
C	+0.720569	-1.258289	-2.545112
C	-1.477864	+0.011489	-2.530848
C	+0.720553	+1.281297	-2.533644
C	-1.481642	-2.533906	-2.543745
C	+2.925945	+0.011511	-2.550369
C	-1.481700	+2.556916	-2.520878
C	-3.658828	-1.257363	-2.540947
C	-3.658846	+1.280313	-2.529507
C	+0.711659	-3.781793	-2.570679
C	+2.909333	-2.512601	-2.574194
C	+2.909316	+2.535721	-2.551474
C	+0.711645	+3.804846	-2.536597
C	-5.121072	-1.252956	-2.057817
C	-4.362625	-0.000173	+0.031635
C	-4.369008	-2.537710	+0.028895
C	-4.368994	+2.537362	+0.051753
C	-2.202275	+3.818312	+1.584988
C	-2.202655	-3.832905	+1.550514
C	-2.192399	+1.260761	+1.540237
C	-2.238442	-1.275148	+1.546152
C	-1.512766	-2.531478	+2.074316
C	-3.660301	-3.831634	+2.047390
C	-3.671718	-1.291895	+2.047470
C	-1.520948	-0.001287	+2.082309
C	-3.623631	+1.247126	+2.092970
C	-1.519250	+2.532257	+2.098283
C	-3.677825	+3.809017	+2.087918

```
C      -5.093552     +1.281586     -0.467513
C      -4.352967     +2.512233     +1.591471
C      -5.085694     -1.264808     -0.467836
C      -4.348238     -0.000151     +1.571571
C      -4.381987     -2.576385     +1.568354
C      -5.099871     +1.297314     -2.007416
C      -5.836206     +0.045955     -2.520740
H      +0.719120     +3.830570     -3.641129   newgto "SV" end
H      +2.917050     +2.561457     -3.656327   newgto "SV" end
H      +0.719016     -3.797698     -3.675394   newgto "SV" end
H      +2.916929     -2.528395     -3.679239   newgto "SV" end
H      -3.688208     -1.252605     -3.645716   newgto "SV" end
H      -3.688326     +1.285401     -3.634285   newgto "SV" end
H      +0.714337     +1.282740     -3.643541   newgto "SV" end
H      -1.478357     +0.016335     -3.640707   newgto "SV" end
H      +0.714340     -1.250036     -3.654969   newgto "SV" end
H      -1.484895     +2.558945     -3.628336   newgto "SV" end
H      +2.918243     +0.016406     -3.657924   newgto "SV" end
H      -1.484850     -2.526257     -3.651178   newgto "SV" end
H      -1.254816     -4.689248     -2.423629   newgto "SV" end
H      -3.460061     -3.415115     -2.408576   newgto "SV" end
H      -3.460097     +3.436790     -2.377749   newgto "SV" end
H      +4.678865     -1.262814     -2.433833   newgto "SV" end
H      +4.678879     +1.284892     -2.422340   newgto "SV" end
H      -1.254717     +4.711103     -2.381236   newgto "SV  end
H      +1.242574     +4.711634     -2.193188   newgto "SV" end
H      +3.432410     -3.426866     -2.239094   newgto "SV" end
H      +1.242632     -4.691607     -2.235405   newgto "SV" end
H      +3.432450     +3.446839     -2.208012   newgto "SV" end
H      -2.718936     -4.704894     -0.333897   newgto "SV" end
H      +5.431201     +0.001670     -0.347642   newgto "SV" end
H      -2.718951     +4.707925     -0.290969   newgto "SV" end
H      +1.976056     -3.425048     -0.154540   newgto "SV" end
H      +1.976150     +3.426247     -0.123676   newgto "SV" end
H      -0.221171     -4.698461     -0.144036   newgto "SV" end
H      -0.221145     +4.699661     -0.101852   newgto "SV" end
H      +4.177082     +2.159461     -0.132118   newgto "SV" end
H      +4.177087     -2.158168     -0.151531   newgto "SV" end
H      +4.412362     -0.004972     +1.103692   newgto "SV" end
H      -1.725841     -4.723315     +1.903697   newgto "SV" end
H      -1.691763     +4.693866     +1.928021   newgto "SV" end
H      -4.883232     +3.420013     -0.266655   newgto "SV" end
H      -4.876867     -3.406193     -0.335419   newgto "SV" end
H      -5.375413     -2.612230     +1.964235   newgto "SV" end
H      -5.345721     +0.031813     +1.957448   newgto "SV" end
H      -5.348079     +2.471470     +1.982618   newgto "SV" end
H      -6.080676     -1.262341     -0.074250   newgto "SV" end
H      -6.094631     +1.278489     -0.089725   newgto "SV" end
H      -5.645275     -2.107902     -2.430878   newgto "SV" end
H      -5.613148     +2.164832     -2.366376   newgto "SV" end
H      -5.895981     +0.069478     -3.588810   newgto "SV" end
H      -6.824273     +0.047810     -2.110097   newgto "SV" end
H      -4.159953     -4.688474     +1.646060   newgto "SV" end
H      -4.202660     +4.667153     +1.723159   newgto "SV" end
H      -3.66702      -3.85430      +3.11713    newgto "SV" end
H      -3.69817      +3.84367      +3.15716    newgto "SV" end
```

```
  H       {xH}          {yH}         +1.11
  end
end
```

B) Second half of unit cell

```
#-----------------------------------------
# Diamond (111) cluster KS scan back-step H2
#-----------------------------------------
#
! UKS BP86 Def2-SVP Def2-SVP/C RI PAL4
%scf
  Convergence    Normal
  MaxIter  500
  Autostart false
  end
%method
  SwitchToSOSCF  false
  ScanGuess Hueckel
  end
#%geom
#  MaxIter   300
#  end
%output
  PrintLevel     mini
#  Print[P_MOs]  1
  end
%MaxCore 6000
%coords
  CTyp           XYZ
  Charge          0
  Mult            7
  pardef
     xH =  0.00, 2.2005, 13;   # atom 1 to 2
     yH = -1.2732, 0.00, 8;    # atom 2 to 1
    end
  coords
  C      +0.000000     +0.000000     +0.000000
  C      +2.200482     -1.273153     -0.011447
  C      -2.203181     -1.270089     +0.006556
  C      +2.200464     +1.273163     +0.000000
  C      -2.203216     +1.270057     +0.017996
  C      +0.001374     +2.543259     +0.014918
  C      +0.001367     -2.543253     -0.007930
  C      -2.192535     +3.797262     +0.045162
  C      -2.192580     -3.797466     +0.010954
  C      +4.383717     +0.000000     -0.000000
  C      -0.736129     -1.268884     -0.487201
  C      +1.464729     +0.002253     -0.490382
  C      -0.736161     +1.273392     -0.475752
  C      -2.919916     -2.542734     -0.492369
  C      -2.919925     +2.547238     -0.469496
  C      -0.747918     -3.797069     -0.507036
```

```
C      +3.659066     -1.252028     -0.514309
C      -0.747908     +3.801589     -0.472891
C      +3.659025     +1.256638     -0.503017
C      -2.912998     +0.002276     -0.488159
C      +1.452365     -2.518941     -0.517384
C      +1.452341     +2.523552     -0.494729
C      -2.938653     -2.514239     -2.037121
C      -2.938722     +2.532573     -2.014417
C      -0.730958     -3.789515     -2.052000
C      +3.639101     -1.266002     -2.059212
C      -0.730991     +3.807893     -2.017890
C      +3.639087     +1.284434     -2.047756
C      -0.743816     -1.262178     -2.051208
C      -0.743858     +1.280638     -2.039776
C      +1.457442     +0.009238     -2.054330
C      +1.459604     -2.537785     -2.069250
C      -2.949620     +0.009221     -2.039815
C      +1.459589     +2.556317     -2.046379
C      +0.720569     -1.258289     -2.545112
C      -1.477864     +0.011489     -2.530848
C      +0.720553     +1.281297     -2.533644
C      -1.481642     -2.533906     -2.543745
C      +2.925945     +0.011511     -2.550369
C      -1.481700     +2.556916     -2.520878
C      -3.658828     -1.257363     -2.540947
C      -3.658846     +1.280313     -2.529507
C      +0.711659     -3.781793     -2.570679
C      +2.909333     -2.512601     -2.574194
C      +2.909316     +2.535721     -2.551474
C      +0.711645     +3.804846     -2.536597
C      -5.121072     -1.252956     -2.057817
C      -4.362625     -0.000173     +0.031635
C      -4.369008     -2.537710     +0.028895
C      -4.368994     +2.537362     +0.051753
C      -2.202275     +3.818312     +1.584988
C      -2.202655     -3.832905     +1.550514
C      -2.192399     +1.260761     +1.540237
C      -2.238442     -1.275148     +1.546152
C      -1.512766     -2.531478     +2.074316
C      -3.660301     -3.831634     +2.047390
C      -3.671718     -1.291895     +2.047470
C      -1.520948     -0.001287     +2.082309
C      -3.623631     +1.247126     +2.092970
C      -1.519250     +2.532257     +2.098283
C      -3.677825     +3.809017     +2.087918
C      -5.093552     +1.281586     -0.467513
C      -4.352967     +2.512233     +1.591471
C      -5.085694     -1.264808     -0.467836
C      -4.348238     -0.000151     +1.571571
C      -4.381987     -2.576385     +1.568354
C      -5.099871     +1.297314     -2.007416
C      -5.836206     +0.045955     -2.520740
H      +0.719120     +3.830570     -3.641129   newgto "SV" end
H      +2.917050     +2.561457     -3.656327   newgto "SV" end
H      +0.719016     -3.797698     -3.675394   newgto "SV" end
H      +2.916929     -2.528395     -3.679239   newgto "SV" end
```

```
  H      -3.688208     -1.252605     -3.645716   newgto "SV" end
  H      -3.688326     +1.285401     -3.634285   newgto "SV" end
  H      +0.714337     +1.282740     -3.643541   newgto "SV" end
  H      -1.478357     +0.016335     -3.640707   newgto "SV" end
  H      +0.714340     -1.250036     -3.654969   newgto "SV" end
  H      -1.484895     +2.558945     -3.628336   newgto "SV" end
  H      +2.918243     +0.016406     -3.657924   newgto "SV" end
  H      -1.484850     -2.526257     -3.651178   newgto "SV" end
  H      -1.254816     -4.689248     -2.423629   newgto "SV" end
  H      -3.460061     -3.415115     -2.408576   newgto "SV" end
  H      -3.460097     +3.436790     -2.377749   newgto "SV" end
  H      +4.678865     -1.262814     -2.433833   newgto "SV" end
  H      +4.678879     +1.284892     -2.422340   newgto "SV" end
  H      -1.254717     +4.711103     -2.381236   newgto "SV  end
  H      +1.242574     +4.711634     -2.193188   newgto "SV" end
  H      +3.432410     -3.426866     -2.239094   newgto "SV" end
  H      +1.242632     -4.691607     -2.235405   newgto "SV" end
  H      +3.432450     +3.446839     -2.208012   newgto "SV" end
  H      -2.718936     -4.704894     -0.333897   newgto "SV" end
  H      +5.431201     +0.001670     -0.347642   newgto "SV" end
  H      -2.718951     +4.707925     -0.290969   newgto "SV" end
  H      +1.976056     -3.425048     -0.154540   newgto "SV" end
  H      +1.976150     +3.426247     -0.123676   newgto "SV" end
  H      -0.221171     -4.698461     -0.144036   newgto "SV" end
  H      -0.221145     +4.699661     -0.101852   newgto "SV" end
  H      +4.177082     +2.159461     -0.132118   newgto "SV" end
  H      +4.177087     -2.158168     -0.151531   newgto "SV" end
  H      +4.412362     -0.004972     +1.103692   newgto "SV" end
  H      -1.725841     -4.723315     +1.903697   newgto "SV" end
  H      -1.691763     +4.693866     +1.928021   newgto "SV" end
  H      -4.883232     +3.420013     -0.266655   newgto "SV" end
  H      -4.876867     -3.406193     -0.335419   newgto "SV" end
  H      -5.375413     -2.612230     +1.964235   newgto "SV" end
  H      -5.345721     +0.031813     +1.957448   newgto "SV" end
  H      -5.348079     +2.471470     +1.982618   newgto "SV" end
  H      -6.080676     -1.262341     -0.074250   newgto "SV" end
  H      -6.094631     +1.278489     -0.089725   newgto "SV" end
  H      -5.645275     -2.107902     -2.430878   newgto "SV" end
  H      -5.613148     +2.164832     -2.366376   newgto "SV" end
  H      -5.895981     +0.069478     -3.588810   newgto "SV" end
  H      -6.824273     +0.047810     -2.110097   newgto "SV" end
  H      -4.159953     -4.688474     +1.646060   newgto "SV" end
  H      -4.202660     +4.667153     +1.723159   newgto "SV" end
  H      -3.66702      -3.85430      +3.11713    newgto "SV" end
  H      -3.69817      +3.84367      +3.15716    newgto "SV" end
  H       {xH}          {yH}         +1.11
  end
end
```

5- Adsorption of Oxygen on Stepped Surface

A) First half of unit cell

```
#-----------------------------------------
# Diamond (111) cluster KS scan back-step O1
#-----------------------------------------
#
! UKS BP86 Def2-SVP Def2-SVP/C RI PAL4
%scf
  Convergence    Normal
  MaxIter  500
  Autostart false
  end
%method
  SwitchToSOSCF  false
  ScanGuess Hueckel
  end
#%geom
#  MaxIter   300
#  end
%output
  PrintLevel     mini
#  Print[P_MOs]  1
  end
%MaxCore 6000
%coords
  CTyp           XYZ
  Charge          0
  Mult            4
  pardef
    xO = -2.2032, 0.00, 13;   # atom 5 to 1
    yO =  0.00, 1.2701, 8;    # atom 1 to 5
    end
  coords
  C      +0.000000     +0.000000     +0.000000
  C      +2.200482     -1.273153     -0.011447
  C      -2.203181     -1.270089     +0.006556
  C      +2.200464     +1.273163     +0.000000
  C      -2.203216     +1.270057     +0.017996
  C      +0.001374     +2.543259     +0.014918
  C      +0.001367     -2.543253     -0.007930
  C      -2.192535     +3.797262     +0.045162
  C      -2.192580     -3.797466     +0.010954
  C      +4.383717     +0.000000     -0.000000
  C      -0.736129     -1.268884     -0.487201
  C      +1.464729     +0.002253     -0.490382
  C      -0.736161     +1.273392     -0.475752
  C      -2.919916     -2.542734     -0.492369
  C      -2.919925     +2.547238     -0.469496
  C      -0.747918     -3.797069     -0.507036
  C      +3.659066     -1.252028     -0.514309
  C      -0.747908     +3.801589     -0.472891
```

```
C      +3.659025     +1.256638     -0.503017
C      -2.912998     +0.002276     -0.488159
C      +1.452365     -2.518941     -0.517384
C      +1.452341     +2.523552     -0.494729
C      -2.938653     -2.514239     -2.037121
C      -2.938722     +2.532573     -2.014417
C      -0.730958     -3.789515     -2.052000
C      +3.639101     -1.266002     -2.059212
C      -0.730991     +3.807893     -2.017890
C      +3.639087     +1.284434     -2.047756
C      -0.743816     -1.262178     -2.051208
C      -0.743858     +1.280638     -2.039776
C      +1.457442     +0.009238     -2.054330
C      +1.459604     -2.537785     -2.069250
C      -2.949620     +0.009221     -2.039815
C      +1.459589     +2.556317     -2.046379
C      +0.720569     -1.258289     -2.545112
C      -1.477864     +0.011489     -2.530848
C      +0.720553     +1.281297     -2.533644
C      -1.481642     -2.533906     -2.543745
C      +2.925945     +0.011511     -2.550369
C      -1.481700     +2.556916     -2.520878
C      -3.658828     -1.257363     -2.540947
C      -3.658846     +1.280313     -2.529507
C      +0.711659     -3.781793     -2.570679
C      +2.909333     -2.512601     -2.574194
C      +2.909316     +2.535721     -2.551474
C      +0.711645     +3.804846     -2.536597
C      -5.121072     -1.252956     -2.057817
C      -4.362625     -0.000173     +0.031635
C      -4.369008     -2.537710     +0.028895
C      -4.368994     +2.537362     +0.051753
C      -2.202275     +3.818312     +1.584988
C      -2.202655     -3.832905     +1.550514
C      -2.192399     +1.260761     +1.540237
C      -2.238442     -1.275148     +1.546152
C      -1.512766     -2.531478     +2.074316
C      -3.660301     -3.831634     +2.047390
C      -3.671718     -1.291895     +2.047470
C      -1.520948     -0.001287     +2.082309
C      -3.623631     +1.247126     +2.092970
C      -1.519250     +2.532257     +2.098283
C      -3.677825     +3.809017     +2.087918
C      -5.093552     +1.281586     -0.467513
C      -4.352967     +2.512233     +1.591471
C      -5.085694     -1.264808     -0.467836
C      -4.348238     -0.000151     +1.571571
C      -4.381987     -2.576385     +1.568354
C      -5.099871     +1.297314     -2.007416
C      -5.836206     +0.045955     -2.520740
H      +0.719120     +3.830570     -3.641129   newgto "SV" end
H      +2.917050     +2.561457     -3.656327   newgto "SV" end
H      +0.719016     -3.797698     -3.675394   newgto "SV" end
H      +2.916929     -2.528395     -3.679239   newgto "SV" end
H      -3.688208     -1.252605     -3.645716   newgto "SV" end
H      -3.688326     +1.285401     -3.634285   newgto "SV" end
```

```
  H      +0.714337     +1.282740     -3.643541   newgto "SV" end
  H      -1.478357     +0.016335     -3.640707   newgto "SV" end
  H      +0.714340     -1.250036     -3.654969   newgto "SV" end
  H      -1.484895     +2.558945     -3.628336   newgto "SV" end
  H      +2.918243     +0.016406     -3.657924   newgto "SV" end
  H      -1.484850     -2.526257     -3.651178   newgto "SV" end
  H      -1.254816     -4.689248     -2.423629   newgto "SV" end
  H      -3.460061     -3.415115     -2.408576   newgto "SV" end
  H      -3.460097     +3.436790     -2.377749   newgto "SV" end
  H      +4.678865     -1.262814     -2.433833   newgto "SV" end
  H      +4.678879     +1.284892     -2.422340   newgto "SV" end
  H      -1.254717     +4.711103     -2.381236   newgto "SV  end
  H      +1.242574     +4.711634     -2.193188   newgto "SV" end
  H      +3.432410     -3.426866     -2.239094   newgto "SV" end
  H      +1.242632     -4.691607     -2.235405   newgto "SV" end
  H      +3.432450     +3.446839     -2.208012   newgto "SV" end
  H      -2.718936     -4.704894     -0.333897   newgto "SV" end
  H      +5.431201     +0.001670     -0.347642   newgto "SV" end
  H      -2.718951     +4.707925     -0.290969   newgto "SV" end
  H      +1.976056     -3.425048     -0.154540   newgto "SV" end
  H      +1.976150     +3.426247     -0.123676   newgto "SV" end
  H      -0.221171     -4.698461     -0.144036   newgto "SV" end
  H      -0.221145     +4.699661     -0.101852   newgto "SV" end
  H      +4.177082     +2.159461     -0.132118   newgto "SV" end
  H      +4.177087     -2.158168     -0.151531   newgto "SV" end
  H      +4.412362     -0.004972     +1.103692   newgto "SV" end
  H      -1.725841     -4.723315     +1.903697   newgto "SV" end
  H      -1.691763     +4.693866     +1.928021   newgto "SV" end
  H      -4.883232     +3.420013     -0.266655   newgto "SV" end
  H      -4.876867     -3.406193     -0.335419   newgto "SV" end
  H      -5.375413     -2.612230     +1.964235   newgto "SV" end
  H      -5.345721     +0.031813     +1.957448   newgto "SV" end
  H      -5.348079     +2.471470     +1.982618   newgto "SV" end
  H      -6.080676     -1.262341     -0.074250   newgto "SV" end
  H      -6.094631     +1.278489     -0.089725   newgto "SV" end
  H      -5.645275     -2.107902     -2.430878   newgto "SV" end
  H      -5.613148     +2.164832     -2.366376   newgto "SV" end
  H      -5.895981     +0.069478     -3.588810   newgto "SV" end
  H      -6.824273     +0.047810     -2.110097   newgto "SV" end
  H      -4.159953     -4.688474     +1.646060   newgto "SV" end
  H      -4.202660     +4.667153     +1.723159   newgto "SV" end
  H      -3.66702      -3.85430      +3.11713    newgto "SV" end
  H      -3.69817      +3.84367      +3.15716    newgto "SV" end
  O       {xO}          {yO}         +1.33
  end
end
```

B) Second half of unit cell

```
#-------------------------------------------
# Diamond (111) cluster KS scan back-step O2
#-------------------------------------------
#
! UKS BP86 Def2-SVP Def2-SVP/C RI PAL4
```

```
%scf
  Convergence    Normal
  MaxIter  500
  Autostart false
  end
%method
  SwitchToSOSCF  false
  ScanGuess Hueckel
  end
#%geom
#  MaxIter   300
#  end
%output
  PrintLevel     mini
#  Print[P_MOs]  1
  end
%MaxCore 6000
%coords
  CTyp           XYZ
  Charge          0
  Mult           4
  pardef
     xO =  0.00, 2.2005, 13;   # atom 1 to 2
     yO = -1.2732, 0.00, 8;    # atom 2 to 1
    end
  coords
  C      +0.000000     +0.000000     +0.000000
  C      +2.200482     -1.273153     -0.011447
  C      -2.203181     -1.270089     +0.006556
  C      +2.200464     +1.273163     +0.000000
  C      -2.203216     +1.270057     +0.017996
  C      +0.001374     +2.543259     +0.014918
  C      +0.001367     -2.543253     -0.007930
  C      -2.192535     +3.797262     +0.045162
  C      -2.192580     -3.797466     +0.010954
  C      +4.383717     +0.000000     -0.000000
  C      -0.736129     -1.268884     -0.487201
  C      +1.464729     +0.002253     -0.490382
  C      -0.736161     +1.273392     -0.475752
  C      -2.919916     -2.542734     -0.492369
  C      -2.919925     +2.547238     -0.469496
  C      -0.747918     -3.797069     -0.507036
  C      +3.659066     -1.252028     -0.514309
  C      -0.747908     +3.801589     -0.472891
  C      +3.659025     +1.256638     -0.503017
  C      -2.912998     +0.002276     -0.488159
  C      +1.452365     -2.518941     -0.517384
  C      +1.452341     +2.523552     -0.494729
  C      -2.938653     -2.514239     -2.037121
  C      -2.938722     +2.532573     -2.014417
  C      -0.730958     -3.789515     -2.052000
  C      +3.639101     -1.266002     -2.059212
  C      -0.730991     +3.807893     -2.017890
  C      +3.639087     +1.284434     -2.047756
  C      -0.743816     -1.262178     -2.051208
  C      -0.743858     +1.280638     -2.039776
```

```
C      +1.457442     +0.009238     -2.054330
C      +1.459604     -2.537785     -2.069250
C      -2.949620     +0.009221     -2.039815
C      +1.459589     +2.556317     -2.046379
C      +0.720569     -1.258289     -2.545112
C      -1.477864     +0.011489     -2.530848
C      +0.720553     +1.281297     -2.533644
C      -1.481642     -2.533906     -2.543745
C      +2.925945     +0.011511     -2.550369
C      -1.481700     +2.556916     -2.520878
C      -3.658828     -1.257363     -2.540947
C      -3.658846     +1.280313     -2.529507
C      +0.711659     -3.781793     -2.570679
C      +2.909333     -2.512601     -2.574194
C      +2.909316     +2.535721     -2.551474
C      +0.711645     +3.804846     -2.536597
C      -5.121072     -1.252956     -2.057817
C      -4.362625     -0.000173     +0.031635
C      -4.369008     -2.537710     +0.028895
C      -4.368994     +2.537362     +0.051753
C      -2.202275     +3.818312     +1.584988
C      -2.202655     -3.832905     +1.550514
C      -2.192399     +1.260761     +1.540237
C      -2.238442     -1.275148     +1.546152
C      -1.512766     -2.531478     +2.074316
C      -3.660301     -3.831634     +2.047390
C      -3.671718     -1.291895     +2.047470
C      -1.520948     -0.001287     +2.082309
C      -3.623631     +1.247126     +2.092970
C      -1.519250     +2.532257     +2.098283
C      -3.677825     +3.809017     +2.087918
C      -5.093552     +1.281586     -0.467513
C      -4.352967     +2.512233     +1.591471
C      -5.085694     -1.264808     -0.467836
C      -4.348238     -0.000151     +1.571571
C      -4.381987     -2.576385     +1.568354
C      -5.099871     +1.297314     -2.007416
C      -5.836206     +0.045955     -2.520740
H      +0.719120     +3.830570     -3.641129   newgto "SV" end
H      +2.917050     +2.561457     -3.656327   newgto "SV" end
H      +0.719016     -3.797698     -3.675394   newgto "SV" end
H      +2.916929     -2.528395     -3.679239   newgto "SV" end
H      -3.688208     -1.252605     -3.645716   newgto "SV" end
H      -3.688326     +1.285401     -3.634285   newgto "SV" end
H      +0.714337     +1.282740     -3.643541   newgto "SV" end
H      -1.478357     +0.016335     -3.640707   newgto "SV" end
H      +0.714340     -1.250036     -3.654969   newgto "SV" end
H      -1.484895     +2.558945     -3.628336   newgto "SV" end
H      +2.918243     +0.016406     -3.657924   newgto "SV" end
H      -1.484850     -2.526257     -3.651178   newgto "SV" end
H      -1.254816     -4.689248     -2.423629   newgto "SV" end
H      -3.460061     -3.415115     -2.408576   newgto "SV" end
H      -3.460097     +3.436790     -2.377749   newgto "SV" end
H      +4.678865     -1.262814     -2.433833   newgto "SV" end
H      +4.678879     +1.284892     -2.422340   newgto "SV" end
H      -1.254717     +4.711103     -2.381236   newgto "SV  end
```

```
  H      +1.242574     +4.711634     -2.193188   newgto "SV" end
  H      +3.432410     -3.426866     -2.239094   newgto "SV" end
  H      +1.242632     -4.691607     -2.235405   newgto "SV" end
  H      +3.432450     +3.446839     -2.208012   newgto "SV" end
  H      -2.718936     -4.704894     -0.333897   newgto "SV" end
  H      +5.431201     +0.001670     -0.347642   newgto "SV" end
  H      -2.718951     +4.707925     -0.290969   newgto "SV" end
  H      +1.976056     -3.425048     -0.154540   newgto "SV" end
  H      +1.976150     +3.426247     -0.123676   newgto "SV" end
  H      -0.221171     -4.698461     -0.144036   newgto "SV" end
  H      -0.221145     +4.699661     -0.101852   newgto "SV" end
  H      +4.177082     +2.159461     -0.132118   newgto "SV" end
  H      +4.177087     -2.158168     -0.151531   newgto "SV" end
  H      +4.412362     -0.004972     +1.103692   newgto "SV" end
  H      -1.725841     -4.723315     +1.903697   newgto "SV" end
  H      -1.691763     +4.693866     +1.928021   newgto "SV" end
  H      -4.883232     +3.420013     -0.266655   newgto "SV" end
  H      -4.876867     -3.406193     -0.335419   newgto "SV" end
  H      -5.375413     -2.612230     +1.964235   newgto "SV" end
  H      -5.345721     +0.031813     +1.957448   newgto "SV" end
  H      -5.348079     +2.471470     +1.982618   newgto "SV" end
  H      -6.080676     -1.262341     -0.074250   newgto "SV" end
  H      -6.094631     +1.278489     -0.089725   newgto "SV" end
  H      -5.645275     -2.107902     -2.430878   newgto "SV" end
  H      -5.613148     +2.164832     -2.366376   newgto "SV" end
  H      -5.895981     +0.069478     -3.588810   newgto "SV" end
  H      -6.824273     +0.047810     -2.110097   newgto "SV" end
  H      -4.159953     -4.688474     +1.646060   newgto "SV" end
  H      -4.202660     +4.667153     +1.723159   newgto "SV" end
  H      -3.66702      -3.85430      +3.11713    newgto "SV" end
  H      -3.69817      +3.84367      +3.15716    newgto "SV" end
  O       {xO}          {yO}         +1.33
  end
end
```

6- Adsorption of Hydroxyl on Stepped Surface

A) First half of unit cell

```
#-----------------------------------------
# Diamond (111) cluster KS scan back-step with OH 1
#-----------------------------------------
#
! UKS BP86 Def2-SVP Def2-SVP/C RI PAL4
! Opt
%scf
  Convergence    Normal
  MaxIter  500
  Autostart false
  end
%method
  SwitchToSOSCF  false
```

```
  ScanGuess Hueckel
  end
#%geom
#  MaxIter  300
#  end
%output
  PrintLevel           mini
#  Print[P_MOs]  1
  end
%MaxCore 6000
%coords
  CTyp            XYZ
  Charge           0
  Mult             3
  pardef
    xO = -2.2032, 0.00, 13;   # atom 5 to 1
    yO =  0.00, 1.2701, 8;    # atom 1 to 5
    end
  coords
  C      +0.000000     +0.000000     +0.000000
  C      +2.200482     -1.273153     -0.011447
  C      -2.203181     -1.270089     +0.006556
  C      +2.200464     +1.273163     +0.000000
  C      -2.203216     +1.270057     +0.017996
  C      +0.001374     +2.543259     +0.014918
  C      +0.001367     -2.543253     -0.007930
  C      -2.192535     +3.797262     +0.045162
  C      -2.192580     -3.797466     +0.010954
  C      +4.383717     +0.000000     -0.000000
  C      -0.736129     -1.268884     -0.487201
  C      +1.464729     +0.002253     -0.490382
  C      -0.736161     +1.273392     -0.475752
  C      -2.919916     -2.542734     -0.492369
  C      -2.919925     +2.547238     -0.469496
  C      -0.747918     -3.797069     -0.507036
  C      +3.659066     -1.252028     -0.514309
  C      -0.747908     +3.801589     -0.472891
  C      +3.659025     +1.256638     -0.503017
  C      -2.912998     +0.002276     -0.488159
  C      +1.452365     -2.518941     -0.517384
  C      +1.452341     +2.523552     -0.494729
  C      -2.938653     -2.514239     -2.037121
  C      -2.938722     +2.532573     -2.014417
  C      -0.730958     -3.789515     -2.052000
  C      +3.639101     -1.266002     -2.059212
  C      -0.730991     +3.807893     -2.017890
  C      +3.639087     +1.284434     -2.047756
  C      -0.743816     -1.262178     -2.051208
  C      -0.743858     +1.280638     -2.039776
  C      +1.457442     +0.009238     -2.054330
  C      +1.459604     -2.537785     -2.069250
  C      -2.949620     +0.009221     -2.039815
  C      +1.459589     +2.556317     -2.046379
  C      +0.720569     -1.258289     -2.545112
  C      -1.477864     +0.011489     -2.530848
  C      +0.720553     +1.281297     -2.533644
```

```
C      -1.481642     -2.533906     -2.543745
C      +2.925945     +0.011511     -2.550369
C      -1.481700     +2.556916     -2.520878
C      -3.658828     -1.257363     -2.540947
C      -3.658846     +1.280313     -2.529507
C      +0.711659     -3.781793     -2.570679
C      +2.909333     -2.512601     -2.574194
C      +2.909316     +2.535721     -2.551474
C      +0.711645     +3.804846     -2.536597
C      -5.121072     -1.252956     -2.057817
C      -4.362625     -0.000173     +0.031635
C      -4.369008     -2.537710     +0.028895
C      -4.368994     +2.537362     +0.051753
C      -2.202275     +3.818312     +1.584988
C      -2.202655     -3.832905     +1.550514
C      -2.192399     +1.260761     +1.540237
C      -2.238442     -1.275148     +1.546152
C      -1.512766     -2.531478     +2.074316
C      -3.660301     -3.831634     +2.047390
C      -3.671718     -1.291895     +2.047470
C      -1.520948     -0.001287     +2.082309
C      -3.623631     +1.247126     +2.092970
C      -1.519250     +2.532257     +2.098283
C      -3.677825     +3.809017     +2.087918
C      -5.093552     +1.281586     -0.467513
C      -4.352967     +2.512233     +1.591471
C      -5.085694     -1.264808     -0.467836
C      -4.348238     -0.000151     +1.571571
C      -4.381987     -2.576385     +1.568354
C      -5.099871     +1.297314     -2.007416
C      -5.836206     +0.045955     -2.520740
H      +0.719120     +3.830570     -3.641129   newgto "SV" end
H      +2.917050     +2.561457     -3.656327   newgto "SV" end
H      +0.719016     -3.797698     -3.675394   newgto "SV" end
H      +2.916929     -2.528395     -3.679239   newgto "SV" end
H      -3.688208     -1.252605     -3.645716   newgto "SV" end
H      -3.688326     +1.285401     -3.634285   newgto "SV" end
H      +0.714337     +1.282740     -3.643541   newgto "SV" end
H      -1.478357     +0.016335     -3.640707   newgto "SV" end
H      +0.714340     -1.250036     -3.654969   newgto "SV" end
H      -1.484895     +2.558945     -3.628336   newgto "SV" end
H      +2.918243     +0.016406     -3.657924   newgto "SV" end
H      -1.484850     -2.526257     -3.651178   newgto "SV" end
H      -1.254816     -4.689248     -2.423629   newgto "SV" end
H      -3.460061     -3.415115     -2.408576   newgto "SV" end
H      -3.460097     +3.436790     -2.377749   newgto "SV" end
H      +4.678865     -1.262814     -2.433833   newgto "SV" end
H      +4.678879     +1.284892     -2.422340   newgto "SV" end
H      -1.254717     +4.711103     -2.381236   newgto "SV" end
H      +1.242574     +4.711634     -2.193188   newgto "SV" end
H      +3.432410     -3.426866     -2.239094   newgto "SV" end
H      +1.242632     -4.691607     -2.235405   newgto "SV" end
H      +3.432450     +3.446839     -2.208012   newgto "SV" end
H      -2.718936     -4.704894     -0.333897   newgto "SV" end
H      +5.431201     +0.001670     -0.347642   newgto "SV" end
H      -2.718951     +4.707925     -0.290969   newgto "SV" end
```

```
  H      +1.976056     -3.425048     -0.154540   newgto "SV" end
  H      +1.976150     +3.426247     -0.123676   newgto "SV" end
  H      -0.221171     -4.698461     -0.144036   newgto "SV" end
  H      -0.221145     +4.699661     -0.101852   newgto "SV" end
  H      +4.177082     +2.159461     -0.132118   newgto "SV" end
  H      +4.177087     -2.158168     -0.151531   newgto "SV" end
  H      +4.412362     -0.004972     +1.103692   newgto "SV" end
  H      -1.725841     -4.723315     +1.903697   newgto "SV" end
  H      -1.691763     +4.693866     +1.928021   newgto "SV" end
  H      -4.883232     +3.420013     -0.266655   newgto "SV" end
  H      -4.876867     -3.406193     -0.335419   newgto "SV" end
  H      -5.375413     -2.612230     +1.964235   newgto "SV" end
  H      -5.345721     +0.031813     +1.957448   newgto "SV" end
  H      -5.348079     +2.471470     +1.982618   newgto "SV" end
  H      -6.080676     -1.262341     -0.074250   newgto "SV" end
  H      -6.094631     +1.278489     -0.089725   newgto "SV" end
  H      -5.645275     -2.107902     -2.430878   newgto "SV" end
  H      -5.613148     +2.164832     -2.366376   newgto "SV" end
  H      -5.895981     +0.069478     -3.588810   newgto "SV" end
  H      -6.824273     +0.047810     -2.110097   newgto "SV" end
  H      -4.159953     -4.688474     +1.646060   newgto "SV" end
  H      -4.202660     +4.667153     +1.723159   newgto "SV" end
  H      -3.667020     -3.854300      3.117130   newgto "SV" end
  H      -3.698170      3.843670      3.157160   newgto "SV" end
  O      {xO}           {yO}          1.42
  H      {xO+0.45866}   {yO-0.7933}   1.73814
  end
end
```

B) Second half of unit cell

```
#-----------------------------------------
# Diamond (111) cluster KS scan back-step with OH 2
#-----------------------------------------
#
! UKS BP86 Def2-SVP Def2-SVP/C RI PAL4
! Opt
%scf
  Convergence    Normal
  MaxIter  500
  Autostart false
  end
%method
  SwitchToSOSCF  false
  ScanGuess Hueckel
  end
#%geom
#  MaxIter  300
#  end
%output
  PrintLevel           mini
#  Print[P_MOs]  1
  end
```

```
%MaxCore 6000
%coords
  CTyp           XYZ
  Charge          0
  Mult            3
  pardef
    xO =  0.00, 2.2005, 13;   # atom 1 to 2
    yO = -1.2732, 0.00, 8;    # atom 2 to 1
    end
  coords
  C      +0.000000     +0.000000     +0.000000
  C      +2.200482     -1.273153     -0.011447
  C      -2.203181     -1.270089     +0.006556
  C      +2.200464     +1.273163     +0.000000
  C      -2.203216     +1.270057     +0.017996
  C      +0.001374     +2.543259     +0.014918
  C      +0.001367     -2.543253     -0.007930
  C      -2.192535     +3.797262     +0.045162
  C      -2.192580     -3.797466     +0.010954
  C      +4.383717     +0.000000     -0.000000
  C      -0.736129     -1.268884     -0.487201
  C      +1.464729     +0.002253     -0.490382
  C      -0.736161     +1.273392     -0.475752
  C      -2.919916     -2.542734     -0.492369
  C      -2.919925     +2.547238     -0.469496
  C      -0.747918     -3.797069     -0.507036
  C      +3.659066     -1.252028     -0.514309
  C      -0.747908     +3.801589     -0.472891
  C      +3.659025     +1.256638     -0.503017
  C      -2.912998     +0.002276     -0.488159
  C      +1.452365     -2.518941     -0.517384
  C      +1.452341     +2.523552     -0.494729
  C      -2.938653     -2.514239     -2.037121
  C      -2.938722     +2.532573     -2.014417
  C      -0.730958     -3.789515     -2.052000
  C      +3.639101     -1.266002     -2.059212
  C      -0.730991     +3.807893     -2.017890
  C      +3.639087     +1.284434     -2.047756
  C      -0.743816     -1.262178     -2.051208
  C      -0.743858     +1.280638     -2.039776
  C      +1.457442     +0.009238     -2.054330
  C      +1.459604     -2.537785     -2.069250
  C      -2.949620     +0.009221     -2.039815
  C      +1.459589     +2.556317     -2.046379
  C      +0.720569     -1.258289     -2.545112
  C      -1.477864     +0.011489     -2.530848
  C      +0.720553     +1.281297     -2.533644
  C      -1.481642     -2.533906     -2.543745
  C      +2.925945     +0.011511     -2.550369
  C      -1.481700     +2.556916     -2.520878
  C      -3.658828     -1.257363     -2.540947
  C      -3.658846     +1.280313     -2.529507
  C      +0.711659     -3.781793     -2.570679
  C      +2.909333     -2.512601     -2.574194
  C      +2.909316     +2.535721     -2.551474
  C      +0.711645     +3.804846     -2.536597
```

```
C      -5.121072     -1.252956     -2.057817
C      -4.362625     -0.000173     +0.031635
C      -4.369008     -2.537710     +0.028895
C      -4.368994     +2.537362     +0.051753
C      -2.202275     +3.818312     +1.584988
C      -2.202655     -3.832905     +1.550514
C      -2.192399     +1.260761     +1.540237
C      -2.238442     -1.275148     +1.546152
C      -1.512766     -2.531478     +2.074316
C      -3.660301     -3.831634     +2.047390
C      -3.671718     -1.291895     +2.047470
C      -1.520948     -0.001287     +2.082309
C      -3.623631     +1.247126     +2.092970
C      -1.519250     +2.532257     +2.098283
C      -3.677825     +3.809017     +2.087918
C      -5.093552     +1.281586     -0.467513
C      -4.352967     +2.512233     +1.591471
C      -5.085694     -1.264808     -0.467836
C      -4.348238     -0.000151     +1.571571
C      -4.381987     -2.576385     +1.568354
C      -5.099871     +1.297314     -2.007416
C      -5.836206     +0.045955     -2.520740
H      +0.719120     +3.830570     -3.641129   newgto "SV" end
H      +2.917050     +2.561457     -3.656327   newgto "SV" end
H      +0.719016     -3.797698     -3.675394   newgto "SV" end
H      +2.916929     -2.528395     -3.679239   newgto "SV" end
H      -3.688208     -1.252605     -3.645716   newgto "SV" end
H      -3.688326     +1.285401     -3.634285   newgto "SV" end
H      +0.714337     +1.282740     -3.643541   newgto "SV" end
H      -1.478357     +0.016335     -3.640707   newgto "SV" end
H      +0.714340     -1.250036     -3.654969   newgto "SV" end
H      -1.484895     +2.558945     -3.628336   newgto "SV" end
H      +2.918243     +0.016406     -3.657924   newgto "SV" end
H      -1.484850     -2.526257     -3.651178   newgto "SV" end
H      -1.254816     -4.689248     -2.423629   newgto "SV" end
H      -3.460061     -3.415115     -2.408576   newgto "SV" end
H      -3.460097     +3.436790     -2.377749   newgto "SV" end
H      +4.678865     -1.262814     -2.433833   newgto "SV" end
H      +4.678879     +1.284892     -2.422340   newgto "SV" end
H      -1.254717     +4.711103     -2.381236   newgto "SV" end
H      +1.242574     +4.711634     -2.193188   newgto "SV" end
H      +3.432410     -3.426866     -2.239094   newgto "SV" end
H      +1.242632     -4.691607     -2.235405   newgto "SV" end
H      +3.432450     +3.446839     -2.208012   newgto "SV" end
H      -2.718936     -4.704894     -0.333897   newgto "SV" end
H      +5.431201     +0.001670     -0.347642   newgto "SV" end
H      -2.718951     +4.707925     -0.290969   newgto "SV" end
H      +1.976056     -3.425048     -0.154540   newgto "SV" end
H      +1.976150     +3.426247     -0.123676   newgto "SV" end
H      -0.221171     -4.698461     -0.144036   newgto "SV" end
H      -0.221145     +4.699661     -0.101852   newgto "SV" end
H      +4.177082     +2.159461     -0.132118   newgto "SV" end
H      +4.177087     -2.158168     -0.151531   newgto "SV" end
H      +4.412362     -0.004972     +1.103692   newgto "SV" end
H      -1.725841     -4.723315     +1.903697   newgto "SV" end
H      -1.691763     +4.693866     +1.928021   newgto "SV" end
```

```
  H      -4.883232     +3.420013     -0.266655   newgto "SV" end
  H      -4.876867     -3.406193     -0.335419   newgto "SV" end
  H      -5.375413     -2.612230     +1.964235   newgto "SV" end
  H      -5.345721     +0.031813     +1.957448   newgto "SV" end
  H      -5.348079     +2.471470     +1.982618   newgto "SV" end
  H      -6.080676     -1.262341     -0.074250   newgto "SV" end
  H      -6.094631     +1.278489     -0.089725   newgto "SV" end
  H      -5.645275     -2.107902     -2.430878   newgto "SV" end
  H      -5.613148     +2.164832     -2.366376   newgto "SV" end
  H      -5.895981     +0.069478     -3.588810   newgto "SV" end
  H      -6.824273     +0.047810     -2.110097   newgto "SV" end
  H      -4.159953     -4.688474     +1.646060   newgto "SV" end
  H      -4.202660     +4.667153     +1.723159   newgto "SV" end
  H      -3.667020     -3.854300      3.117130   newgto "SV" end
  H      -3.698170      3.843670      3.157160   newgto "SV" end
  O      {xO}           {yO}          1.42
  H      {xO+0.45866}   {yO-0.7933}   1.73814
  end
end
```